Chapter 11

INDUSTRIAL APPLICATIONS TO NEW CLEAN BURNING, COST COMPETITIVE FUELS

11.1 THE INCREASINGLY CATACLYSMIC CLIMACTIC EVENTS FACING MANKIND

11.1.1 Foreword

Some of the biggest needs of mankind to contain increasingly cataclysmic climactic events due to global warming and other large environmental problems are: 1) Remove and recycle carbon dioxide from our atmosphere; 2) Develop means for the processing of carbon dioxide in automotive exhaust; and 3) Develop new clean burning cost competitive fuels (see the content of this chapter for details).

The biggest threat to mankind in this field is the lack at this writing in all developed countries of political will to invest public funds in serious resolutions of our environmental problems. All governmental investments in the sector known to this author have been made for the *appearance* of favoring the environment while in reality favoring the myopic and self-destructing interests of the organized petroleum cartel, as it is the case for investment of public funds in hydrogen (see Section 11.1.3 for the huge environmental problems caused by current hydrogen production via the reformation of fossil fuels, while multiplying the profits of the petroleum cartel).

It should be stressed that the solution of large societal problems must be supported by *public* funds, since it is unethical to expect that individuals pay for the cost. Yet, all the research presented in this chapter has been supported by *private* funds due to the lack of public funds following solicitations by the author in the U.S.A., Continental Europe, Russia, China, Japan, Australia, and other developed countries.

One way to understand the gravity of environmental problems is to note that this chapter has been written during the month of September 2005 at

the Institute for Basic Research in Florida, when the southern belt of the U.S.A. had been exposed to some eighteen hurricanes and devastated by the hurricanes Kathrina and Rita, with additional hurricanes expected before the end of the 2005 season. Increasingly cataclysmic climactic events are expected in the years ahead, until the entire southern belt of the U.S.A. will become uninhabitable.[1]

Similar increasingly cataclysmic climactic events are occurring in the rest of the world. As an example, the mountain region of the Andes in Peru is experiencing an exodus of the local farmers toward the cities due to the lack of snow in winter, with expected major drought the following summer and consequential inability to grow crops.

Also, *The Economist* in England published in the fall of 2004 a report from the U. S. Pentagon releasing for the first time data on the slow down of the Gulf Stream due to the decreased density and salinity of the North Atlantic caused by the melting of the ice in the North Pole region. The complete halting of the Gulf Stream is now beyond scientific doubt, the only debatable issue remaining is that of the date, at which time England is expected to suffer from extreme cold in winter and extreme temperature in summer.

The list of similar increasingly cataclysmic climactic events all over the world could now be endless.

It is at this point were the efforts for the construction of hadronic mechanics, superconductivity and chemistry acquire their full light. In fact, all possibilities of resolving our huge environmental problems via the use of conventional doctrines were long exhausted, as better illustrated in this and in the next chapter, thus establishing the need for suitable covering disciplines beyond any possible doubt.

All scientists have a direct responsibility to contribute, or at least not to oppose, serious efforts toward the solution of these increasingly cataclysmic problems via the traditional scientific process of trial and errors, by implementing genuine scientific democracy, ethics and accountability vis a vis mankind, not via a formal academic parlance, but in actual deeds, the only ones having social as well as scientific value, beginning with the admission that *the dominance of the entire universe by the rather limited Einsteinian doctrines is a purely political - nonscientific posture, and its era has now ended in favor of covering theories for physical conditions unthinkable during Einstein's times.*

[1] At the end of the 2005 hurricane season Florida was hit by *twenty two* major climactic events, so many that the U.S. Weather Bureau exhausted all 21 letters of the English alphabet and had to name the 22-nd storm from the Greek alphabet. There is no need to wait a few years to understand that the devastating climactic events expected in the next few years are due to the lack of serious political will NOW.

Figure 11.1. A view of one of the primary responsibilities for current increasingly cataclysmic climatic events: the pollution caused by fossil fueled electric power plants.

11.1.2 Origin of the Increasingly cataclysmic Climactic Events

According to official data released by the U. S. Department of Energy[2], by ignoring the world-wide consumption of natural gas and coal, *we consumed in 2003 about* 74×10^6 *barrels of crude oil (petroleum) per day, corresponding to the daily consumption of about* 3×10^9 *gallons (g) or* 1.4×10^{10} *liters (L) of gasoline per day.*

When adding the world consumption of natural gas and coal, *the world consumption of fossil fuels in 2003 should be conservatively estimated to be equivalent to* 1.5×10^7 *barrels per day, corresponding to the gasoline equivalent of* 7.5×10^8 *gallon or* 2.8×10^{11} *liters per day.*

Such a disproportionate consumption is due to the average daily use in 2003 of about $1,000,000,000$ cars, $1,000,000$ trucks, $100,000$ planes plus an unidentifiable number of additional vehicles of military, agricultural, industrial and other nature, plus the large consumption of fossil fuels by electric power plants around the world.

The data for 2004 are not reported here because still debated, and estimated to be of the order of 90×10^6 barrels of crude oil (petroleum) per day. Future

[2]See, e.g., the web site http://www.eia.doe.gov/emeu/international/energy.html

MARKET (Fuel Source)	Current U.S. Daily Market Usage (1999 Statistics)
Oil	U.S.A. - 882.8 million tons (25.5% share of world total usage) = 18,490 thousand barrels daily
Natural Gas	U.S.A. - 555.3 million tons oil equivalent (26.9% of world total usage) = 617 billion cubic meters
Coal	U.S.A. - 543.3 million tons oil equivalent (25.5% of world total usage) = 543.3 million tons oil equivalent (25.5% of world total usage)

Figure 11.2. Official data on the 2003 disproportionate consumption of fossil fuels in the U.S.A. alone.

consumption can be best illustrated by noting that, according to official data of the Chinese government, *China is building* $500,000,000$ *(yes, five hundred million) new cars by 2015, and that the need for petroleum, in China for the year 2006 will correspond to the world consumption for 2004, including China.*

The extremely serious environmental problems caused by the above disproportionate combustion of fossil fuels can be summarized as follows:[3]

(1) **The combustion of fossil fuels releases in our atmosphere about sixty millions metric of tons carbon dioxide CO_2 per day that are responsible for the first large environmental problem known as "global warning" or "green house effect."**[4] Of these only 30 millions metric tons

[3]See for details the web site http://www.magnegas.com/technology/part6.htm. The reader should note that the calculations in this web site only treat the 2003 consumption of crude oil for automotive use. Consequently, the data therein should be multiplied by three to reach realistic values for 2003.
[4]The value of 60 million tons of CO_2 per day is easily obtained from the chemical reaction in the combustion of the indicated daily volume of fossil fuels (see for details http://www.magnegas.com/technology/part6.htm

are estimated to be recycled by our ever decreasing forests. This implies the release in our atmosphere of about thirty millions metric tons of unrecycled green house gases per day, which release is the cause of the "global warming" now visible to everybody through climactic episodes such as floods, tornadoes, hurricanes, etc. of increasing catastrophic nature.

(2) **The combustion of fossil fuels causes the permanent removal from our atmosphere of about 21 millions metric tons of breathable oxygen per day, a second, extremely serious environmental problem known as "oxygen depletion."**[5] Even though not disclosed by political circles and newsmedia, the very admission of an "excess" CO_2 in our atmosphere (that is, CO_2 no longer recycled by plants) is an admission of oxygen depletion because the "O_2 in the excess "CO_2" was originally breathable oxygen. Hence, by recalling the atomic weight of CO_2 and O_2, we have the value $\frac{32}{44} \times 30 \times 10^6 = 21.8 \times 10^8$ tons of lost oxygen per day.

It appears that, prior the introduction of oxygen depletion by the author in 2000, everybody ignored the fact that *the combustion of fossil fuels requires atmospheric oxygen.* Since only the global warming is generally considered, it appears that *newsmedia, governments and industries alike ignored the fact that we need oxygen to breath.* Only more recently, various environmental groups, unions and other concerned groups are becoming aware that *the increasing heart problems in densely populated area are indeed due to local oxygen depletion caused by excessive fossil fuel combustion.*

(3) **The combustion of fossil fuels releases in our atmosphere about fifteen millions metric tons of carcinogenic and toxic substances per day.** This third, equally serious environmental problems is euphemistically referred to by the newsmedia as "atmospheric pollution"', while in reality it refers to the primary source of the widespread increase of cancer in our societies. For instance, it has been established by various medical studies (generally suppressed by supporters of the oil cartel) that *unless of genetic origin, breast cancer is due to the inhaling of carcinogenic substances in fossil fuels exhaust.* These studies have gone so far as to establish that breast cells are very receptive to a particular carcinogenic substance in fossil fuel exhaust. After all, responsible citizens should remember and propagate (rather than myopically suppress) the fact that *the U. S. Environmental Protection Agency has formally admitted that diesel exhaust is carcinogenic.* A moment of reflection is sufficient for anybody in good faith to see that we inhale on a daily basis carcinogenic substances from gasoline exhaust in an amount that is ten thousands times bigger than carcinogenic substances ingested with food.

[5]The "oxygen depletion" was first introduced by the author at the 2000 Hydrogen World Conference held in Munich, Germany (see the web site http://www.magnegas.com/technology/part6.htm).

Figure 11.3. A picture of frequent environmental disasters caused by the spill of crude oil from tankers following accidents. The replacement of crude oil with a gaseous fuel will eliminate the environmental damage, with the exception of hydrogen because, in the event the cargo of this tanker had been composed of hydrogen, its release in the atmosphere, its immediate rising to the ozone layer, and its very rapid reaction with O_3 would create a hole in the ozone layer of the size of the State of Rhode Island, with consequential increase of skin and other cancers on Earth (see Section 11.1.3 for details).

This is another serious environmental problem that has remained virtually ignored by all until recently due to the widespread misinformation by the newsmedia. However, the existence of this third major environmental problem caused by fossil fuel combustion has now propagated to environmental, union and other circles with predictable legal implications for the fossil fuel industry and its major users, unless suitable corrective measures are initiated, as it occurred for the tobacco industry.

It is hoped that people trapped in traffic, thus inhaling the carcinogenic fumes from the vehicle in front, will remember the above evidence and assume an active role in the support of environmentally acceptable fuels because it is written throughout history that people have the government and system they deserve.

There exist numerous additional environmental problems caused by the *global* study of fossil fuels, that is, not only the environmental problems caused by their combustion, but also those caused by their production and transportation. The latter problems are omitted here for brevity and also because the

dimension of problems 1), 2) and 3) is a sufficient call for persons in good faith.

11.1.3 Serious Environmental Problems Caused by Hydrogen, Natural Gas, Ethanol, Biogases and Fuels with Molecular Structure

Whenever facing the ever increasing cataclysmic climactic events caused by fossil fuel combustion, a rather widespread belief is that the solution already exists and it is given by *hydrogen* for the large scale fuel uses of the future because hydrogen is believed to be "the cleanest fuel available to mankind."

Due to the potentially lethal implications for mankind, it is necessary to dispel this belief and indicate that, *the current production and combustion of hydrogen, whether for an internal combustion engine or for a fuel cell, causes a global pollution much greater than that caused by gasoline when compared for the same energy outputs.*

Hydrogen is indeed an environmentally acceptable fuel, but only when its production and use verify the following conditions:

CONDITION I: Hydrogen is produced via the electrolytic separation of water;

CONDITION II: The electricity used for electrolysis originates from clean and renewable energy sources, such as those of hydric, solar or wind nature; and

CONDITION III: The oxygen produced by the electrolytic process is freely released in the environment so that the subsequent hydrogen combustion leaves unchanged the existing oxygen content of our atmosphere.

However, the reality in the production and use of hydrogen is dramatically different than the above ideal conditions. In fact, hydrogen is today produced in its greatest percentage via reformation processes of fossil fuels such as methane CH_4, via the use of highly polluting electric power plants, and no oxygen is released in the atmosphere during production.

Reformation processes are preferred over electrolysis not only because of the low efficiency of the electrolytic separation of water,[6] but also due to the fact that the primary drive in the current international support for hydrogen as a fuel is to permit the petroleum cartel to multiply the profits (because the profits from the sale of the hydrogen content of fossil fuels are a multiple of the profits from the direct sale of fossil fuels, as better indicated below.)

[6]Electrolytic plants for the separation of water have an efficiency of the order of 0.8, thus yielding an efficiency for hydrogen production by volume of the order of 0.5, as compared to the efficiency in the production of magnegas discussed in the subsequent sections of this chapter that can be 10.5 in industrial recycler, that is, 21 times bigger than that of electrolysis.

Renewable sources of electricity, even though manifectly valuable, are so minute with respect to the enormity of the demand for fuel that cannot be taken into serious consideration. Nuclear power plants also cannot be taken into serious consideration until governments finally provide serious financial support for basic research on the stimulated decay of radioactive nuclear waste by nuclear power plants themselves, rather than the currently preferred "storage" of nuclear waste in in depositories nobody wants to have near-by. These aspects begin to illustrate the reason hadronic mechanics, superconductivity and chemistry were developed, as studied in more details in the next chapter.

When inspected in real terms, the current production, transportation and use of hydrogen, if implemented in large scale such as that of fossil fuels, cause the following very serious environmental problems:

A) **Alarming oxygen depletion caused by hydrogen combustion,** namely, the permanent removal of breathable oxygen from our atmosphere and its conversion into water vapor H_2O. By remembering that oxygen is the very basis of life, we are here referring to one of the most serious environmental problems facing mankind that can become potentially lethal for large scale combustion of hydrogen irrespective of whether used as fuel or in fuel cells. When TV programs show water vapor coming out of car exhaust running on hydrogen, they are actually showing one of the most alarming environmental problems facing mankind.

It should be indicated that *gasoline combustion causes much less oxygen depletion than hydrogen combustion,* for various reasons. The first is that gasoline combustion turns atmospheric oxygen into CO_2 that is food for plants, since the chlorophyll process turns CO_2 into breathable O_2 while maintaining C for plant growth. Therefore, the oxygen depletion caused by gasoline and fossil fuels in general is only that for the *excess* of CO_2 that cannot be any longe recycled by plants due to their enormous daily releases, combined with the ongoing forest depletion.

By comparison, hydrogen turns breathable oxygen into water vapors. At this point equivocal technicians indicate that "plants also recycle water into oxygen,", which statement is correct because without water plants die, as well known. Nevertheless, if proffered by experts, the statement may be dishonest because they do not mention the fact that *our atmosphere is full of water vapor as shown by clouds and rain.* Hence, the additional water vapor originating from hydrogen combustion cannot possibly be recycled by plants. By comparison, the CO_2 content in our atmosphere was less than 1% one century ago, in which case the excess due to fossil fuel combustion was, at least initially, recycled by plants, and this is the very reason the human race is still alive today despite the current immense fossil fuel consumption the world over.

Yet another reason favoring environmentally the combustion of gasoline over hydrogen is that *the oxygen depletion caused by hydrogen combustion*

is a large multiple of that caused by gasoline combustion. This additional environmental problem can be seen as follows. Gasoline combustion is based on the synthesis of CO, one of the most esoenergetic chemical reactions known to man, that releases 255 Kcal/mole, followed by the synthesis of CO_2 that releases about 85 Kcal/mole, and other reactions for a total of at least 335 Kcal/mole. By comparison, the sole chemical reaction in hydrogen combustion is the synthesis of H_2O releasing about 57 Kcal/mole. A first year graduate student in chemistry can then compute the multiplier needed for the oxygen depletion caused by gasoline combustion to reach that of hydrogen combustion, of course, under the same energy output.

B) **Alarming environmental problems caused by current hydrogen production.** The reformation of methane and other fossil fuels for hydrogen production requires large amounts of energy because of the necessary breaking of strong molecular bonds such as CH_4. In this case, all byproducts of the reformation, such as the "green house gas" CO_2, are released into the environment. A first year graduate student in chemistry can then prove (although his/her teacher may disagree for personal academic gains) that the CO_2 released in the atmosphere for hydrogen production from CH_4 is a large multiple of the CO_2 produced in gasoline combustion.

Hence, simple calculations establish that *the current methods of hydrogen production, transportation and use release in the atmosphere carcinogenic substances, green house gases and other contaminants that are at least twenty times bigger than the contaminants releases by the gasoline production and combustion in contemporary cars with efficient catalytic converters.*

In fact, the production of hydrogen requires large amounts of energy while, by comparison, gasoline production requires considerably less energy because crude oil comes out of the group at pressure without any need of electricity, while refining processes of crude oil into gasoline are mostly chemical in nature, thus requiring minimal electric energy. The global pollution caused by gasoline is therefore essentially restricted to the pollution caused by transportation and combustion.

Being an environmentalist, the author certainly does not support gasoline as the dominant fuel. Nevertheless, scientific honesty requires the admission that *gasoline is much less polluting than hydrogen as currently produced when considered on a global scale including production, transportation and combustion.*

C) **Alarming threat to the ozone layer caused by hydrogen seepage and losses.** Another serious environmental problem caused by hydrogen is due to its *seepage,* namely, the fact that, being composed by the smallest molecule on Earth, hydrogen escapes through container walls irrespective of the used material and thickness. Consequently, the large scale use of hydrogen must take into account the inevitable release of free hydrogen that, being very

light, instantly rises to the upper layer of our atmosphere all the way to the *ozone layer,* resulting in its depletion because hydrogen and ozone have one of the fastest known chemical reactions

$$H_2 + O_3 \quad \rightarrow \quad H_2O + O_2. \tag{11.1.1}$$

Again, *gasoline is preferable over hydrogen also in regard to the ozone layer.* In fact, gasoline is liquid and its vapors are heavy, thus being unable to reach the ozone layer. Also, all byproducts of gasoline combustion are heavy and they simply cannot rise to the ozone layer. Assuming that some tornado carries byproducts of gasoline combustion all the way up to the ozone layer, they have no known reaction with the ozone that could compare with that of hydrogen, Eq. (11.1.1).

D) **Alarming environmental problems caused by the need to liquify hydrogen.** Gasoline contains about $110,000$ British Thermal Units (BTU) per gallon (g) while hydrogen contains about 300 BTU per standard cubic foot (scf). Consequently, the "Gasoline Gallon Equivalent' (GGE)' is given by 366 scf of hydrogen. Hence, the hydrogen equivalent of an average 20 gallon gasoline tank would require $7,320$ scf of hydrogen, namely, *a volume of hydrogen so big to require a trailer for its transportation in automotive uses.*

This is the reason all manufacturers testing cars running on hydrogen as a fuel, such as BMW, GM, Honda, and others, have been forced to use *liquified hydrogen.* At this point the environmental problems caused by use of hydrogen as an automotive fuel become truly serious, e.g., because hydrogen liquifies close to the absolute zero degree temperature, thus requiring large amounts of electric energy for its liquefaction, with consequential multiplication of pollution. Additional significant amounts of energy are needed to maintain the liquid state because the spontaneous transition from the liquid to the gas state is explosive without any combustion (because of the rapidity of the transition when the cooling systems ceases to operate).

At the 2000 Hydrogen World Meeting held in Munich, Germany, under BMW support, a participant from Florida stated that "If one of my neighbors in Florida purchases a car operating on liquid hydrogen, I will sell my house because in the event that neighbor leaves the car parked in his driveway to spend the weekend in Las Vegas, and the cooling systems fails to operate due to the Florida summer heat, the explosion due to the transition of state back to the gaseous form will cause a crater."

E) **Prohibitive hydrogen cost.** Commercial grade hydrogen (not the pure hydrogen needed for fuel cells) currently retails in the USA at $\$0.18/scf$. By comparison, natural gas retails at about $\$0.01/scf$. But hydrogen contains $300 BTU/scf$, while natural gas contains $1,050 BTU/scf$. Consequently, $\frac{1,050}{300} \times \$0.18 = \$0.63$, namely, *commercial grade hydrogen currently sells in the U.S.A. at* **sixty three times** *the cost of natural gas,* a very high cost

Element	MagneGas (MG)	Natural Gas	Gasoline	EPA Standards
Hydro-carbons	0.026 gm/mi	0.380 gm/mi 2460% of MG emission	0.234 gm/mi 900% of MG emission	0.41 gm/mi
Carbon Monoxide	0.262 gm/mi	5.494 gm/mi 2096% of MG emission	1.965 gm/mi 750% of MG emission	3.40 gm/mi
Nitrogen Oxides	0.281 gm/mi	.732 gm/mi 260% of MG emission	0.247 gm/mi 80% of MG emission	1.00 gm/mi
Carbon Dioxide	235 gm/mi	646.503 gm/mi 275% of MG emission	458.655 gm/mi 195% of MG emission	No EPA standard exists for Carbon Dioxide
Oxygen	9%-12%	0.5%-0.7% 0.04% of MG emission	0.5%-0.7% 0.04% of MG emission	No EPA standard exists for Oxygen

Figure 11.4. Summary of comparative measurements combustion exhaust of the new magnegas fuel (described in Section 11.3 below), natural gas and gasoline conducted at the EPA accrtedited automotive laboratory of Liphardt & Associatesd of Long Island, New York in 2000 (see for details the website http://www.magnegas.com/technology/part6.htm). As one can see, contrary to popular belief, under the same conditions (same car with same weight used with the same computerized EPA routine, for the same duration of time), natural gas exhaust contains 61% "more" hydrocarbons, about 41% "more" green hoouse gases, and about 200% "more" nitrogen oxides than gasoline exhaust.

that is a reflection of the low efficiency of the available processes for hydrogen production.

But, unlike magnegas and natural gas, hydrogen cannot be significantly carried in a car in a compressed form, thus requiring its liquefaction that is very expensive to achieve as well as to maintain. Consequently, simple calculations establish that *the actual cost of hydrogen in a liquified form for automotive use is at least* 200 *times the cost of fossil fuels,*

There is no credible or otherwise scientific doubt that, under the above generally untold large problems, hydrogen has no realistic chance of becoming a serious alternative for large use without basically *new* technologies and processes.

The above refers to the use of hydrogen as an automotive fuel for internal combustion engines. The situation for the use of hydrogen in fuel cells is essentially the same, except for different efficiencies between internal combustion engines and fuel cells that have no relevance for environmental profiles.

A possible resolution, or at least alleviation, of these problems is presented in Section 11.5.

Another widespread misrepresentation existing in alternative fuels is the belief that "the combustion of natural gas (or methane) is cleaner than that

of gasoline," with particular reference to a presumed reduction of carcinogenic and green house emissions. This misrepresentation is based on the visual evidence that the flame of natural gas is indeed cleaner than that of gasoline or other liquid fuels. However, natural gas is gaseous while gasoline is liquid, with an increase of density in the trantion from the former to the latter of about $1,500$ units. Consequently, when the pollutants in the flame of natural gas are prorated to the density of gasoline, the much more polluting character of natural energes.

In any case, recent measurements reviewed later on in this chapter have disproved the above belief because, *under identical performances, natural gas is much more polluting than gasoline* (see Figure 11.3).

Further widespread misrepresentations exist for *ethanol, biogases,* and other conventional fuels, that is, fuels possessing the conventional molecular structure, because generally presented as cleaner than gasoline. In effect, ethanol combustion exhaust is the most carcinogenic among all fuels, the pollution caused by biogases is truly alarming, and the same occur for all remaining available conventional fuels.

In addition, ethanol. biogases and otehr fuels of agricultural origin leave large carbon deposits on spark plugs, piiston rings and otehr component, by decreasing considerably the life of the engines.

Hence, the mere inspection of the tailpipe exhaust is today a view of the past millennium, if not motivated by equivocal commercial, political or academic interests. The sole approach environmentally acceptable today is *the study of the global environmental profile pertaining to fuels, that including the environmental pollution causes by the production, storage, transportation, and combustion.*

In closing, equivocal commercial, political and academic interests should be made aware that, following the success of the lawsuits against the tobacco industry, environmental groups in Berlin, Washington, Tokyo and other cities are apparently preparing lawsuits for trillion dollars punitive compensation against any large scale producer or user of polluting fuel. Therefore, it appears that the best way to confront supporters of hydrogen, ethanol, biofuels and other highly polluting fuels is that via a judicial process. After all, we should never forget that the future of mankind is at stake on these issues.

11.1.4 Basic Needs for the Survival of Mankind

The most basic need for the very survival of our contemporary societies in view of the disproportionate use of fossil fuels and the increasingly cataclysmic climactic events caused by the pollutants in their combustion exhaust can be summarized as follows:

(1) **Develop "new" processes for the nonpolluting, large scale production of electricity,** that is, processes beyond the now exhausted pre-

dictive capacities of conventional doctrines. Whether for electrolysis or other uses, electricity is and will remain the basic source of energy for the synthesis of new fuels. At the same time, hydro, thermal and wind sources of energy, even though very valuable, are dramatically insufficient to fulfill the present, let alone the future needs of clean energy. Nuclear power plants have been severely damaged by governmental obstructions, both in the U.S.A., Europe and other countries, against new processes for the stimulated decay of radioactive nuclear waste by the power plants themselves, in favor of a politically motivated storage of the radioactive waste in depositories so much opposed by local societies, thus preventing nuclear power to be a viable alternative.[7] Additionally, both the "hot fusion' and the "cold fusion" have failed to achieve industrially viable results to date, and none is in sight at this writing. The need for basically "new" clean sources of electricity is then beyond scientific doubt. This need is addressed in the next chapter because, as we shall see, the content of this chapter is a necessary pre-requisite.

(2) **Build a large number of large reactors for the large scale removal and recycling of the excess CO_2 in our atmosphere.** The containment of future production of CO_2 is basically insufficient because the existing amount in our atmosphere is sufficient to cause increasingly cataclysmic climactic events. Therefore, another major problem facing mankind is the removal of the CO_2 already existing in our atmosphere. This problem is addressed in the next subsection.

(3) **it Develop "new" fuels that are not derivable from crude oil and are capable of achieving full combustion,** that is, fuels structurally different than all known fuels due to their highly polluting character. The production of new fuels not derivable from crude oil is necessary in view of the exploding demand for fossil fuels expected from the construction in China of $500,000,000$ new cars and other factors, as well as the expected end of the petroleum reserves. This need is addressed in this chapter. the need for fuels with a new chemical structure is set by the impossibility for all available fuels, those with conventional molecular structure, to achieve full combustion. This need is addressed in this chapter.

11.1.5 Removing Carbon Dioxide from our Atmosphere and Car Exhaust

Nowadays, we have in our atmosphere a large excess CO_2 estimated to be from 100 to 300 times the CO_2 percentage existing at the beginning of

[7]For governmental politics opposing new methods for the stimulated decay of radioactive nuclear waste, one may visit the web site http://www.nuclearwasterecycling.com

the 20-th century, which excess is responsible for the "global worming" and consequential devastating climactic events.

A typical illustration is given by the Gulf of Mexico whose waters have reached in August, 2005, such a high temperature (95^oF) to kill dolphins and other marine species. This sad environmental problem is due to the fact that CO_2 is heavier than any other gas in the atmosphere, thus forming a layer on the top of the water that traps Sun light, with the resulting increase of water temperature.

All predictions establish that the current rate of CO_2 release in our atmosphere will eventually cause the water of the Gulf of Mexico to reach in the summer a steaming state, with consequential impossibility to sustain life, the only debatable aspect being the time of these lethal conditions in the absence of corrective action.

The *only* possible, rational solution of the problem is the *removal of* CO_2 *from our atmosphere via molecular filtration or other methods and its processing into noncontaminant gases.*

Other solutions, such as the pumping of CO_2 underground jointly with petroleum production as adopted by the petroleum company StatOil in Norway and other companies, are definitely unacceptable on environmental grounds because of the risk that the green house gas may resurface at some future time with catastrophic consequences. In fact, being a gas under very high pressure when under grounds, it is only a question of time for the CO_2 to find its way back to the surface.[8]

The technology for the molecular separation of CO_2 from our atmosphere is old and well established, thus requiring the construction of equipment in large sizes and numbers for installation in a sufficient number of location to yield appreciable results.

To understand the dimension for the sole Gulf of Mexico there is the need of a number of recyclers located in barges and/or in coastal area capable of processing at least 10 millions metric tons of air per day.

After clarifying that the technology for the removal of CO_2 from our atmosphere is fully available (only the political will is still absent at this writing in virtually all developed nations), the next issue is the selection of the appropriate processing of CO_2 into environmentally acceptable species.

According to extensive research in the problem conducted by the author and his associates, *the most efficient method for recycling* CO_2 *is that based on flowing the gas at high pressure through an electric arc* [5]. In fact, the arc decomposes the CO_2 molecule into carbon precipitates and breathable oxygen

[8]In reality, petroleum companies pump CO_2 underground to increase the pressure of release of near-by crude oil, and certainly not to help the environment.

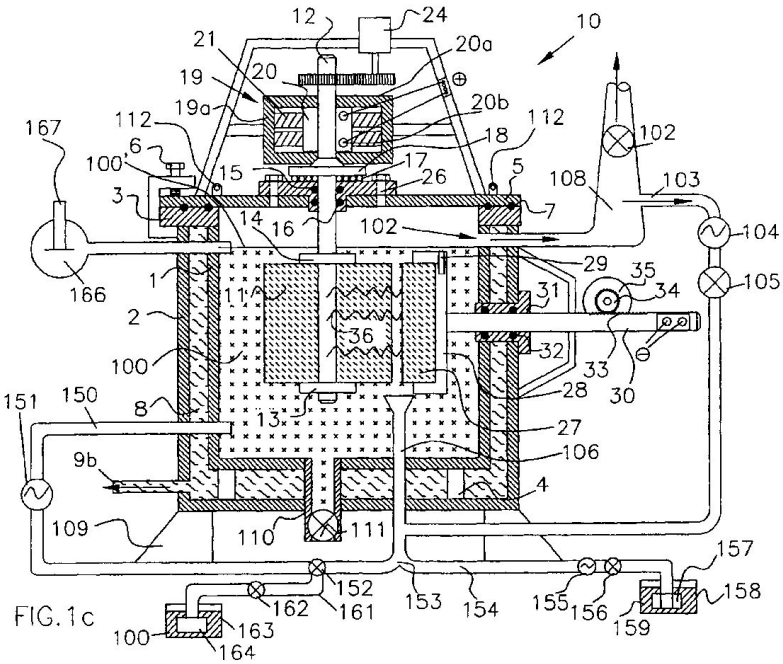

Figure 11.5. A schematic view of a preferred embodymnent for the recycling of CO_2 into C and O_2 via the use the PlasmaArcFlow technology of Refs.[5]. the main principle is that, following its separation from the atmosphere, the most efficient mean for breaking down the CO_2 bond is, by far, the electric arc..

that can be released into the atmosphere to correct the oxygen depletion caused by fossil fuels.

Needless to say, these "CO_2 Recycling Plants can additionally remove from the environment circinogenic and other toxic pollutants via the use of the same technology of molecular sep[aration and processing.

Numerous other processes are also expected to be possible for the removal of the CO_2 excess from our atmosphere, and their indication to the author for quotation in possible future editions of this monograph would be appreciated.

Whatever environmentally acceptable solution is suggested, the main needs for serious and responsible governments is to stop the debate and discussions and initiate action *now,* when the economies of developed countries are still somewhat solid, because, later on, increasingly cataclysmic climatic events combined with increases in fossil fuel costs may eventually cause the collapse

of said economies, at which points nations will not have the immense financial resources needed for the removal of the excess CO_2 in our planet.

IIn closing, the reader should be aware that current technologies permit the large scale production, thus at low cost, of special CO_2 absorbing cartridges that can be houses in conventional car exhaust pipes and replaced periodically. the removal of CO_2 is done via special chemicals or other means.Additional possibilities are given by passing the exhaust through a series of arcs for the recycling of CO_2 into C and breathable O_2.

In short, in this chapter we show that current technologies do indeed permit the production of environmentally acceptable fuels, while in the next chapter we shall show that other technologies permit new clean energies. Mankind is exposed to increasing cataclysmic climactic events not only because of the *lack of political will* for any action that could be considered minimally responsible at this writing (fall 2005) in any and all so-called developed countries, but also because the political will continues to serve the oil cartel, as demonstrated by the political support of hydrogen, of course, produced from fossil fuels, despite having extremely serious environmental problems identified in the preceding subsection

11.2 THE NEW CHEMICAL SPECIES OF MAGNECULES

11.2.1 Introduction

The origin of the alarming environmental problems increasingly afflicting our planet are not due to fossil fuels per se, but rather to the strength of their conventional valence bond, since that strength has prohibited the achievement of full combustion during the past one hundred years of efforts. In fact, most of the atmospheric pollution caused by fossil fuels is due to "chunks" (such as dimers) of uncombusted fuel that are carcinogenic primarily because consisting of incomplete molecules.

In view of the above occurrence, this author proposed in Ref. [1] of 1998 a new chemical species that, by central assumption, is based on a bond much *weaker* than that of valence bonds so as to permit full combustion. For certain technical reasons indicated below the new species was submitted under the name of *magnecules* in order to distinguish the species from the conventional "molecules," and the new species is known today as *Santilli magnecules.*

In this chapter we report industrial research with the investment of several millions of dollars from private corporations that followed the proposal of Santilli magnecules [1], and resulted in the identification of three distinct new gaseous fuels with the novel magnecular structure, all achieving the original objective of full combustion without toxic substances in the exhaust. Several

other substances with magnecular structure are under study and they will be reported in specialized technical journals.

This chapter is organized as follows. We shall first present the hypothesis of Santilli magnecules; we shall then study the industrial methods needed for their production, the features to be detected experimentally, and the analytic equipment needed for the detection of the new species. We shall then study three distinct gaseous fuels with magnecular structure and outline their rather vast experimental verifications. We shall finally study the experimental evidence for magnecular structures in liquids and other related aspects.

To begin, let us recall that the only chemical species with a clearly identified bond which was known prior to the advent of hadronic chemistry was that of *molecules* and related *valence bonds*, whose identification dates back to the 19-th century, thanks to the work by Avogadro (1811), Canizzaro (1858), and several others, following the achievement of scientific measurements of atomic weights.

Various candidates for possible additional chemical species are also known, such as the delocalized electron bonds. However, none of them possess a clearly identified attractive force clearly distinct from the valence.

Also, various molecular clusters have been studied in more recent times, although they either are unstable or miss a precise identification of their internal attractive bond.

An example of unstable molecular cluster occurs when the internal bond is due to an *electric polarization* of atomic structures, that is, a deformation from a spherical charge distribution without a net electric charge to an ellipsoidal distribution in which there is the predominance of one electric charge at one end and the opposite charge at the other end, thus permitting atoms to attract each other with opposite electric polarities. The instability of these clusters then follows from the known property that the smallest perturbation causes nuclei and peripheral electrons to reacquire their natural configuration, with the consequential loss of the polarization and related attractive bond.

An example of molecular clusters without a clear identification of their internal attractive bond is given by *ionic clusters*. In fact, ionized molecules have the *same positive charge* and, therefore, they *repel*, rather than attract, each other. As a result, not only the internal attractive bond of ionic clusters is basically unknown at this writing, but, when identified, it must be so strong as to overcome the repulsive force among the ions constituting the clusters.

In 1998, R. M. Santilli submitted in paper [1] (and then studied in details in monograph [2]) the hypothesis of a new type of stable clusters composed of molecules, dimers and atoms under a new, clearly identified, attractive internal bond which permits their industrial and practical use. The new clusters were called **magnecules** (patents pending) because of the dominance of magnetic effects in their formation, as well as for pragmatic needs of differentiations

with the ordinary molecules, with the understanding that a technically more appropriate name would be *electromagnecules*.

The following terminology will be used herein:

1) The word *atom* is used in its conventional meaning as denoting a stable atomic structure, such as a hydrogen, carbon or oxygen, irrespective of whether the atom is ionized or not and paramagnetic or not.

2) The word *dimer* is used to denote part of a molecule under a valance bond, such as H–O, H–C, *etc.*, irrespective of whether the dimer is ionized or not, and whether it belongs to a paramagnetic molecule or not;

3) The word *molecule* is used in its internationally known meaning of denoting stable clusters of atoms under conventional, valence, electron bonds, such as H_2, H_2O, C_2H_2, *etc.*, irrespective of whether the molecule is ionized or not, and paramagnetic or not;

4) The word *magnecule* is used to denote stable clusters of two or more molecules, and/or dimers and/or atoms and any combination thereof formed by a new internal attractive bond of primarily magnetic type identified in detail in this chapter; the word *magnecular* will be used in reference to substances with the structure or features of magnecules;

5) The words *chemical species* are used to denote an essentially pure population of stable clusters with the same internal bond, thus implying the conventional chemical species of molecules as well as that of magnecules, under the condition that each species admits an ignorable presence of the other species.

In this chapter we study the theoretical prediction permitted by hadronic mechanics and chemistry of the new chemical species of magnecules and its experimental verifications, which were apparently presented for the first time by Santilli in memoir [1] of 1998.

11.2.2 The Hypothesis of Santilli Magnecules

The main hypothesis, studied in details in the rest of this Chapter, can be formulated as follows:

DEFINITION 11.2.1 [1,2] (patented and international patents pending [5]): **Santilli magnecules** *in gases, liquids, and solids consist of stable clusters composed of conventional molecules, and/or dimers, and/or individual atoms bonded together by opposing magnetic polarities of toroidal polarizations of the orbits of at least the peripheral atomic electrons when exposed to sufficiently strong external magnetic fields, as well as the polarization of the intrinsic magnetic moments of nuclei and electrons. A population of magnecules constitutes a chemical species when essentially pure, i.e., when molecules or other species are contained in very small percentages in a directly identifiable form. Santilli magnecules are characterized by, or can be identified via the following main features:*

I) Magnecules primarily exist at large atomic weights where not expected, for instance, at atomic weights which are ten times or more the maximal atomic weight of conventional molecular constituents;

II) Magnecules are characterized by large peaks in macroscopic percentages in mass spectrography, which peaks remain unidentified following a search among all existing molecules;

III) Said peaks admit no currently detectable infrared signature for gases and no ultraviolet signature for liquids other than those of the conventional molecules and/or dimers constituting the magnecule;

IV) Said infrared and ultraviolet signatures are generally altered (a feature called "mutation") with respect to the conventional versions, thus indicating an alteration (called infrared or ultraviolet mutation) of the conventional structure of dimers generally occurring with additional peaks in the infrared or ultraviolet signatures not existing in conventional configurations;

V) Magnecules have an anomalous adhesion to other substances, which results in backgrounds (blank) following spectrographic tests which are often similar to the original scans, as well as implying the clogging of small feeding lines with consequential lack of admission into analytic instruments of the most important magnecules to be detected;

VI) Magnecules can break down into fragments under sufficiently energetic collisions, with subsequent recombination with other fragments and/or conventional molecules, resulting in variations in time of spectrographic peaks (called time mutations of magnecular weights);

VII) Magnecules can accrue or lose during collision individual atoms, dimers or molecules;

VIII) Magnecules have an anomalous penetration through other substances indicating a reduction of the average size of conventional molecules as expected under magnetic polarizations;

IX) Gas magnecules have an anomalous solution in liquids due to new magnetic bonds between gas and liquid molecules caused by magnetic induction;

X) Magnecules can be formed by molecules of liquids which are not necessarily solvable in each other;

XI) Magnecules have anomalous average atomic weights in the sense that they are bigger than that of any molecular constituent and any of their combinations;

XII) A gas with magnecular structure does not follow the perfect gas law because the number of its constituents (Avogadro number), or, equivalently, its average atomic weight, varies with a sufficient variation of the pressure;

XIII) Substances with magnecular structure have anomalous physical characteristics, such as anomalous specific density, viscosity, surface tension, etc., as compared to the characteristics of the conventional molecular constituents;

XIV) Magnecules release in thermochemical reactions more energy than that released by the same reactions among unpolarized molecular constituents;

XV) All the above characteristic features disappear when the magnecules are brought to a sufficiently high temperature, which varies from species to species, called Curie Magnecular Temperature; in particular, combustion eliminates all magnetic anomalies resulting in an exhaust without magnecular features.

Magnecules are also called:

A) **elementary** *when only composed of two molecules*;

B) **magneplexes** *when entirely composed of several identical molecules*;

C) **magneclusters** *when composed of several different molecules.*

Finally, magnecules are called:

i) **isomagnecules** *when having all single-valued characteristics and being reversible in time, namely, when they are characterized by isochemistry (see Chapter 9);*

ii) **genomagnecules** *when having all single-valued characteristics and being irreversible in time, namely, when they are characterized by genochemistry;* and

iii) **hypermagnecules** *when having at least one multi-valued characteristic and being irreversible in time, namely, when they are characterized by hyperchemistry.*

The primary objective of this chapter is, first, to study the characteristic features of magnecules from a theoretical viewpoint, and then present independent experimental verifications for each feature.

All magnecules studied in this chapter are, strictly speaking, isomagnecules because single valued and reversible. The reader should be aware that all correct calculations implying single-valued irreversible chemical processes, such as chemical reactions in general, should be done with genomagnecules. Finally, all biological; structure will inevitably require the use of hypermagnecules as illustrated in Chapter 5.

The reader should keep in mind that *magnegas*, the new, clean combustible gas developed by the author [1,2,5], of Largo, Florida, has precisely a magnecular structure from which it derives its name. Nevertheless, we shall identify in this chapter other gases, liquids and solids with a magnecular structure.

By denoting the conventional valence bond with the symbol "–" and the new magnetic bond with the symbol "×", examples of *elementary magnecules* in gases and liquids are respectively given by

$$\{\mathrm{H}-\mathrm{H}\} \times \{\mathrm{H}-\mathrm{H}\}, \quad \{\mathrm{O}-\mathrm{O}\} \times \{\mathrm{O}-\mathrm{C}-\mathrm{O}\}, \ \textit{etc.}, \tag{11.2.1a}$$

$$\{\mathrm{C}_{15}-\mathrm{H}_{20}-\mathrm{O}\} \times \{\mathrm{C}_{15}-\mathrm{H}_{20}-\mathrm{O}\}, \ \textit{etc.}; \tag{8.1b}$$

examples of *magneplexes* in gases and liquids are respectively given by

$$\{\mathrm{H}-\mathrm{H}\} \times \{\mathrm{H}-\mathrm{H}\} \times \{\mathrm{H}-\mathrm{H}\} \times \ldots, \ \textit{etc.}, \tag{11.2.2a}$$

$$\{\mathrm{H}-\mathrm{O}-\mathrm{H}\} \times \{\mathrm{H}-\mathrm{O}-\mathrm{H}\} \times \ldots, \ \textit{etc.}; \tag{11.2.2b}$$

and examples of *magneclusters* are given by

$$\{\mathrm{H}-\mathrm{H}\} \times \{\mathrm{C}-\mathrm{O}\} \times \{\mathrm{O}-\mathrm{C}-\mathrm{O}\} \times \{\mathrm{C}=\mathrm{O}\} \times \ldots, \ \textit{etc.}, \tag{11.2.3a}$$

$$\{\mathrm{C}_{13}-\mathrm{H}_{18}-\mathrm{O}\} \times \{\mathrm{C}_{14}-\mathrm{H}_{12}-\mathrm{O}_3\} \times \{\mathrm{C}_{15}-\mathrm{H}_{20}-\mathrm{O}\} \times \ldots, \ \textit{etc.} \tag{11.2.3b}$$

A generic representation of a gas magnecules requires the presence of individual atoms and dimers, such as:

$$\{\mathrm{H}-\mathrm{H}\} \times \{\mathrm{C}-\mathrm{O}\} \times \mathrm{H} \times \{\mathrm{H}-\mathrm{O}-\mathrm{H}\} \times \mathrm{C} \times \{\mathrm{H}-\mathrm{O}\} \times \ldots, \ \textit{etc.} \tag{11.2.4}$$

One of the most important features of magnecules is their anomalous release of energy in thermochemical reactions (Feature XIV of Definition 8.2.1), in view of its evident importance for the industrial development of new clean fuels such as magnegas (Sects. 7.10 and 7.11).

As we shall see in detail later on, this feature is crucially dependent on the existence within the magnecules of individual atoms, such as H, C and O, and/or individual unpaired dimers, such as H–O and H–C. In fact, at the breakdown of the magnecules due to combustion, these individual atoms and dimers coupled themselves into conventional molecules via known exothermic reactions such as

$$\begin{gathered} \mathrm{H}+\mathrm{H} \rightarrow \mathrm{H}_2 + 105 \text{ Kcal/mole}, \\ \mathrm{C}+\mathrm{O} \rightarrow \mathrm{CO} + 255 \text{ Kcal/mole}, \\ \mathrm{H}-\mathrm{O}+\mathrm{H} \rightarrow \mathrm{H}_2\mathrm{O} + 28 \text{ Kcal/mole}, \ \textit{etc.}, \end{gathered} \tag{11.2.5}$$

with consequential release during combustion of a large amount of energy that does not exist in fuels with a conventional molecular structure.

In reading this chapter, the reader should keep in mind that, in view of the above important industrial, consumer and environmental implications, a primary emphasis of the presentation is the study of magnecules with the largest possible number of *unpaired atoms and dimers*, rather than molecules.

In inspecting the above representation of magnecules, the reader should also keep in mind that their linear formulation in a row is used mainly for practical purposes. In fact, the correct formulation should be via *columns*, rather than rows, since the bond occurs between one atom of a given molecule and an atom of another molecule, as we shall see in detail later on.

11.2.3 The Five Force Fields Existing in Polarized Atoms

The attractive bond responsible for the creation of magnecules originates within the structure of individual *atoms*. Therefore, it is recommendable to initiate our study via the identification of all force fields existing in a conventional atomic structure.

The sole fields in the atomic structure studied by chemists prior to Ref. [1] were the intrinsic electric and magnetic fields of electrons and nuclei (see Fig. 11.6). It was proved a century ago that these fields can only produce *valence bonds*, thus explaining the reason why molecules were the only form of atomic clustering with a clear bond admitted by chemistry until recently.

Santilli's [1] main contribution has been the identification of a *new force field in the atomic structure*, which is sufficiently strong to permit a new chemical species.

Since the inception of atomic physics, the electron of the hydrogen atom (but not necessarily peripheral electrons of more complex atoms) has been assumed to have a spherical distribution, which is indeed the case for isolated and unperturbed atomic structures (see also Fig. 811.6).

However, electrons are charged particles, and all charges rotating in a planar orbit create a magnetic field in the direction perpendicular to the orbital plane, and such to exhibit the North polarity in the semi-space seeing a counter-clockwise rotation (see Fig. q11.6..B).

A main point of Ref. [1] is that the distribution in space of electron orbits is altered by sufficiently strong external magnetic fields. In particular, the latter cause the transition from the conventional spherical distribution to a new distribution with the same cylindrical symmetry of the external field, and such to exhibit magnetic polarities opposite to the external ones (Fig. 11.6.C).

Therefore, the magnetic fields of atoms *are not* solely given by the intrinsic magnetic fields of the peripheral electrons and of nuclei because, under the application of a sufficiently strong external magnetic field, atoms exhibit the additional magnetic moment caused by a polarization of the electron orbits. This third magnetic field was ignored by chemists until 1998 (although not by physicists) because nonexistent in a conventional atomic state.

As a matter of fact, it should be recalled that *orbits are naturally planar in nature, as established by planetary orbits, and they acquire a spherical distribution in atoms because of various quantum effects, e.g., uncertainties.* Therefore, in the absence of these, all atoms would naturally exhibit *five* force fields and not only the four fields currently assumed in chemistry.

On historical grounds it should be noted that theoretical and experimental studies in physics of the hydrogen atom subjected to an external (homogeneous) magnetic field date to Schrödinger's times.

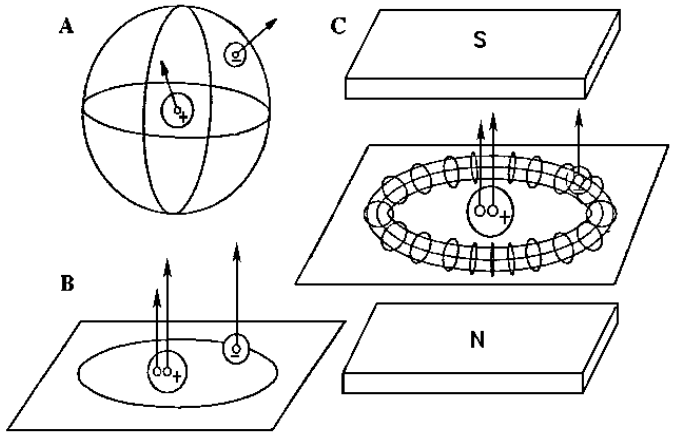

Figure 11.6. A schematic view of the force fields existing in the hydrogen atom. Fig. 11.6.A depicts an isolated hydrogen atom in its conventional spherical configuration when at absolute zero degree temperature, in which the sole force fields are given by the electric charges of the electron and of the proton, as well as by the intrinsic magnetic moments of the same particles. Fig. 11.6.B depicts the same hydrogen atom in which the orbit of the peripheral electron is polarized into a plane. In this case there is the emergence of a fifth field, the magnetic dipole moment caused by the rotation of the electron in its planar orbit. Fig. 11.6.C depicts the same hydrogen atom under an external magnetic field which causes the transition from the spherical distribution of the peripheral electron as in Fig. 11.6.A to a new distribution with the same cylindrical symmetry as that of the external field, and such to offer magnetic polarities opposite to the external ones. In the latter case, the polarization generally occurs within a toroid, and reaches the perfectly planar configuration of Fig. 11.6.B only at absolute zero degree temperature or under extremely strong magnetic fields.

11.2.4 Numerical Value of Magnecular Bonds

In the preceding section we have noted that a sufficiently strong external magnetic field polarizes the orbits of peripheral atomic electrons resulting in a magnetic field which does not exist in a conventional spherical distribution. Needless to say, the same external magnetic fields also polarize the intrinsic magnetic moments of the peripheral electrons and of nuclei, resulting into *three net magnetic polarities* available in an *atomic* structure for a new bond.

When considering molecules, the situation is different because valence electrons are bonded in singlet couplings to verify Pauli's exclusion principle, as per our hypothesis of the *isoelectronium* of Chapter 9. As a result, their net magnetic polarities can be assumed in first approximation as being null. In this case, only *two* magnetic polarities are available for new bonds, namely, the magnetic field created by the rotation of paired valence electrons in a polarized orbit plus the intrinsic magnetic field of nuclei.

It should be noted that the above results persist when the inter-electron distance of the isoelectronium assumes orbital values. In this case the total intrinsic magnetic moment of the two valence electrons is also approximately null in average due to the persistence of antiparallel spins and, therefore, antiparallel magnetic moments, in which absence there would be a violation of Pauli's exclusion principle.

The calculation of these *polarized magnetic moments at absolute zero degree temperature* is elementary [1]. By using rationalized units, the magnetic moment $M_{e\text{-orb}}$. of a polarized orbit of one atomic electron is given by the general quantum mechanical law:

$$M_{\text{e-orb.}} = \frac{q}{2m} L\mu, \tag{11.2.6}$$

where L is the angular momentum, μ is the rationalized unit of the magnetic moment of the electron, $q = -e$, and $m = m_e$.

It is easy to see that *the magnetic moment of the polarized orbit of the isoelectronium with characteristics (4.25) coincides with that of one individual electron*. This is due to the fact that, in this case, in Eq. (11.2.6) the charge in the numerator assumes a double value $q = -2e$, while the mass in the denominator also assumes a double value, $m = 2m_e$, thus leaving value (8.6) unchanged.

By plotting the various numerical values for the ground state of the hydrogen atom, one obtains:

$$M_{\text{e-orb.}} = M_{\text{isoe-orb.}} = 1,859.59\mu. \tag{11.2.7}$$

By recalling that in the assumed units the proton has the magnetic moment 1.4107 μ, we have the value [1]:

$$\frac{M_{\text{e-orb.}}}{M_{\text{p-intr.}}} = \frac{1,856.9590}{1.4107} = 1,316.33, \tag{11.2.8}$$

namely, *the magnetic moment created by the orbiting in a plane of the electron in the hydrogen atom is 1,316 times bigger than the intrinsic magnetic moment of the nucleus*, thus being sufficiently strong to create a bond.

It is evident that the *polarized magnetic moments at ordinary temperature* are smaller than those at absolute zero degrees temperature. This is due to the fact that, at ordinary temperature, the perfect polarization of the orbit in a plane is no longer possible. In this case the polarization occurs in a *toroid*, as illustrated in Fig. 8.2, whose sectional area depends on the intensity of the external field.

As an illustrative example, under an external magnetic field of 10 Tesla, an *isolated hydrogen atom* has a total magnetic field of the following order of magnitude:

$$M_{\text{H-tot.}} = M_{\text{p-intr.}} + M_{\text{e-intr.}} + M_{\text{e-orb.}} \approx 3,000\mu, \tag{11.2.9}$$

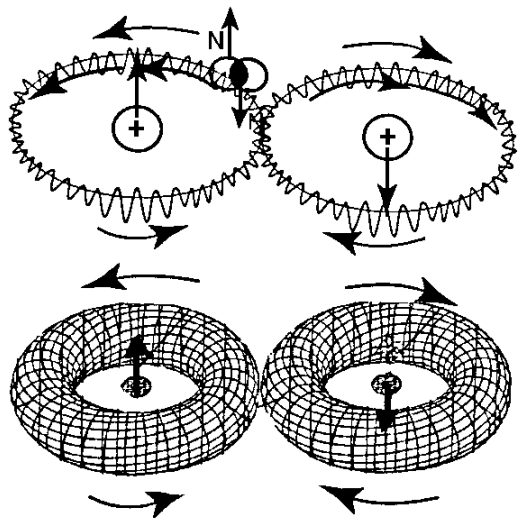

Figure 11.7. A schematic view of the magnetic fields of the isochemical model of the hydrogen molecule with isoelectronium assumed to be a stable quasi-particle. The top view represents the molecule at absolute zero degree temperature with polarization of the orbit in a plane, while the bottom view represents the molecule at ordinary temperature with a polarization of the orbit within a toroid. In both cases there is the disappearance of the *total intrinsic* magnetic moments of the electrons because they are coupled in the isoelectronium with antiparallel spin and magnetic moments due to Pauli's exclusion principle. The *lack* of contribution of the intrinsic magnetic moments of the electrons persists even when the isoelectronium has dimension much bigger than 1 fm, because the antiparallel character of the spins and magnetic moments persists, resulting in an average null total intrinsic magnetic moment of the electrons. Therefore, the biggest magnetic moment of the hydrogen molecule which can be obtained via polarizations is that of the electrons *orbits*. Note, as recalled in Sect. 9.2, the *oo*-shaped (also called figure eight) configuration has been recently proved in mathematics to be one of the most stable solutions of the N-body problem.

while the same hydrogen atom under the same conditions, when a component of a *hydrogen molecule* has the smaller value

$$M_{\text{H}_2\text{-tot.}} = M_{\text{p-intr.}} + M_{\text{isoe-orb.}} \approx 1,500\mu, \tag{11.2.10}$$

again, because of the absence of the rather large contribution from the intrinsic magnetic moment of the electrons, while the orbital contribution remains unchanged.

The above feature is particularly important for the study of magnecules and their applications because it establishes the theoretical foundations for the presence of isolated atoms in the structure of magnecules since *the magnetic*

bonds of isolated atoms can be at least twice stronger than those of the same atoms when part of a molecule.

An accurate independent verification of the above calculations was conducted by M.G. Kucherenko and A.K. Aringazin [3], who obtained the following value via the use of alternative models,

$$\frac{M_{\text{e-orb.}}}{M_{\text{p-intr.}}} \approx 1,315\mu. \tag{11.2.11}$$

Needless to say, the quantized value of the angular momentum of the ground state of the conventional (unpolarized) hydrogen atom is null, $L = 0$, thus implying a null magnetic moment, $M = 0$. This occurrence confirms the well known feature that the magnetic moment of the orbit of the peripheral electron of a conventional (unpolarized) hydrogen atom is null.

Consequently, expressions (8.6)-(8.11) should be considered under a number of clarifications. First, said expressions refer to *the orbit of the peripheral electron under an external magnetic field* which implies an evident alteration of the value of the magnetic moment. Note that this external magnetic field can be either that of an electric discharge, as in the PlasmaArcFlow reactors, or that of another polarized hydrogen atom, as in a magnecule. This occurrence confirms a main aspect of the new chemical species of magnecules, namely, that the plane polarization of the orbits of the peripheral atomic electron is stable if and only if said polarization is coupled to another because, if isolated, the plane polarization is instantly lost due to rotations with recover the conventional spheroidal distribution of the orbits.

Moreover, expressions (11.2.6)-(11.2.11) refer to the angular momentum of the orbit of the peripheral electron *polarized in a plane*, rather than that with a spherical distribution as in the conventional ground state of the hydrogen atom. The latter condition, alone, is sufficient to provide a non-null quantized orbital magnetic moment.

Finally, the value $L = 1$ needed for expressions (11.2.6)-(11.2.11) can be obtained via *the direct quantization of the plane polarization of a classical orbit*. These aspects have been studied in detail by Kucherenko and Aringazin [2] and Aringazin [8] (see Appendix 8.A). These studies clarify a rather intriguing property mostly ignored throughout the 20-th century according to which, contrary to popular beliefs, *the quantized angular momentum of the ground state of the hydrogen atom is not necessarily zero, because its value depends on possible external fields*.

It is important to note that the magnetic polarizations herein considered are *physical notions*, thus being best expressed and understood via *actual orbits* as treated above rather than *chemical orbitals*. This is due to the fact that *orbits are physical entities* actually existing in nature, and schematically represented in the figures with standing waves, in semiclassical approximation.

By contrasts, *orbitals are purely mathematical notions* given by probability density. As a result, magnetic fields can be more clearly associated with orbits rather than with orbitals.

Despite the above differences, it should be stressed that, magnetic polarizations can also be derived via the *orbitals* of conventional use in chemistry. For example, consider the description of an isolated atom via the conventional Schrödinger equation

$$H|\psi\rangle = \left(\frac{p^2}{2m} + V\right)|\psi\rangle = E|\psi\rangle, \tag{11.2.12}$$

where $|\psi\rangle$ is a state in a Hilbert space. Orbitals are expressed in terms of the probability density $|\langle\psi| \times |\psi\rangle|$. The probability density of the electron of a hydrogen atom has a spherical distribution, namely, the electron of an isolated hydrogen atom can be found at a given distance from the nucleus with the same probability in any direction in space.

Assume now that the same hydrogen atom is exposed to a strong external homogeneous and static magnetic field B. This case requires the new Schrödinger equation,

$$\left((p - \frac{e}{c}A)^2/2m + V\right)|\psi'\rangle = E'|\psi'\rangle, \tag{11.2.13}$$

where A is vector-potential of the magnetic field B. It is easy to prove that, in this case, the new probability density $|\langle\psi'| \times |\psi'\rangle|$ possesses a *cylindrical symmetry* precisely of the type indicated above, thus confirming the results obtained on physical grounds. A similar confirmation can be obtained via the use of Dirac's equation or other chemical methods.

An accurate recent review of the Schrödinger equation for the hydrogen atom under external magnetic fields is that by A.K. Aringazin [8], which study confirms the toroidal configuration of the electron orbits which is at the foundation of the new chemical species of magnecules. A review of Aringazin studies is presented in Appendix 11 .A. As one can see, under an external, strong, homogeneous, and constant magnetic fields of the order of 10^{13} Gauss $= 10^7$ Tesla, the solutions of Schrödinger equation of type (8.13) imply the restriction of the electron orbits within a single, small-size toroidal configuration, while the excited states are represented by the double-splitted toroidal configuration due to parity.

Intriguingly, the binding energy of the ground state of the H atom is much higher than that in the absence of an external magnetic field, by therefore confirming another important feature of the new chemical species of magnecules, that of permitting new means of storing energy within conventional molecules and atoms, as discussed later on in this chapter.

For magnetic fields of the order of 10^9 Gauss, spherical symmetry begins to compete with the toroidal symmetry, and for magnetic fields of the order of

10^5 Gauss or less, spherical symmetry is almost completely restored by leaving only ordinary Zeeman effects. This latter result confirms that the creation of the new chemical species of magnecules in gases as per Definition 8.2.1 requires very strong magnetic fields. The situation for liquids is different, as shown later on also in this chapter.

The magnetic polarization of atoms larger than hydrogen is easily derived from the above calculations. Consider, for example, the magnetic polarization of an isolated atom of oxygen. For simplicity, assume that an external magnetic field of 10 Tesla polarizes only the two peripheral valence electrons of the oxygen. Accordingly, its total polarized magnetic field of orbital type is of the order of twice value (8.9), *i.e.*, about 6,000 μ. However, when the same oxygen atom is bonded into the water or other molecules, the maximal polarized magnetic moment is about half the preceding value.

Note the dominance of the magnetic fields due to polarized electron *orbits* over the intrinsic *nuclear* magnetic fields. This is due not only to the fact that the former are 1,316 times the latter, but also to the fact that nuclei are at a relative great distance from peripheral electrons, thus providing a contribution to the bond even smaller than that indicated. This feature explains the essential novelty of magnecules with respect to established magnetic technologies, such as that based on *nuclear magnetic resonances.*

Note also that a main mechanism of polarization is dependent on an external magnetic field and the force actually providing the bond is of magnetic type. Nevertheless, the ultimate origin is that of charges rotating in an atomic orbit. This illustrates that, as indicated in Sect. 11.2.1, the name "magnecules" was suggested on the basis of the predominant magnetic origin, as well as for the pragmatic differentiation with molecules without using a long sentence, although a technically more appropriate name would be "electromagnecules."

Needless to say, the polarization of the orbits is not necessarily restricted to valence electrons because the polarization does not affect the quantum numbers of any given orbit, thus applying for all atomic electrons, including those of complete inner shells, of course, under a sufficiently strong external field. As a consequence, *the intensity of the magnetic polarization generally increases with the number of atomic electrons*, namely, the bigger is the atom, the bigger is, in general, its magnetic bond in a magnecule.

Ionizations do not affect the *existence* of magnetic polarizations, and they may at best affect their *intensity*. An ionized hydrogen atom is a naked proton, which acquires a polarization of the direction of its magnetic dipole moment when exposed to an external magnetic field. Therefore, an ionized hydrogen atom can indeed bond magnetically to other polarized structures. Similarly, when oxygen is ionized by the removal of one of its peripheral electrons, its remaining electrons are unchanged. Consequently, when exposed to a strong magnetic field, such an ionized oxygen atom acquires a magnetic polarization

which is similar to that of an unpolarized oxygen atom, except that it lacks the contribution from the missing electron. Ionized molecules or dimers behave along similar lines. Accordingly, the issue as to whether individual atoms, dimers or molecules are ionized or not will not be addressed hereon.

The magnetic polarizations here considered are also independent as to whether the substance considered is paramagnetic or not. This is evidently due to the fact that the polarization deals with the individual orbits of individual peripheral electrons, irrespective of whether paired or unpaired, belonging to a saturate shell or not. Therefore, the issue as to whether a given substance is paramagnetic or not will be ignored hereon.

Similarly, the polarizations here considered do not require molecules to have a net total magnetic polarity, which would be possible only for paramagnetic substances, again, because they act on individual orbits of individual atomic electrons.

We should also indicate that another verification of our isochemical model of molecular structures is the resolution of the inconsistency of the conventional model in predicting that all substances are paramagnetic, as illustrated in Figs. 1.4 and 1.5.

Recall that the atoms preserve their individualities in the conventional molecular model, thus implying the *individual* acquisition of a magnetic polarization under an external field, with consequential net total magnetic polarities for all molecules which is in dramatic disagreement with experimental; evidence.

By comparison, in the isochemical molecular model the valence electrons are actually bonded to each other, with consequential *oo*-shaped orbit around the respective nuclei. This implies that the rotational directions of the *o*-branches are opposite to each other. In turn, this implies that magnetic polarizations are also opposite to each other, resulting in the lack of a net magnetic polarity under an external field, in agreement with nature (see Figs. 4.5 and 8.3 for more details).

11.2.5 Production of Magnecules in Gases, Liquids and Solids

At its simplest, the creation of magnecules can be understood via the old method of magnetization of a paramagnetic metal by induction. Consider a paramagnetic metal which, initially, has no magnetic field. When exposed to a constant external magnetic field, the paramagnetic metal acquires a permanent magnetic field that can only be destroyed at a sufficiently high temperature varying from metal to metal and called the *Curie Temperature*.

The mechanism of the above magnetization is well known. In its natural unperturbed state, the peripheral atomic electrons of a paramagnetic metal have a space distribution that results in the lack of a total magnetic field.

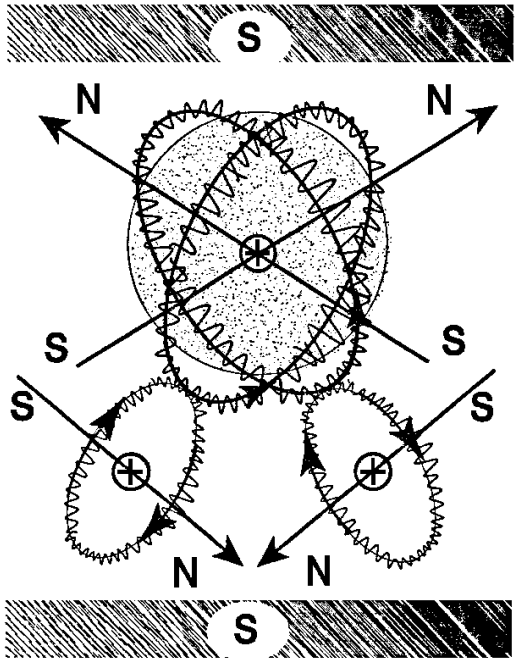

Figure 11.8. A schematic view of the resolution for the case of the water molecule of the inconsistent prediction of the conventional molecular model that water is paramagnetic (Fig. 1.14), as permitted by the Santilli-Shillady isochemical model of water molecule (Chapter 9). As one can see, the resolution is given by the impossibility for the water molecule to acquire a net magnetic polarity. Note the complexity of the geometry of the various magnetic fields which, according to ongoing research, apparently permits the first explanation on scientific record of the 105° angle between the two H–O dimers. The corresponding resolution for the case of the hydrogen is outlined in Fig. 9.5.

However, when exposed to an external magnetic field, the orbits of one or more unpaired electrons are polarized into a toroidal shape with end polarities opposite to those of the external field.

This mechanism is called magnetic induction, and results in a stable chain of magnetically polarized orbits from the beginning of the metal to its end with polarities North-South/North-South/North-South/ ... This chain of polarizations is so stable that it can only be destroyed by high temperatures.

The creation of magnecules can be essentially understood with a similar polarization of the peripheral electron orbits, with the main differences that: no total magnetic polarization is necessary; the polarization generally apply to all electrons, and not necessarily to unpaired electrons only; and the substance need not to be paramagnetic.

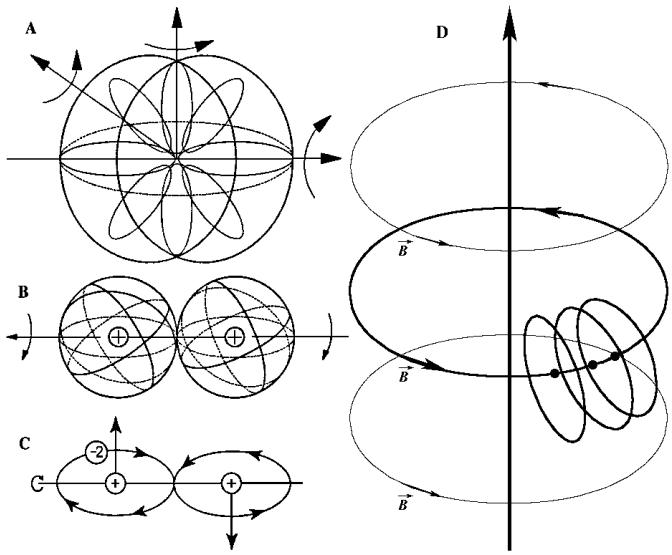

Figure 11.9. A schematic view of the main mechanism underlying the creation of magnecules, here illustrated for the case of the hydrogen molecule. It consists in the use of sufficiently strong external magnetic fields which can progressively eliminate all rotations, thus reducing the hydrogen molecule to a configuration which, at absolute zero degrees temperature, can be assumed to lie in a plane. The planar configuration of the electron orbits then implies the manifestation of their magnetic moment which would be otherwise absent. The r.h.s. of the above picture outlines the geometry of the magnetic field in the immediate vicinity of an electric arc as described in the text for the case of hadronic molecular reactors (Chapter 12). Note the *circular* configuration of the magnetic field lines around the electric discharge, the *tangential* nature of the symmetry axis of the magnetic polarization of the hydrogen atoms with respect to said circular magnetic lines, and the consideration of hydrogen atoms at *orbital distances* from the electric arc 10^{-8} cm, resulting in extremely strong magnetic fields proportional to $(10^{-8})^{-2} = 10^{16}$ Gauss, thus being ample sufficient to create the needed polarization (see Appendix 8.A for details).

To illustrate these differences, consider a diamagnetic substance, such as the hydrogen at its gaseous state at ordinary pressure and temperature. As well known, the hydrogen molecule is then a perfect sphere whose radius is equal to the diameter of a hydrogen atom, as illustrated in Fig. 11.9.A. The creation of the needed magnetic polarization requires the use of external magnetic fields capable, first, to remove the rotation of the atoms, as illustrated in Fig. 11.9.B, and then the removal of the internal rotations of the same, resulting in a planar configuration of the orbits as illustrated in Fig. 11.9 .C.

Once the above polarization is created in two or more hydrogen molecules sufficiently near each other, they attract each other via opposite magnetic

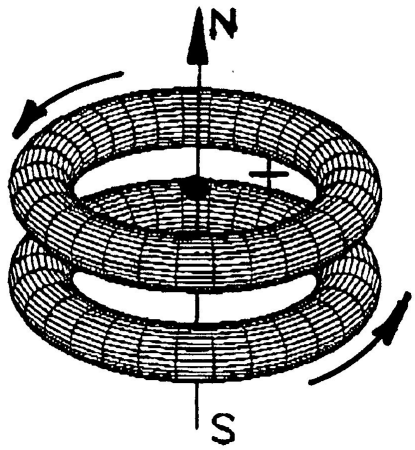

Figure 11.10. A schematic view of the simplest possible bi-atomic magnecule whose bond originates from the toroidal polarization of the orbits of peripheral atomic electrons. A first main difference with conventional molecular bonds is that, under sufficiently strong external magnetic fields, the magnecular bond may occur independently from the existence or not of valence electrons. Consequently, the two polarized atoms depicted in this figure can be arbitrarily chosen, while for conventional molecular bonds the atoms are restricted to verify known valence rules. Another major difference is that, by central conception to achieve full combustion for the case of fuels (see Section 11.1), the magnecular bond is much weaker than the molecular bond. In fact, due to its magnetic origin, the bond of this picture ceases to exist at a given temperature (the Curie Temperature) that, for the case of gaseous fuels with magnecular structure, it is usually given by the flame temperature. The main industrial as well as social result is that gaseous fuels with magnecular structure do achieve indeed total combustion without any toxic substance in its exhaust, something impossible for fuels with molecular structure, as proved by various cases studied in the subsequent sections of this chapter. Another implication also of major industrial and social relevance is that fuels with magnecular structure can be synthesized in such a way to be internally rich in oxygen (usually of liquid, rather than atmospheric origin) in order to replenish the atmospheric oxygen already depleted by fossil fuels, something equally impossible for fuels with molecular structure, as also studied later on in this chapter.

polarities, resulting in the elementary magnecules of Fig. 11.10.A. Additional elementary magnecules can then also bond to each other, resulting in clusters with a number of constituents depending on the conditions considered.

A most efficient industrial production of gas and liquid magnecules is that via the *PlasmaArcFlow Reactors* [5]. As we shall see via the experimental evidence presented below, said reactors can produce an essentially pure popula-

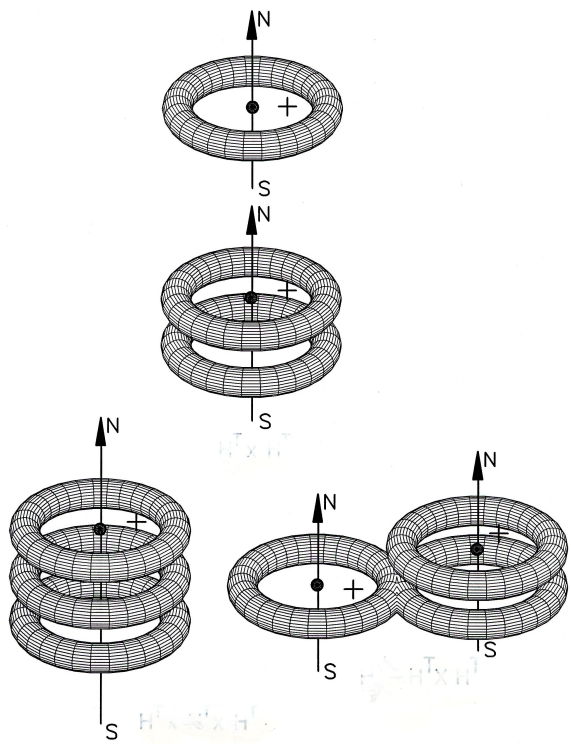

Figure 11.11. A schematic view of the simplest possible multiatomic magnecular bonds. Case A illustrates the *elementary hydrogen magnecule*. The subsequent case is that of four hydrogen atoms $(H \times H) \times (H \times H)$ (or two hydrogen molecules $H - H) \times (H - H)$) under a magnecular bond that has atomic weight very close to that of the helium. Therefore, the detection in a GC-MS scan of a peak with 4 a.m.u., by no means, necessarily identifies the helium because the peak could belong to the hydrogen magnecule. Case B illustrates a magnecule composed by a molecule and a dimer. Case C illustrates the hypothesis submitted in this monograph that the structure with 3 a.m.u. generally interpreted as a conventional "molecule" H_3 may in reality be a magnecule between a hydrogen molecule and an isolated hydrogen atom. This is due to the fact that, once the two valence electrons of the hydrogen molecule are bonded-correlated, they cannot admit the same valence bond with a third electron for numerous physical reasons, such as: the bond cannot be stable because the former is a Boson while the latter is a Fermion; the former has charge $-2e$ while the latter has charge $-e$, thus resulting in a large repulsion; *etc.*

tion of gas and liquid magnecules without appreciable percentages of molecules directly detectable in the GC- or LC-MS.

The reason for these results is the intrinsic geometry of the PlasmaArcFlow itself. Recall that this technology deals with a DC electric arc submerged

within a liquid waste to be recycled. The arc decomposes the molecules of the liquid into its atomic constituents; ionizes the same; and creates a plasma of mostly ionized H, C and O atoms at about $3,500°$ K. The flow of the liquid through the arc then continuously removes the plasma from the arc following its formation. Said plasma then cools down in the surrounding liquid, and a number of chemical reactions take place resulting in the formation of magnegas which bubbles to the surface of the liquid where it is collected for industrial or consumer use.

To understand the creation of a *new chemical species* defined according to Sect. 11.2.1 as an essentially pure population of *gas magnecules*, recall that magnetic fields are inversely proportional to the square of the distance,

$$F_{\text{magnetic}} = \frac{m_1 m_2}{r^2}. \tag{11.2.14}$$

Therefore, an atom in the immediate vicinity of a DC electric arc with 1,000 A and 30 V, experiences a magnetic field which is inversely proportional to the square of the *orbital* distance $r = 10^{-8}$ cm, resulting in a magnetic field proportional to 10^{16} units.

No conventional space distribution of peripheral atomic electrons can exist under these extremely strong magnetic fields, which are such to generally cause the polarization of the orbits of *all* atomic electrons, and not only those of valence type, as well as their essential polarization in a plane, rather than a toroid.

As soon as two or more molecules near each other possessing such an extreme magnetic polarization are created, they bond to each other via opposing magnetic polarities, resulting in the elementary magnecule of Fig. 11.8.A.

Moreover, as shown earlier, isolated atoms have a magnetic field with an intensity double that of the same atom when belonging to a molecule. Therefore, as soon as created in the immediate vicinity of the electric arc, individual polarized atoms can bond to polarized molecules without any need to belong themselves to a molecule, as illustrated in Fig. 11.10.C.

Finally, recall that the PlasmaArcFlow is intended to destroy liquid molecules such as that of water. It then follows that the plasma can also contain individual highly polarized molecular fragments, such as the dimer H–O. The notion of gas magnecules as per Definition 8.2.1 then follows as referred to stable clusters of molecules, and/or dimers, and/or isolated atoms under an internal attractive bond among opposing polarities of the magnetic polarization of the orbits of peripheral electrons, nuclei and electrons when the latter are not coupled into valence bonds.

Effective means for the creation of an essentially pure population of *liquid magnecules* are given by the same PlasmaArcFlow Reactors. In fact, during its flow through the DC arc, the liquid itself is exposed to the same extreme magnetic fields as those of the electric arc indicated above. This causes the

creation of an essentially pure population of liquid magnecules composed of highly polarized liquid molecules, dimers of the same liquid, and individual atoms, as established by LC-MS/UVD tests.

One way to create an essentially pure population of *solid magnecules* is given by freezing the new chemical species at the liquid level and then verifying that the latter persists after defrosting, as confirmed by various tests. Therefore, the case of solid magnecules is ignored hereon for simplicity.

By denoting with the arrow $\uparrow$ the vertical magnetic polarity North-South and with the arrow $\downarrow$ the vertical polarity South-North, and by keeping the study at the absolute zero degree temperature, when exposed to the above indicated extreme magnetic fields, the hydrogen molecule H–H can be polarized into such a form that the orbit of the isoelectronium is in a plane with resulting structure $\mathrm{H}_\uparrow - \mathrm{H}_\downarrow$ (Fig. 11.7).

The elementary hydrogen magnecule can then be written

$$\{\mathrm{H}^a_\uparrow - \mathrm{H}^b_\downarrow\} \times \{\mathrm{H}^c_\uparrow - \mathrm{H}^d_\downarrow\}, \tag{11.2.15}$$

where: a, b, c, d denote different atoms; the polarized hydrogen atom $\mathrm{H}^a_\uparrow$ is bonded magnetically to the polarized atom $\mathrm{H}^c_\uparrow$ with the South magnetic pole of atom a bonded to the North pole of atom c; and the North polarity of atom b is bonded to the South polarity of atom d (see, again, Fig. 8.5.A). This results in a strong bond due to the flat nature of the atoms, the corresponding mutual distance being very small and the magnetic force being consequently very large. Moreover, unlike the case of the unstable clusters due to electric polarization discussed in Sect. 11.2.1, the above magnetic bonds are very stable because motions due to temperature apply to the bonded couple (11.2.15) as a whole.

For other magnecules we can then write

$$\{\mathrm{H}_\uparrow - \mathrm{H}_\downarrow\} \times \{\mathrm{C}_\uparrow - \mathrm{O}_\downarrow\}; \tag{11.2.16}$$

or, more generally

$$\{\mathrm{H}_\uparrow - \mathrm{H}_\downarrow\} \times \mathrm{H}_\downarrow \times \{\mathrm{C}_\uparrow - \mathrm{O}_\downarrow\} \times \{\mathrm{H}_\uparrow - \mathrm{O}_\downarrow\} \times \{\mathrm{H}_\uparrow - \mathrm{C}_\downarrow - \mathrm{A} - \mathrm{B} - \mathrm{C} \ldots\} \times \ldots, \tag{11.2.17}$$

where A, B, and C are generic atoms in a conventional molecular chain and the atoms without an indicated magnetic polarity may indeed be polarized but are not necessarily bonded depending on the geometric distribution in space.

Magnecules can also be formed by means other than the use of external magnetic fields. For instance, magnecules can be produced by electromagnetic fields with a distribution having a cylindrical symmetry; or by microwaves capable of removing the rotational degrees of freedom of molecules and atoms, resulting in magnetic polarizations. Similarly, magnecules can be formed by subjecting a material to a pressure that is sufficiently high to remove the orbital

rotations. Magnecules can also be formed by friction or by any other means not necessarily possessing magnetic or electric fields, yet capable of removing the rotational degrees of freedom within individual atomic structures, resulting in consequential magnetic polarizations.

It is, therefore, expected that a number of substances which are today listed as of unknown chemical bond, may eventually result to have a magnecular structure.

Magnecules of type (8.15) may well have been detected in past mass spectrometric measurements, but believed to be the helium (because its molecular weight is very close to that of the helium). In fact, the same happens for the "molecule" H_3 which, in reality may be the magnecule of Fig. 11.10.C.

The destruction of magnecules is achieved by subjecting them to a temperature greater than the magnecules Curie Temperature which varies from magnecule to magnecule.

11.2.6 New Molecular Internal Bonds

As indicated in Sect. 11.2.2, and verified experimentally later on, the IR signatures of conventional molecules such as CO_2 are mutated due to the appearance of two new peaks which do not exist for the conventional molecule. By recalling that peaks in the IR signature generally represent bonds, this evidence indicates the capability by the CO_2 molecule to acquire new internal bonds in addition to those of conventional valence type.

The magnetic polarization at the foundations of magnecules predicts the existence of these new internal bonds and permits their quantitative study. Recall that external magnetic fields can polarize the orbit of valence electrons, but cannot possibly break or alter valence bonds. Recall that, consequently, sufficiently strong external magnetic fields can polarize the orbits of all atomic electrons, and not only those of the valence electrons.

Consider then a conventional molecule such as C=O. When exposed to the extreme magnetic fields as existing in the PlasmaArcFlow technology, the orbits of all internal electrons can be polarized, individually, for the carbon and the oxygen, in addition to the polarization of the two pairs of valence bonds. Note that the planes of these polarizations need not be necessarily parallel to each other, because their relative orientation dependents on the geometry at hand.

One of the various possible geometries is that in which the plane of the polarization of the internal electrons is perpendicular to that of the two pairs of valence bonds. In this case we have the birth of a *new bond of magnetic origin in the interior of a conventional molecule*, which is evidently given by the alignment of the two polarities North-South and North-South in the carbon and oxygen, and the consequential attraction of opposite polarities of different atoms, as illustrated in Fig. 11.11.A.

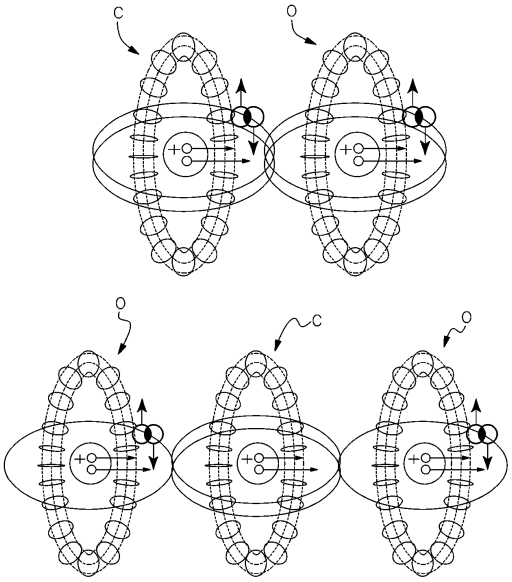

Figure 11.12. A schematic view for the cases of C=O and O–C–O of the polarization of internal atomic electrons, while preserving conventional valence bonds, and the consequential creation of new bonds in conventional molecules which are not of valence type, as later on verified experimentally via IR scans.

For the case of the O–C–O molecule we can evidently have two internal bonds of magnetic type in addition to the valence bonds, which are also given by the alignment of the magnetic polarities, resulting in one new bond for the O–C dimer and a second one for the C–O dimer, as illustrated in Fig. 11.11.B.

As we shall see later on, the above new internal molecular bonds have major industrial and consumer implications, inasmuch as they permit the production of fuels capable of releasing under combustion anomalous amounts of energy, with consequential reduction of pollutants in the exhaust, as already proved by magnegas.

Needless to say, the creation of new internal bonds is an extreme case of IR mutation. In reality, numerous other weaker forms of mutations without the appearance of new peaks are possible and their study is left to the interested reader.

11.2.7 Main Features for the Detection of Magnecules

The experimental detection of gas magnecules requires the verification of a number of characteristic features of magnecules identified in Definition 8.2.1. In the following we focus the reader's attention on the main features of gas

magnecules which must be verified via GC-MS tests. The remaining features will be considered later on.

Feature 1: Appearance of unexpected heavy MS peaks.
Gas magnecules are generally heavier than the heaviest molecule in a given gas. Peaks in the GC-MS are, therefore, expected in macroscopic percentages with atomic weights bigger than the heaviest molecule. As a concrete example, the heaviest molecule in magnegas in macroscopic percentage is CO_2 with 44 a.m.u. Therefore, GC-MS scans should only show background noise if set for over 44 a.m.u. On the contrary, peaks in macroscopic percentages have been detected in magnegas all the way to 1,000 a.m.u.

Feature 2: Unknown character of the unexpected MS heavy peaks.
To provide the initial premises for the detection of magnecules, all MS peaks of feature 1 should result in being "unknown" following the computer search among all known molecules, usually including a minimum of 150,000 molecules. Evidently, this lack of identification of the peaks, *per se*, does not guarantee the presence of a new chemical species.

Feature 3: Lack of IR signature of the unknown MS peaks.
Another necessary condition to claim the detection of magnecules is that the unknown MS peaks of feature 1 should have no IR signature other than that of the molecules and/or dimers constituents. This feature guarantees that said heavy peaks cannot possibly represent molecules, thus establishing the occurrence of a new chemical species. In fact, only very few and very light molecules can have such a perfect spherical symmetry to avoid IR detection, while such a perfect spherical symmetry is manifestly impossible for large clusters. In regard to the constituents we are referring to IR signatures, *e.g.*, of the CO_2 at 44 a.m.u. in a cluster having 458 a.m.u.

Feature 4: Mutation of IR signatures.
The infrared signatures of conventional molecules constituting magnecules are expected to be *mutated*, in the sense that the shape of their peaks is not the conventional one. As indicated in the preceding section, the mutations most important for industrial applications are those due to the presence of *new IR peaks* representing new internal bonds. Nevertheless, various other forms of IR mutations are possible.

Feature 5: Mutation of magnecular weights.
While molecules preserve their structure and related atomic weight at conventional temperatures and pressures, this is not the case for gas magnecules, which can *mutate* in time, that is, change their atomic weight with consequen-

tial change of the shape and location of their MS peaks. Since we are referring to gases whose constituents notoriously collide with each other, magnecules can break-down during collisions into fragments which can then recombine with other fragments or other magnecules to form new clusters.

Feature 6: Accretion or emission of individual atoms, dimers or molecules.

Magnecules are expected to experience accretion or emission of individual atoms, dimer or molecules without necessarily breaking down into parts. It follows that the peaks of Feature 1 are not expected to remain the same over a sufficient period of time for the same gas under the same conditions.

Feature 7: Anomalous adhesion.

Magnetically polarized gases have anomalous adhesion to walls of disparate nature, not necessarily of paramagnetic character, as compared to the same unpolarized gas. This is due to the well-known property that magnetism can be propagated by induction, according to which a magnetically polarized molecule with a sufficiently intense magnetic moment can induce a corresponding polarization of valence and/or other electrons in the atoms constituting the wall surface. Once such a polarization is created by induction, magnecules can have strong magnetic bonds to the indicated walls. In turn, this implies that the background of GC-MS following scans and conventional flushing are often similar to the scan themselves. As a matter of fact, backgrounds following routine flushing are often used to identify the most dominant magnecules. Notice that the magnetic polarization here considered does not require that the walls of the instrument are of paramagnetic type, since the polarization occurs for the orbits of arbitrary atoms.

Magnetically polarized gases additionally have mutated physical characteristics and behavior because the very notion of polarization of electron orbits implies physical alterations of a variety of characteristics, such as average size. Mutations of other characteristics are then consequential.

We should finally recall that the above features are expected to disappear at a sufficiently high temperature, evidently varying from gas to gas (Curie Temperature), while the features are expected to be enhanced at lower temperature and at higher pressure, and survive liquefaction.

11.3 THE UNAMBIGUOUS DETECTION OF MOLECULES AND MAGNECULES

11.3.1 Selection of Analytic Instruments

Current technologies offer an impressive variety of analytic instruments (see, *e.g.*, Ref. [4]), which include: Gas Chromatography (GC), Liquid Chromatography (LC), Capillary Electrophoresis Chromatography (CEC), Supercritical Chromatography (SCC), Ion Chromatography (IC), Infrared Spectroscopy (IR), Raman Spectroscopy (RS), Nuclear Magnetic Resonance Spectroscopy (NMRS), X-Ray Spectroscopy (XRS), Atomic Absorption Spectroscopy (AAS), Mass Spectrometry (MS), Laser Mass Spectrometry (LMS), Flame Ionization Spectrometry (FIS), and others.

Only some of these instruments are suitable for the detection of magnecules and, when applicable, their set-up and use are considerably different than those routinely used with great success for molecules.

Among all available chromatographic equipment, that suitable for the detection of gas magnecules is the GC with column having ID of at least 0.32 mm operated according to certain criteria outlined below. By comparison, other chromatographs do not appear to permit the entrance of large magnecules, such as the CEC, or be potentially destructive of the magnecules to be detected, such as the IC.

Among all available spectroscopic equipment, that preferable is the IR, with the understanding that such an instrument is used in a *negative* way, that is, to verify that the magnecule considered has no IR signature. The RS may also result in being preferable in various cases, while other instruments, such as the NMRS do not appear to be capable of detecting magnecules despite their magnetic nature, evidently because NMRS are most effective for the detection of microscopic magnetic environment of H-nuclei rather than large structures. Other spectroscopic instruments have not been studied at this writing.

In regard to spectrometric equipment, the most recommendable one is the low ionization MS due to the fact that other instruments seemingly destroy magnecules at the time of their detection. The study of other spectrometric equipment is left to interested researchers. Chemical analytical methods (i.e. via chemical reactions) to *detect* gas magnecules are probably not very effective since they necessarily destroy the magnecules in reaction.

As it is well known, when used individually, the above suggested instruments have considerable limitations. For instance, the GC has a great resolution of a substance into its constituent, but it has very limited capabilities to identify them. By comparison, the MS has great capabilities to identify individual species, although it lacks the ability to separate them.

For these reasons, some of the best analytic instruments are given by the combination of two different instruments. Among them, the most recommend-

able one is the GC combined with the MS, and denoted GC-MS. A similar occurrence holds for the IR combined to the GC-MS. As indicated since the early parts of this Chapter, the best instrument for the detection of both molecules and magnecules in gases is the GC-MS equipped with the IRD denoted GC-MS/IRD while that for liquids is the LC-MS equipped with UVD and denoted LC-MS/UVD.

Among a large variety of GC-MS instruments, only a few are truly effective for the detection of gas magnecules for certain technical reasons identified below. The instrument which has permitted the first identification of magnecules and remains the most effective at this writing (despite its considerable age for contemporary standards) is the GC Hewlett-Packard (HP) model 5890 combined with the MS HP model 5972 equipped with a large ID column and feeding line operated at the lowest temperature permitted by the instrument (about 10° C) and the longest elusion time (about 25 min).

A secondary function of the IRD is that of identifying the *dimers constituting a magnecule*, a task which can be fulfilled by various IRD. That which was used for the original discovery of magnecules and still remains effective (again, despite its age by current standards) is the IRD HP model 5965, when operated with certain criteria identified below.

A most insidious aspect in the detection of magnecule is the protracted use of any given instrument with great success in the detection of conventional molecules, and the consequential expectation that the same instrument should work equally well for the detection of magnecules, resulting in an analysis without any real scientific value because:

i) the species to be detected may not even have entered the instrument, as it is routinely the case for small syringes and feeding lines particularly for liquid magnecules (which can be so big as to be visible to the naked eye, as shown later on in this chapter);

ii) the species to be detected may have been destroyed by the measurement itself, as it is routinely the case for instruments operated at very high temperature, or flame ionization instruments which, when used for combustible gases with magnecular structure, cause the combustion of magnecules at the very time of their detection; or

iii) the detection itself may create magnecules which do not exist in the original species, as it is the case of peaks with 3 a.m.u. discussed in Fig. 11.10.

In conclusion, the separation between a true scientific measurement and a personal experimental belief requires extreme scientific caution in the selection of the analytic instrument, its use, and the interpretation of the results.

11.3.2 Unambiguous Detection of Molecules

As it is well known, a *gas molecule* is identifiable by unique and unambiguous GC-MS peaks, which are distinctly different from those of any other gas

molecule. In addition, this GC-MS identification can be confirmed by IRD peaks and related resonating frequencies, which are also distinctly different for different gas molecule. Additional confirmations are possible using other analytic methods, such as those based on average molecular weight, chemical reactions and other procedures.

The advent of the new chemical species of magnecules suggests a re-examination of these analytic methods and procedures so as to separate personal opinions from actual scientific identifications. Such a re-examination is warranted by the fact that, due to extended use, claims of specific molecular identifications are nowadays generally voiced via the use of only one analytic detector.

As an illustration, most contemporary analytic laboratories conduct chemical analyses on gases via the sole use of the IRD. However, *infrared detectors do not identify complete molecules, since they can only identify the bond in their dimers*. For instance, for the case of H_2O, the IRD does not identify the complete molecule, but only its dimer H–O.

This method of identification of molecules is certainly acceptable for gases whose lack of magnetic polarization has been verified by the analysts. However, the same method is highly questionable for gases of unknown origin. In fact, we shall soon show experimental evidence of clear IR signatures for molecules which have no MS identification at all, in which case the claim of such a molecule evidently has no scientific value.

The inverse occurrence is equally questionable, namely, the claim of a given molecule from its sole identification in the MS without a confirmation of exactly the same peak in the IRD. In fact, there are several MS peaks in magnetically polarized gases which may be easily identified with one or another molecule, but which have no IR signature at all at the MS value of the atomic weight, in which case the claim of molecular identification evidently has no scientific value.

Note that the great ambiguities in the separate use of disjoint GC-MS and IRD. In fact, in this case there is no guarantee or visible evidence that exactly the same peak is jointly inspected under the MS and, separately, the IRD. In fact, a given molecule can be tentatively identified in the MS at a given a.m.u., while the same molecule may indeed appear in the IRD, although at a different value of a.m.u., in which case, again, the claim to have detected a given molecule is a personal experimental belief, rather than a scientific truth.

In conclusion, *a serious scientific identification of any given molecule requires the joint use of at least two different analytic methods, both giving exactly the same result for exactly the same peak in a unique and unambiguous way, such as the detection via MS scans with unequivocal computer identifications, confirmed by IR scans without ambiguities, thus requiring the use of GC-MS equipped with IRD.*

Additional ambiguities result from the rather widespread belief that molecules are the only possible chemical species in nature, in which case small deviations from exact identifications are generally ignored for the specific intent of adapting experimental evidence to pre-existing knowledge, rather than modifying old interpretations to fit new experimental evidence. This widespread tendency is also a reason why magnecules have not been identified until now.

As an illustration, suppose that: a GC-MS equipped with IRD detects a peak with 19 a.m.u.; said peak is identified by the MS search as the water molecule with 18 a.m.u.; and the IRD confirms the presence of the HO-dimer. Under these conditions, it is almost universally accepted in contemporary analytic laboratories that said peak with 19 a.m.u. represents the water molecule, and the spurious single a.m.u. is just an "impurity" or something to be ignored, in which case, however, we do not have a true scientific identification of the species.

In fact, it is well possible that the peak at 19 a.m.u. is constituted by a highly polarized water molecule magnetically bonded to one isolated hydrogen atom with structure

$$\{H_{\downarrow} - O_{\uparrow\uparrow} - H_{\downarrow}\} \times H_{\downarrow}. \tag{11.3.1}$$

In this case, according to our terminology, the peak at 19 a.m.u. is a magnecule and *not* a molecule, even though the MS search gives 99.99% confidence and the IR search gives 100% confidence that the species is the ordinary water molecule. After all, the magnecular bond is transparent to current IR detection, then, the latter confirms an erroneous belief.

At any rate, no claim on the peak with 19 a.m.u. can be truly scientific or otherwise credibly, unless it explains in a specific and numerical way, without vague nomenclatures, how the single a.m.u. entity is attached to the water molecule.

Recall that the valence bond requires singlet couplings to verify Pauli's exclusion principle. As a consequence, coupled pairs of valence electrons are *Bosonic states with zero spin*. Under these conditions, no nomenclature suggesting one or another type of valence can credible explain the bonding of one single H atom to the H–O–H molecule because it would imply the bond of a *Fermion with spin* 1/2 (the valence electron of the hydrogen) with a *Boson* (the coupled valence electron pair of the water), which bond is an impossibility well known in particle physics. By comparison, the magnecular hypothesis identifies the *attractive* character of the bond in a clear and unambiguous way, and then its *numerical value* (8.9).

The detection of *liquid molecules* has problems greater than those for gas molecules, because liquid magnecules can be so big to be visible by the naked eye, in which case only their conventional molecular constituents are generally permitted to enter current instruments, resulting again in a lack of real detection.

In conclusion, the separation in the identification of molecules between a true scientific process and a personal experimental belief requires extreme care before claiming that a certain peak characterizes a molecule, since possible ambiguities exist in all cases, from small to large atomic weights. In the final analysis, as stressed above, the difference between a molecule and a magnecule may be given by what is generally considered noise, or instrument malfunction.

The most unreassuring occurrence is that all GC-MS equipped with IRD identified by this author in the USA following a laborious search belong to military, governmental, or law enforcement institutions, and none of them was identified in commercial or academic laboratories. Therefore, the great majority of analytic laboratories lack the very instrument necessary for a final and unequivocal identification of a conventional *molecules*, let alone that of magnecules.

11.3.3 Unambiguous Detection of Magnecules

Since magnecules have properties very different from those of conventional molecules, the experimental detection of magnecules requires a special care. In particular, methods which have been conceived and developed for the detection of molecules are not necessarily effective for the detection of the different chemical species of magnecules precisely in view of the indicated differences.

The first indication of a possible *gas magnecule* is given by MS peaks with large atomic weight which cannot be explained via conventional molecular hypotheses. The second indication of a gas magnecule is given by the lack of identification of said heavy peaks in the MS following a search among all known molecules. A third indication of a gas magnecule then occurs when said unknown MS peak has no IR signature, except those of its constituents with much smaller atomic weight, which occurrence establishes the lack of a valence bond. Final identification of a gas magnecule requires the knowledge of the method used in the production of the gas and other evidence.

As it is the case also for molecules, a serious spectrographic analysis of magnecules requires GC-MS detectors necessarily equipped with IRD, because only such an instrument permits the direct test of the *same peaks* under both the MS and IR scan. Again, if the IRD operates separately from the GC-MS, the indicated joint inspection is not possible; the IRD can only detect ordinary molecular dimers; the experimental belief that the MS peak must be a molecule is then consequential.

As a concrete example verified later on with actual tests, consider the spectrographic analysis of magnegas. This is a light gas whose heaviest molecule in macroscopic percentages should be the CO_2 at 44 a.m.u. Consider now an MS peak of magnegas at 481 a.m.u. It is evident that, while small deviations could be adapted to quantum chemistry, large deviations of such an order of magnitude cannot be reconciled with established knowledge in a credible way,

thus permitting the hypothesis that the MS peak in a *light* gas with 481 a.m.u. can be a magnecule. The MS scan of the peak soon establishes the impossibility for the computer to identify the peak among all existing molecules. When the GC-MS is equipped with IRD, the analyst can scan the same peak with 481 a.m.u. under the IRD and detect no signature at the 481 a.m.u. value, the only IR signature being that at 44 a.m.u. of the CO_2 as well as those of smaller molecules. The production of the gas under intense magnetic fields then confirm that the peak here considered at 481 a.m.u. is indeed a magnecule composed of a large number of ordinary light molecules, dimers and individual atoms, in accordance with Definition 8.2.1.

Note that the IRD scan in the above test has solely identified conventional molecules without any additional unknown. Yet, the conclusion that the gas considered is solely composed of molecule would be nonscientific for numerous reasons, such as: 1) magnetic bonds are transparent to IR scans with available frequencies; 2) there is no IR detection, specifically, at 481 a.m.u.; and 3) IRD do not detect molecules, but only dimers.

Therefore, even though the IRD has detected CO_2 in the above test, the actual detection was for the C–O dimer, in which case the claim of the presence of the full CO_2 molecule is a personal opinion, and not an experimental fact.

The anomalous energy content, weigh and other features of magnegas confirm the above conclusions, because the latter can only be explained by assuming that a certain percentage of IR counts is indeed due to complete molecules, while the remaining percentage is due to unpaired dimers trapped in the magnecules. The freeing of these dimers and atoms at the time of the combustion, and their re-combination into molecules as in Eqs. (8.5) then explains the anomalous energy content.

In addition to the above basic requirements, numerous other precautions in the use of the GC-MS equipped with IRD are necessary for the detection of magnecules, such as:

i) the MS equipment should permit measurements of peaks at ordinary temperature, and avoid the high temperatures of the GC-MS column successfully used for molecules;

ii) the feeding lines should be cryogenically cooled;

iii) the GC-MS/IRD should be equipped with feeding lines of at least 0.5 mm ID;

iv) the GC-MS should be set to detect peaks at large atomic weights usually not expected; and

v) the ramp time should be the longest allowed by the instrument, *e.g.*, of at least 25 minutes.

It should be stressed that *the lack of verification of any one of the above conditions generally implies the impossibility to detect magnecules*. For instance, the use of a feeding line with 0.5 mm ID is un-necessarily large for a

conventional light gas, while it is necessary for a gas with magnecular structure such as magnegas. This is due to the unique adhesion of the magnecules against the walls of the feeding line, resulting in occluded lines which prevent the passage of the most important magnecules to be detected, those with large atomic weight.

Similarly, it is customary for tests of conventional gases to use GC-MS with columns at high temperature to obtain readings in the shortest possible time, since conventional molecules are perfectly stable under the temperatures here considered. The use of such method would equally prevent the test of the very species to be detected, because, as indicated earlier, they have a characteristic Curie Temperature at which all magnetic features are lost. Magnecules are stable at ordinary temperatures and, consequently, they should be measured at ordinary temperatures.

Along similar lines, recall that GC-MS with a short ramp time are generally used for rapidity of results. Again, the use of such a practice, which has been proven by extensive evidence to be effective for molecules, prevents clear detection of magnecules. If the ramp time is not of the order of 25 minutes, *e.g.*, it is of the order of one minute, all the peaks of magnecules generally combine into one single large peak, as described below. In this case the analyst is generally lead to inspect an individual section of said large peak. However, in so doing, the analyst identifies conventional molecules constituting the magnecule, and not the magnecule itself.

When these detectors with short ramp times are equipped with IRD, the latter identify the infrared signatures of individual conventional molecules constituting said large unique peak, and do not identify the possible IR signature of the single large peak itself. Therefore, a GC-MS with short ramp time is basically unsuited for the detection of magnecules because it cannot separate all existing species into individual peaks.

In conclusion, the experimental evidence of the above occurrences establishes the need in the detection of gas magnecules of *avoiding, rather than using, techniques and equipment with a proved efficiency for molecules*, thus avoiding the use of GC-MS without IRD, with short ramp time, high column temperatures, microscopic feeding lines, and other techniques. On the contrary, new techniques specifically conceived for the detection of magnecules should be worked out.

The conditions for scientific measurements of *liquid magnecules* via LC-MS/UVD are more stringent than those for gases, because of the great increase, in general, of the atomic weight of liquid magnecules which are generally much larger than the IR of conventionally used feeding lines, as shown below.

This implies the possible erroneous claim that magnecules do not exist because they are not detected by the LC-MS, while in reality the magnecule to be detected could not enter into at all into the instrument.

11.3.4 Apparent Magnecular Structure of H and O

As it is well known, chemistry has identified in GC-MS tests clusters with 3 a.m.u., which can only be constituted of three H atoms, H_3, while the familiar ozone O_3 has been known since quite some time. These structures are generally assumed to be molecules, that is, to have a valence bond according to one nomenclature or another, although this author is aware of no in depth theoretical or experimental identification of the attractive force necessary to bond the third atom to a conventional molecule.

There are serious doubts as to whether such a conventional molecular interpretation will resist the test of time as well as of scientific evidence. To begin, a fundamental property of valence bonds is that *valence electrons correlate in pairs.* Since the H_3 and O_3 structures contain the molecules H_2 and O_2 in which all available valence electrons are already bonded in pairs, the belief that an additional third valence electron could be correlated to the preceding ones violates basic chemical knowledge on valence.

Moreover, we have stressed earlier that the assumption of a third valence electron bonded to a valence pair is in violation of basic physical knowledge, because it would require the bond of a Fermion (the third electron with spin 1/2) with a Boson (the singlet valence pair with spin 0) both possessing the same negative charge. Such a hypothetical bond under molecular conditions would violate various laws in particle physics, e.g., it would imply a necessary violation of Pauli-s exclusion principle since the assumed "triplet" of electrons would have *two* identical electrons in the same structure with the same energy.

In view of the above (as well as other) inconsistencies, we here assume that *the familiar H_3 and O_3 clusters are magnecules consisting of a third H and O atom magnetically bonded to the conventional H_2 and O_2 molecules, respectively, along the structure of Fig. 11.11.C.* Note that this assumption is fully in line with Definition 8.2.1 according to which a magnecule also occurs when one single atom is magnetically bonded to a fully conventional molecule.

The plausibility of the above structure is easily illustrated for the case of O_3. In fact, the oxygen is known to be paramagnetic, and the ozone is known to be best created under an electric discharge. These are the ideal conditions for the creation of a magnetic polarization of the orbits of (at least) the paramagnetic electrons. The attraction of opposing magnetic polarities is then consequential, and so is the magnetic bond of the third oxygen to the oxygen molecule, resulting in the magnecule $O_2 \times O$.

The above magnecular interpretation of O_3 is confirmed by various GC-MS detections of peaks with 32 a.m.u. in a magnetically treated gas originally

composed of pure oxygen, in which case the sole possible interpretation is that of two magnetically bonded oxygen molecules, resulting in the magnecule $O_2 \times O_2$.

The plausibility of the magnecular interpretation is less trivial for the H_3 structure since hydrogen is diamagnetic. Nevertheless, the assumption remains equally plausible by recalling that a central feature of the new chemical species of magnecules is that *the magnetic polarization occurs at the level of each individual atom, and not at the level of a diamagnetic molecule, whose total magnetic moment remains null as illustrated in Fig. 11.7.*

In particular, the magnecular interpretation of the MS peaks at 3 a.m.u. is numerical and without ambiguities. Recall that GC equipment works by ionizing molecules. When testing a hydrogen gas, a number of H_2 molecules are separated into individual H atoms by the ionization itself. Moreover, the ionization occurs via the emission of electrons from a filament carrying current, which is very similar to that of the PlasmaArcFlow Reactors producing magnecules. Under these conditions, the filament of the GC can not only separate H-molecules but also polarize them when sufficiently close to the filament. Once such polarizations are created, their bond is a known physical law, resulting in the magnecule of Fig. 11.11, *i.e.*

$$\{H_{\downarrow} - H_{\uparrow}\} \times H_{\downarrow}. \tag{11.2.19}$$

As one can see, under the magnecular structure the bond is manifestly attractive, very strong, and numerically identified in Eq. (11.3.9). Other interpretations of the peak at 3 a.m.u. are here solicited, provided that, to be credible, they are not of valence type and the internal bond is identified in a clear, unambiguous, and numerical way.

The magnecular interpretation of H_3 is confirmed by numerous GC-MS detections of a cluster with 4 a.m.u. in a magnetically treated gas which originally was composed by pure hydrogen, under which conditions such a peak can only be constituted by two hydrogen molecules resulting in the magnecule $H_2 \times H_2$ illustrated in Fig. 11.11.

It is an easy prediction that numerous peaks detected in contemporary GC-MS or LC-MS equipment may need a magnecular re-interpretation since, as indicated earlier, the method of detection itself can create magnecules. This is typically the case when the comparison of a given MS cluster with the actual peak of a given molecules contains additional lines.

As a specific example, when the peak representing a hexanal molecule (whose heaviest constituent has 100 a.m.u.) contains additional lines at 133 a.m.u., 166 a.m.u., and 207 a.m.u., it is evident that the latter lines cannot cluster with the hexanal molecule via valence bond. The plausibility of the magnecular interpretation is then evident.

For copies of the GC-MS scans mentioned in this section, which are not reproduced here for brevity, we suggest the interested reader to contact the author.

11.3.5 Need for New Analytic Methods

In closing, we should stress that the methods for the detection and identification of magnecules are at their infancy and numerous issues remain open at this writing (spring 2001). One of the open issues relates to several detections in magnegas of IR signatures apparently belonging to complex molecules, such as light hydrocarbons, while such molecules have not been identified in the MS scans. This occurrence creates the realistic possibility that certain complex magnecules may indeed have an IR signature in view of their size. More specifically, as indicated earlier, magnecules are assumed to be transparent to currently available IRD because their inter-atomic distance is expected to be 10^4 times smaller than the inter-atomic distance in molecules, thus requiring test frequencies which simply do not exist in currently available IRD.

However, such an argument solely applies for magnecules with small atomic weight, such as the elementary magnecules of Fig. 11.10. On the contrary, magnecules with heavy atomic weight may well have an IR signature and, in any case, the issue requires specific study.

This possibility is confirmed by the fact that magnegas is created via underliquid electric arcs whose plasma can reach up to $10{,}000^o$ K. The insistence that light hydrocarbons could survive in these conditions, let alone be created, is not entirely clear. This direct observation is confirmed by the fact that no hydrocarbon has been detected in the combustion of magnegas. In fact, the cars running on magnegas (see next section) operate without catalytic converter. Direct analysis of the combustion exhaust show a *negative count* of hydrocarbons, that is, the exhaust contains less hydrocarbons than the local atmosphere which is used for basic calibration of the instrument.

In summary, we have a case in which light hydrocarbons are seemingly indicated by IR scans to exist in small percentages in magnegas, while no hydrocarbon has ever been identified in the MS scans, no hydrocarbon is expected to survive at the extreme temperatures of the electric arcs used for their production, and no hydrocarbon has been detected in the combustion exhaust.

These occurrences illustrate again that the identification of conventional molecules via the sole use of IR scans or, equivalently, the sole use of MS scans, is, in general, a mere personal opinion without scientific foundations.

11.4 MAGNEGASES, THE COMBUSTIBLE GASES WITH A MAGNECULAR STRUCTURE

11.4.1 PlasmaArcFlow Reactors for Recycling Liquid Waste into the Clean Burning Cost Competitive Magnegas Fuel

In this section we summarize the results of corporate research following the investment of several millions of dollars for the conception and industrial development by the author of the first new gaseous fuels with magnecular structure, today known as *Santilli Magnegases*^{TM} (patented and international patents pending [5]), verifying the following main conditions:

1) Achievement of full combustion without any toxic content in the exhaust, thanks to its magnecular structure (Section 11.1.1);

2) Achievement of exhaust rich in breathable oxygen originating from liquids (rather than from our atmosphere) so as to replenish the oxygen depleted by fossil fuel combustion and converted into excess CO_2;

3) Have a thermodynamical equivalence with natural gas so that all equipment running on natural gas (cars, electric generators, furnaces, etc.) can also run on magnegas without structural modifications;

4) Be lighter than air and have a natural scent so that in case of leaks the gas can be easily detected and rises for safety;

5) Be synthesized via the recycling of liquid waste (such as automotive liquid wastes, city, farm or ship sewage, etc.), so as to decrease the environmental problems caused by the latter;

6) Be cost competitive with respect to fossil fuels thanks to a highly efficient and non-contaminant production process;

7) Permit the achievement of fuel independence from crude oil (petroleum) thanks to the continuous local availability as feedstock, for instance, of city sewage 24 hours per day.

The term "magnegases" is today referred to *all gaseous fuels possessing Santilli's magnecular structure.* from now on we shall study in this section a specific type of "magnegas" obtained via a new combustion of carbon obtained via a submerged electric arc. Consequently, the type of magnegas treated in this section contains carbon. other types of magnegases without carbon will be studied in the next sections.

The equipment that has been developed for the production of type of magnegas here considered is given by *Santilli's hadronic reactors of molecular type* (Class III), also known as PlasmaArcFlow^{TM} Reactors (patented and international patents pending [5]), that were first built by the author in 1998 in Florida, U.S.A., , and are now in regular production and sale the world over (see the figures and web site [5b] for pictures).

Figure 11.13. Picture of a 250 Kw Santilli's Hadronic Reactor (also called PlasmaArcFlow Reactor) with the panels of its completely automatic and remote controls, to recycle liquid waste into magnegas usable for any fuel application, a large amount of heat and carbonaceous precipitates used to produce the electrodes. This Reactor can produce up to 5000, 000 scf (140 millions liters) of magnegas per week of 24 hours work per day corresponding to 3, 000 gasoline gallon equivalent (11, 000 gasoline liter equivalent) of magnegas per week computed on the basis that: 1) Gasoline contains about 110, 000 BTU/g (about 29, 000 BTU/liter); 2) Magnegas has the low energy content of 750 BTU/scf (26 BTU/liter); and 3) the "gasoline gallon equivalent" is given by about 150 scf of magnegas ("gasoline liter equivalent" is given by about 29 liters of magnegas). PlasmaArcFlow reactors are completely self-contained. Consequently, they release no solid, liquid or gas to the environment and cause no noise or odor pollution (see website [5b] for details).

PlasmaArcFlow Reactors use a submerged DC electric arc between carbon-base electrodes to achieve the complete recycling of essentially any type of (nonradioactive) liquid waste into the clean burning magnegas fuel, heat usable via exchangers, and carbonaceous precipitates used for the production of electrodes. The reactors are ideally suited to recycle antifreeze waste, oil waste, sewage, and other contaminated liquids, although they can also process ordinary fresh water. The best efficiency is achieved in these reactors for the recycling of carbon-rich liquids, such as crude oil or oil waste.

The new PlasmaArcFlow technology is essentially based on flowing liquids through a submerged DC arc with at least one consumable carbon electrode (see Figures 11.8 and 11.9). The arc decomposes the liquid molecules and the carbon electrode into a plasma at about $5,000^oC$, which plasma is composed of mostly ionized H, O and C atoms. The technology moves the plasma away from the electric arc immediately following its formation, and controls the

recombination of H, O and C into magnegas, that bubbles to the surface where it is collected with various means. Other solid substances generally precipitate at the bottom of the reactor where they are periodically collected.

Since magnegas is formed under the extremely intense magnetic fields at atomic distances from the electric arc, its chemical structure is that of all possible magnecules with increasing atomic mass that can be formed from the H, C and O atoms, such as

$$H - H, \quad H \times H, \quad (H - H) \times H \quad H \times H \times H;$$

$$C - H, \quad C \times H, \quad (C - H) \times H, \quad C - O,$$

$$C \times O, \quad C \times (O - O), \quad etc. \tag{11.4.1}$$

where we should note that the bond between C and O can be single, double, and triple valence type as well as of magnecular nature.

When reduced to *atomic* (rather than molecular) percentages, magnegas produced from pure water is composed of about

$$66\% H, \quad 22\% O, \quad 11\% C. \tag{11.4.2}$$

As we shall see in this section, under GC-MS/IRD detectors magnegas shows peaks from 2 amu to 1,000 amu even when produced from pure water. To understand the anomaly ands the *necessity* of a new chemical species to avoid nonscientific beliefs, the reader should be aware that the maximal molecular species predicted by quantum chemistry for magnegas produced from water is CO_2 with 44 amu.

Chemical structure (11.3.1) also explains the capability of magnegas to have combustion exhaust without any toxic components, while being rich of breathable oxygen up to 14% and more (see later on). In fact, the combustion exhaust of magnegas are given by

$$50 - 55\% H_2O, \quad 12 - 14\% O_2, \quad 5 - 7\% CO_2, \quad atmospheric \quad gases. \tag{11.4.3}$$

where the CO_2 content originates from the combustion of conventional carbon monoxide, that of triple bonded nature $\equiv O$ and the stochiometric ratio magnegas/atmosphere is taken into consideration.

the availability in the exhaust of a ;large percentage of breathable oxygen is primarily due to the magnecular bond of oxygen with other species that breaks down at the *Magnegas Curie temperature* generally coinciding with the flame temperature at which all bonds of magnetic origin cease to exhaust. consequently, *magnegas exhaust is solely composed of conventional molecules without any magnecular content.*

The large percentage in the exhaust of breathable oxygen is also due to the conventional single $C - O$ and double bonded species $C = O$ that are

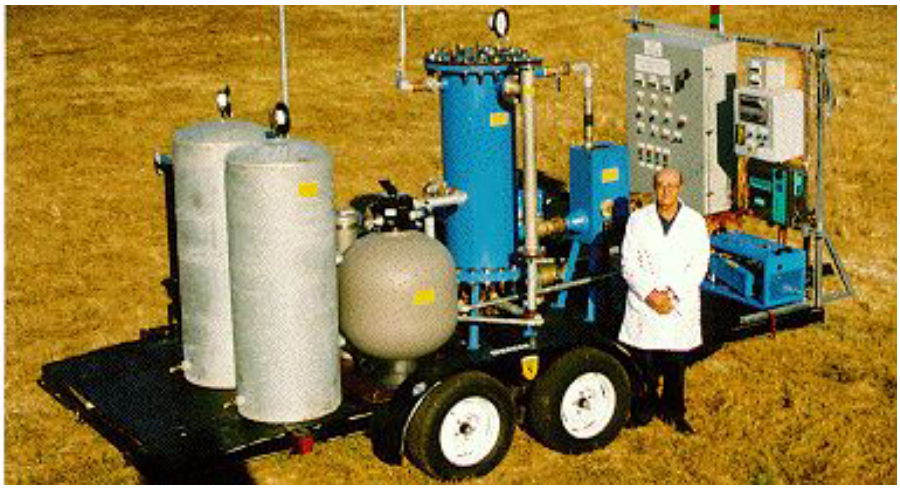

Figure 11.14. Picture of a 50 Kw Santilli's Hadronic Reactor (PlasmaArcFlow Recycler) mounted on a trailer for mobility to conduct test recycling where liquid wastes are located. This recycler can produce up to $84,000$ scf (up to $2.4M$ liters) of magnegas per week corresponding to about 560 gasoline gallon equivalent ($2,100$ gasoline liter equivalent) of magnegas per week (see website [5b] for details).

unstable and can decompose into gaseous oxygen and carbon precipitate when the combustion is at atmospheric pressure (because high pressure $C - O$ and $C = O$ can turn into $C \equiv O$).

the efficiency of Santilli's hadronic reactor of Class III is very high because their primary source of energy is given by a new type of highly efficient and clean combustion of carbon, releasing energy that is at last 30 times the electric energy used by the arc.

In fact, we have the following *Scientific Efficiency* (SE) of PlasmaArcFlow Reactors that is evidently always *smaller* than one due to the conservation of the energy and the inevitable dispersions

$$SE = \frac{E_{tot}^{out}}{E_{tot}^{in}} = \frac{(E_{MG} + E_{heat})}{(Earc + E_{carbon} + E_{unknown})} < 1, \tag{11.4.4}$$

where E_{MG} is the combustion energy contained in magnegas, E_{heat} is the heat acquired by the liquid feedstock and the vessel,$Earc$ is the electric energy used by the arc, E_{carbon} is the energy produced by the combustion of carbon in the plasma, and $E_{unknown}$ is an unknown source of energy due to the fact that the sum $E_{arc} + E_{carbon}$ cannot explain the total energy output (see later on in this section and the next chapter).

At the same time we have the following *Commercial Efficiency* (CE) given by the preceding one *without* the inclusion of the energy produced by the carbon combustion because the carbon content of the liquid feedstock generally brings an *income,* rather than a cost, since it is contained in the liquid waste to be, and without the unknown source of energy since it also carries no cost recycled

$$CE = \frac{E_{tot}^{out}}{E_{tot}^{in}} = \frac{(E_{MG} + E_h eat)}{Earc} >> 1, \tag{11.4.5}$$

which value is much bigger than one because, as indicated above, the energy caused by the combustion of carbon in the plasma under the electric arc and the unknown energy are a large multiple of the electric energy used by the arc.

When operated at atmospheric pressure, at 50 Kw power and at ambient temperature, the above commercial efficiency has a minimum value of about 5. However, the efficiency of Santilli's hadronic reactors increases (nonlinearly) with the increase of pressure, power and operating temperature and can assume rather high value. For instance, when operating a PlasmaArcFlow Recycler at about 150 psi (10 bars), 300 Kw and 275^oF (125^oC), the commercial efficiency can be of the order of 30, that is, per each unit of electric energy used by the arc, the reactor produces 30 times that energy in a combination of energy contained in magnegas and usable heat.

The above very high commercial efficiency of PlasmaArcFlow reactors illustrates the reason why magnegas is cost competitive with respect to all available fossil fuels.

By comparison, one should note that, in other methods based on underwater arcs, the stationary character of the plasma within the arc implies the creation of large percentages of CO_2 resulting in a CO_2 content of the exhaust much greater than that of gasoline and natural gas, measured by the author to be of the order of 18%. The resulting fuel is then environmentally unacceptable since CO_2 is responsible for the green house effect.

Recall that the primary source of the large glow created by underwater arcs is the recombination of H and O into H_2O following its separation. This recombination is the reason for the low efficiency of underwater arcs and consequential lack of industrial development until recently.

By comparison, the PlasmaArcFlow causes the removal of H and O from the arc immediately following their creation, thus preventing their recombination into H_2O, with consequential dramatic increase of the efficiency, that is, of the volume of combustible gas produced per Kwh.

A Ferrari 308 GTS, an SUV, two Honda and other automobiles have been converted by the author to operate on magnegas. One of these vehicles has been subjected to intensive tests at an EPA certified automotive laboratory in Long Island, New York reviewed in details in the next subsection, which

Figure 11.15. A picture of a Ferrari 308 GTSi 1980 and two Honda Civic cars converted by the author to operate with the new clean burning magnegas without catalytic converter, yet surpassing all EPA exhaust requirements, having no carcinogenic or other toxic substance in the exhaust, reducing of about 50% the CO_2 emission due to gasoline combustion, reducing the operating temperature of about 25%, and emitting in the exhaust 10% to 14% breathable oxygen (see website [5b] for details).

tests have established that magnegas exhaust surpasses all EPA requirements *without catalytic converter*, and confirmed data (11.3.3).

In addition to the production of magnegas as a fuel, *the PlasmaArcFlow Reactors can be viewed as the most efficient means for producing a new form of hydrogen, called MagneHydrogen^{TM}, a carbon-free version of magnegas, with energy content and output greater than the conventional hydrogen, and at a cost smaller than that of the latter* (see next section).

Figure 11.16. A picture of a Chevrolet Suburban SUV 1992 converted by the author to operate as a bifuel gasoline/magnegas with a switch on the dashboard permitting to pass from one fuel to the other while driving. Bifuel cars are produced by numerous carmakers to operate on gasoline and natural gas. The same cars can operate on magnegas (in place of natural gas) with the sole adjustment of the pressure regulator to optimize the stochiometric ratio air/fuel, since the latter for magnegas is much smaller than that for natural gas because magnegas is very rich internally in oxygen, thus requiring a fraction of the air needed by natural gas to operate. These bifuel cars are ideally suited for the magnegas technology because, when magnegas runs out, one can still reach the magnegas refilling station on gasoline (see website [5b] for details).

11.4.2 Surpassing by Magnegas Exhaust of EPA Requirements without Catalytic Converter

As indicated above, while the chemical composition of magnegas is new, the chemical composition of magnegas combustion exhaust is fully conventional, and it has been measured with accuracy.

The tests were conducted by an EPA accredited automotive laboratory of Long Island, new York, on a Honda Civic Natural Gas Vehicle (NGV) VIN number 1HGEN1649WL000160 (the white car of Fig. 11x10), produced in 1998 to operate with Compressed Natural Gas (CNG). The car was purchased new in 1999 and converted to operate on Compressed MagneGas (CMG) in early 2000. All tests reported in this section were done with magnegas produced by recycling antifreeze waste. The conversion from CNG to CMG was done via:

1) the replacement of CNG with CMG in a 100 liter tank at 3,600 psi which contains about 1,000 cf of magnegas;

2) the disabling of the oxygen sensor because magnegas has about 20 times more oxygen in the exhaust than natural gas, thus causing erroneous readings by the computer set for natural gas; and

3) installing a multiple spark system to improve magnegas combustion.

The rest of the vehicle was left unchanged, including its computer.

Comparative tests on performance (acceleration, full load, etc.) have established that *the output power of the vehicle operating on compressed magnegas is fully equivalent to that of the same car operating on compressed natural gas.*

Comparative tests on consumption also indicate similar results. In fact, measurements of magnegas consumption per hour in ordinary city driving were conducted with the following results:

$$\begin{array}{ll} \text{Tank capacity:} & \text{1,096 cf at 3,500 psi,} \\ \text{Total duration:} & \text{about 2.5 hours,} \\ \text{Consumption:} & \text{about 7 cf/minute.} \end{array} \tag{11.4.6}$$

As one can see, a magnegas pressure tank of 1,500 cf at 5,000 psi would provide a range of about 4 hours, which is amply sufficient for all ordinary commuting and travel needs. Measurements of magnegas consumption rate per mile on highway are under way, and they are expected to yield essentially the same results holding for natural gas, namely,

$$\text{Gasoline gallon equivalent: 120 cf of magnegas.} \tag{11.4.7}$$

Preliminary measurements of magnegas combustion exhaust were conducted by the laboratory *National Technical Systems, Inc.*, of Largo, Florida, resulting in the following exhaust composition under proper combustion:

$$\begin{array}{ll} \text{Water vapor:} & \text{50\% - 60\%,} \\ \text{Oxygen:} & \text{10\% - 12\%,} \\ \text{Carbon dioxide:} & \text{6\% - 7\%,} \\ \text{Balance:} & \text{atmospheric gases,} \\ \text{Hydrocarbons, carbon monoxide,} & \\ \text{nitrogen oxides:} & \text{in parts per million (ppm).} \end{array} \tag{11.4.8}$$

Detailed magnegas exhaust measurements were then conducted at the EPA Certified, Vehicle Certification Laboratory *Liphardt & Associates* of Long Island, New York, under the Directorship of *Peter di Bernardi*, via the Varied Test Procedure (VTP) as per EPA Regulation 40-CFR, Part 86.

These EPA tests consisted of three separate and sequential tests conducted in November 2000 on a computerized dynamometer, the first and the third tests using the vehicle at its maximal possible capability to simulate an uphill travel at 60 mph, while the second test consisted in simulating normal city driving.

Three corresponding bags with the exhaust residues were collected, jointly with a fourth bag containing atmospheric contaminants. The final measurements expressed in grams/mile are given by the average of the measurements on the three EPA test bags, less the measurements of atmospheric pollutants in the fourth bag.

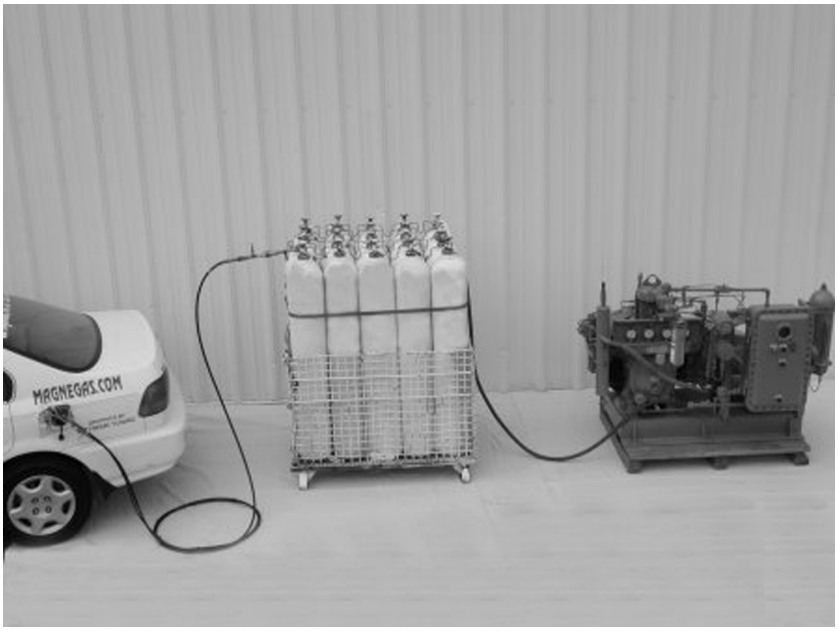

Figure 11.17. [8] A picture of the *Magnegas Refilling Station*, consisting of a standard compressor as used for natural gas and pressure bottles. The simplicity of this station should be compared with the complexity of corresponding stations for liquid hydrogen. Note that the station depicted in this figure allows current *distributors* of fuel, such as gasoline stations, to become *fuel producers*. The refill is achieved by connecting the a pressure bottle with a pressure tank in the trunk of the car; it is faster than the refill with gasoline; and it is much safer than the latter because gasoline, being liquid, spills and explodes if ignited, while magnegas, being a gas, does not spill and if ignited, burns fast in air without explosion (see website [5b] for details).

The following three measurements were released by Liphardt & Associates:
1) Magnegas exhaust measurements with catalytic converter:

HYDROCARBONS:	0.026 grams/mile, which is 0.063 of the EPA standard of 0.41 grams/mile;	
CARBON MONOXIDE:	0.262 grams/mile, which is 0.077 of the EPA standard of 3.40 grams/mile;	
NITROGEN OXIDES:	0.281 grams/mile, which is 0.28 of the EPA standard of 1.00 grams/mile;	(11.4.9)
CARBON DIOXIDE:	235 grams/mile, corresponding to about 6%; there is no EPA standard on CO_2 at this time;	
OXYGEN:	9.5% to 10%; there is no EPA standard for oxygen at this time.	

The above tests have established the important feature that *magnegas exhaust with catalytic converter imply a reduction of about 1/15 of current EPA requirement*.

2) Magnegas exhaust measurements without catalytic converter in the same car and under the same conditions as (1):

HYDROCARBONS:	0.199 grams/mile, which is 0.485 of the EPA standard of 0.41 grams/mile;	
CARBON MONOXIDE:	2.750 grams/mile, which is 0.808 of the EPA standard of 3.40 grams/mile;	(11.4.10)
NITROGEN OXIDE:	0.642 grams/mile, which is 0.64 of the EPA standard of 1.00 grams/mile;	
CARBON DIOXIDE:	266 grams/mile, corresponding to about 6%;	
OXYGEN:	9.5% to 10%.	

As a result of the latter tests, the laboratory *Liphardt & Associates* released the statement that *magnegas exhaust surpasses the EPA requirements* without *the catalytic converter*. As such, magnegas can be used in *old cars without catalytic converter while meeting, and actually surpassing EPA emission standards*.

3) Natural gas exhaust measurements without catalytic converter in the same car and under the same conditions as (1):

HYDROCARBONS:	0.380 grams/mile, which is 0.926 of the EPA standard of 0.41 grams/mile;	
CARBON MONOXIDE:	5.494 gram/mile, which is 1.615 of the EPA standard of 3.40 grams/mile;	
NITROGEN OXIDES:	0.732 grams/mile, which is 0.73 the EPA standard of 1.00 grams/mile;	(11.4.11)
CARBON DIOXIDE:	646.503 grams/mile, corresponding to about 9%;	
OXYGEN:	0.5% to 0.7%.	

The latter tests established the important property that *the combustion of natural gas emits about 2.5 times the CO_2 emitted by magnegas without catalytic converter. Note that, as well known, natural gas exhaust without catalytic converter does not meet EPA requirements*.

As an additional comparison for the above measurements, a similar Honda car running on indolene (a version of gasoline) was tested in the same laboratory with the same EPA procedure, resulting in the following data:

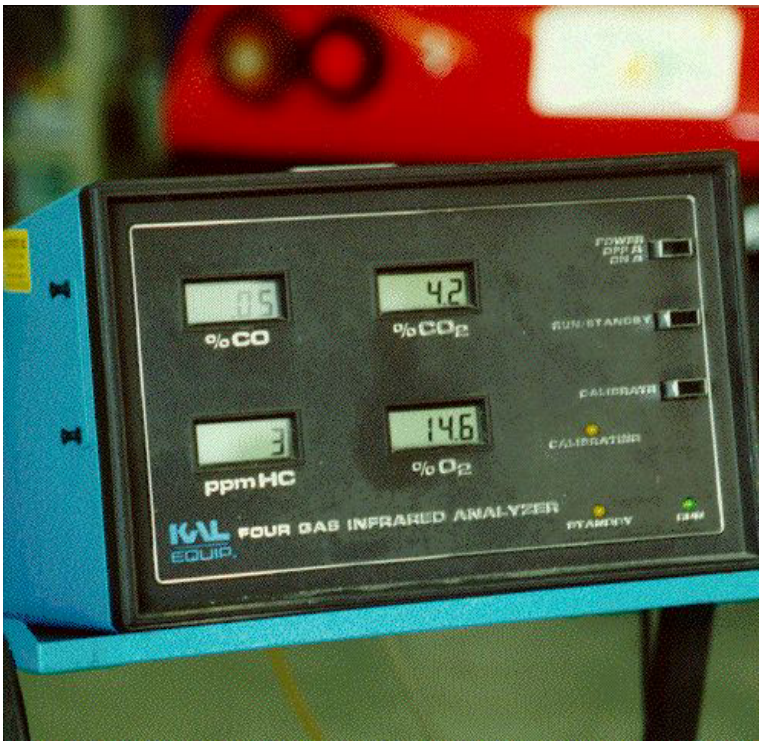

Figure 11.18. A picture of the readings of a 4-ways exhaust analyzer testing the exhaust of the Ferrari 308 GTSi of a preceding picture operating on magnegas "without" catalytic converter. Note: the presence of 14% breathable oxygen in the exhaust; about half the CO_2 produced by the same car when running on gasoline; the very few detected hydrocarbons originate from engine oil seeping through the piston rings because magnegas "cannot" contain hydrocarbons since it is synthesized at the $5,000^oC$ of the arc at which temperature no hydrocarbon can survive; the very small content of CO in the exhaust is due to poor combustion because CO is fuel for magnegas, while it is a byproduct of the combustion for fossil fuels, as a result of which detecting CO in the exhaust of a car running on magnegas is the same as detecting gasoline in the exhaust of a car running on gasoline (see website [5b] for details).

4) Gasoline (indolene) exhaust measurements conducted on a two liter Honda KIA:

Hydrocarbons:	0.234 grams/mile equal to 9 times the corresponding magnegas emission;	
Carbon monoxide:	1.965 grams/mile equal to 7.5 times the corresponding magnegas emission;	
Nitrogen oxides:	0.247 grams/mile equal to 0.86 times the corresponding magnegas emission;	(11.4.12)
Carbon dioxide:	458.655 grams/mile equal to 1.95 times the corresponding of magnegas emission,	
Oxygen:	No measurement available.	

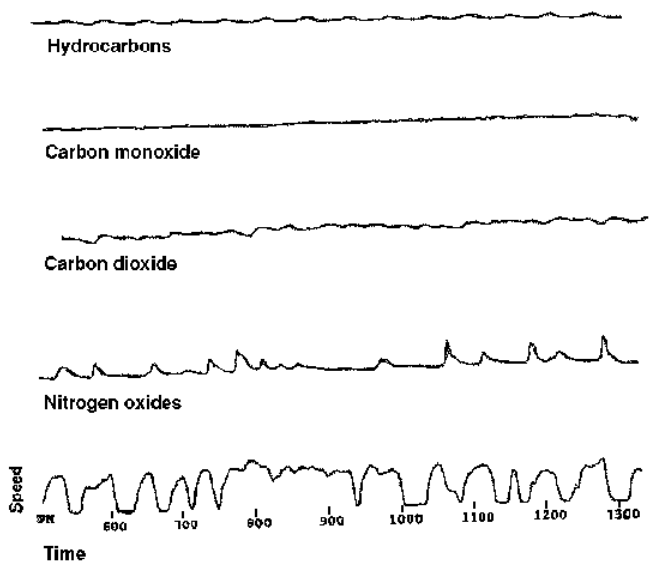

Figure 11.19. An illustration of the city part of the reported EPA test according to Regulation 40-CFR, Part 86, conducted at the Vehicle Certification Laboratory *Liphardt & Associates* of Long Island, New York on a Honda Civic Natural Gas Vehicle converted to magnegas by the author.. The first three diagrams illustrate the very low combustion emission of magnegas in city driving, by keeping in mind that most of measured emission is due to the heavy duty, hill climbing part of the EPA test. The fourth diagram on nitrogen oxides is an indication of insufficient cooling of the engine. The bottom diagram indicates the simulated speed of the car versus time, where flat tracts simulate idle portions at traffic lights.

The above data establish the environmental superiority of magnegas over natural gas and gasoline. The following comments are now in order:

1) Magnegas does not contain (heavy) hydrocarbons since it is created at $3{,}500^o$ K. Therefore, the measured hydrocarbons are expected to be due to combustion of oil, either originating from magnegas compression pumps (thus contaminating the gas), or from engine oil.

2) Carbon monoxide is fuel for magnegas (while being a combustion product for gasoline and natural gas). Therefore, any presence of CO in the exhaust is evidence of insufficient combustion.

3) The great majority of measurements originate from the first and third parts of the EPA test at extreme performance, because, during ordinary city traffic, magnegas exhaust is essentially pollutant free [5].

Figure 11.20. It is generally ignored that cruiseships leave a trail of marine death since they release in the ocean an average of 100,000 gallons of highly contaminated liquid wastes per day. The magnegas technology [5] was developed to resolve this problem via the on board recycling of all liquid waste into purified forms reusable on board without any release in the ocean.

4) Nitrogen oxides are not due, in general, to the fuel (whether magnegas or other fuels), but to the temperature of the engine and other factors, thus being an indication of the quality of its cooling system. Therefore, for each given fuel, including magnegas, NOx's can be decreased by improving the cooling system and via other means.

5) The reported measurements of magnegas exhaust do not refer to the best possible combustion of magnegas, but only to the combustion of magnegas in a vehicle whose carburization was developed for natural gas. Alternatively, the test was primarily intended to prove that magnegas is interchangeable with natural gas without any major automotive changes, while keeping essentially the same performance and consumption. The measurements for combustion specifically conceived for magnegas are under way.

We should also indicate considerable research efforts under way to further reduce the CO_2 content of magnegas exhaust via disposable cartridges of CO_2-absorbing chemical sponges placed in the exhaust system (patent pending). Additional research is under way via *liquefied magnegas* obtained via *catalytic* (and *not* conventional) liquefaction, which liquid is expected to have an anomalous energy content with respect to other liquid fuels, and an expected consequential decrease of pollutants. As a result of these efforts, the achievement of an exhaust essentially free of pollutants and CO_2, yet rich in oxygen, appears to be within technological reach.

11.4.3 Anomalous Chemical Composition of Magnegas

As studied in the preceding section, the chemical composition of the magnegas exhaust is conventional and, therefore, can be tested with established analytic equipment and methods. However, the chemical composition of magnegas itself cannot be successfully tested with the same equipment and methods due to its novelty.

To begin, numerous tests in various analytic laboratories reviewed in below have established that magnegas results in being characterized by large peaks in macroscopic percentage all the way to $1,000$ a.m.u., which peaks remain individually unidentified by the MS computer after scanning all known molecules.

By comparison, quantum chemistry predicts that the heaviest molecule in a *light* gas such as magnegas should only have 44 a.m.u., while offering no explanation whatever, not even remote or indirect on the existence of detectable teaks all the way to $1,000$ a.m.u.

The above differences are so drastic to provide clear experimental evidence on the fact that the magnegas structure is characterized by a *new chemical species* not predicted or considered by quantum chemistry until now.

Besides the inability to identify the clusters composing magnegas via the computer search among all known molecules, the chemical structure of magnegas is equally unidentifiable via InfraRed Detectors (IRD), because the new peaks composing magnegas have no IR signature at all, thus establishing the presence of bonds of non-valence type (because these large clusters cannot possibly be all symmetric).

Moreover, the IR signature of conventional molecules such as CO results in being *mutated* (in the language of hadronic mechanics) with the appearance of new peaks, which evidently indicate *new* internal bonds in *conventional* molecules.

In addition to all the above, dramatic differences between the prediction of quantum chemistry and reality exist for the energy content of magnegas. For instance, when produced with PlasmaArcFlow Reactors operating an electric arc between at least one consumable electrode within pure water, quantum chemistry predicts that magnegas should be a mixture of 50% H_2 and 50% CO, with traces of O_2 and CO_2.

This prediction is dramatically disproved by the fact that *both the* CO *and the* CO_2 *peaks do not appear in the MS scan in the predicted percentages, while they appear in the IR scan although in a mutated form.*

Moreover, quantum chemistry predicts that the indicated composition consisting of 50% H_2 and 50% CO should have an energy content of about 315 BTU/cf, namely, an energy content insufficient to cut metal. This prediction

is also disproved by the experimental evidence that *magnegas cuts metal at least 50% faster than acetylene (which has 2,300 BTU/cf).*

Such a performance in metal cutting is more indicative of a *plasma cutting* feature, such as the metal cutting via a plasma of ionized hydrogen atoms which recombine into H_2 when cooling in the metal surface, thus releasing the energy needed for metal cutting. The problem is that magnegas is at room temperature when used for metal cutting, and it is subjected to ordinary combustion, thus requiring basically new approaches for its correct interpretation.

Nevertheless, the plasma cutting feature is indicative of the presence of isolated atoms and dimers in the magnegas structure which recombine under combustion, thus yielding a behavior and a performance similar to that of plasma cutters.

In fact, as also shown later on, GC-MS scans have indicated the presence in the anomalous peaks of *individual atoms of hydrogen, oxygen, and carbon* evidently in addition to individual molecules.

To conclude, the composition of magnegas in H, C and O *atoms* can be easily identified from the liquid used in the reactors. For instance, when magnegas is produced from water, it is composed of 50% H, 25% O, and 25% C, with corresponding percentages for other liquids such as antifreeze, crude oil, etc.

However, all attempts to reduce the chemical composition of magnegas to conventional molecules conducted by the author as well as independent chemists, have been disproved by a variety of experimental evidence.

In particular, any belief that magnegas is entirely composed by ordinary molecules, such as H_2 and CO, is disproved by experimental evidence via GC-MS and IRD detectors.

The only possible scientific conclusion at this writing is that *magnegas is composed of a new chemical species* studied below.

11.4.4 GC-MS/IRD Measurements of Magnegas at the McClellan Air Force Base

Santilli [1] had predicted that gases produced from underwater electric arcs had the new chemical structure of magnecules as clusters of molecules, dimers and individual atoms as per Definition 8.2.1, in which case conventional chemical structure (8.20) is valid only in first approximation.

Following a laborious search, Santilli [*loc. cit.*] located a GC-MS equipped with IRD suitable to measure magnecules at the *McClellan Air Force Base* in North Highland, near Sacramento, California. Thanks to the invaluable assistance and financial support by *Toups Technologies Licensing, Inc.*, of Largo, Florida, GC-MS/IRD measurements were authorized at that facility on magnegas with conventional chemical structure (8.20).

On June 19, 1998, Santilli visited the analytic laboratory of *National Technical Systems* (NTS) located at said *McClellan Air Force Base* and using

instruments belonging to that base. The measurements on magnegas were conducted by analysts Louis A. Dee, Branch Manager, and Norman Wade who operated an *HP GC model 5890, an HP MS model 5972, equipped with an HP IRD model 5965.* Upon inspection at arrival, the instrument met all conditions indicated in the preceding sections then, and only then, measurements were permitted.

Thanks to a professional cooperation by the NTS analysts, the equipment was set at all the unusual conditions indicated later on. In particular, the equipment was set for the analytic method VOC IRMS.M utilizing an HP Ultra 2 column 25 m long with a 0.32 mm ID and a film thickness of 0.52 μm. It was also requested to conduct the analysis from 40 a.m.u. to the instrument limit of 500 a.m.u. This condition was necessary to avoid the expected large CO peak of magnegas at 28 a.m.u.

Moreover, the GC-MS/IRD was set at the low temperature of 10°C; the biggest possible feeding line with an ID of 0.5 mm was installed; the feeding line itself was cryogenically cooled; the equipment was set at the longest possible ramp time of 26 minutes; and a linear flow velocity of 50 cm/sec was selected. A number of other technical requirements are available in the complete documentation of the measurements.

The analysts first secured a documentation of the *background* of the instrument prior to any injection of magnegas (also called *blank*). Following a final control that *all* requested conditions were implemented, the tests were initiated. The results, reported in part via the representative scans of Figs. 8.7 to 8.12, constitute the first direct experimental evidence of the existence of magnecules in gases.

After waiting for 26 minutes, sixteen large peaks appeared on the MS screen between 40 and 500 a.m.u. as shown in Fig. 11.21. Each of these sixteen MS peaks resulted to be "unknown," following a computer search of database on all known molecules available at *McClellan Air Force Base*, as illustrated in Fig. 11.22 No identifiable CO_2 peak was detected at all in the MS spectrum between 40 and 500 a.m.u., contrary to the presence of 9% of such a molecule in magnegas as per conventional analyses (8.20).

Upon the completion of the MS measurements, exactly the same range of 40 to 500 a.m.u. was subjected to IR detection. As expected, none of the sixteen peaks had any infrared signature at all, as shown in Fig. 11.14. Furthermore, the IR scan for these MS peaks shows only one peak, that belonging to CO_2, with additional small peaks possibly denoting traces of other substances.

Note that the IR signature of the other components, such as CO or O_2 *cannot* be detectable in this IR test because their atomic weights are below the left margin of the scan. In addition, the IR peak of CO_2 is itself mutated from that of the unpolarized molecule, as shown in Fig. 11.24. Note that the mutation is due to the appearance of *two new peaks* which are absent in the

```
Information from Data File:
File        : C:\HPCHEM\1\DATA\0618004.D
Operator    : NAW
Acquired    : 18 Jun 98   3:01 pm using AcqMethod VOC_IRMS
Sample Name: TOUP'S TECH
Misc Info   : 1ML LOOP; 10C @ ULTRA COLUMN
Vial Number: 1
CurrentMeth: C:\HPCHEM\1\METHODS\DEFAULT.M
```

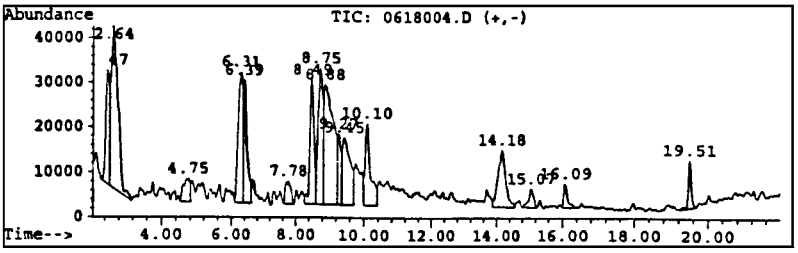

Retention Time	Area	Area %	Ratio %
Total Ion Chromatogram			
2.474	1753306	5.386	32.724
2.644	5091514	15.641	95.030
4.754	641528	1.971	11.974
6.307	2737749	8.411	51.098
6.390	2211258	6.793	41.272
7.782	592472	1.820	11.058
8.490	2357396	7.242	43.999
8.754	2784829	8.555	51.977
8.882	5357812	16.460	100.000
9.265	1123809	3.452	20.975
9.448	2421234	7.438	45.191
10.098	1946292	5.979	36.326
14.177	2129791	6.543	39.751
15.073	435208	1.337	8.123
16.085	389822	1.198	7.276
19.509	577433	1.774	10.777

Figure 11.21. A reproduction of the MS peaks providing the *first experimental evidence of the existence of magnecules* identified on June 19, 1998, by analysts *Louis A. Dee* and *Norman Wade* of the branch of *National Technical; Systems* (NTS) located at the *McClellan Air Force Base* in North Highland, near Sacramento, California, with support from *Toups Technologies Licensing, Inc.* (TTL) of Largo, Florida. The scan is restricted from 40 a.m.u to 500 a.m.u. The peaks refer to magnegas produced via an electric arc between consumable carbon electrodes within ordinary tap water with conventional chemical composition (8.20). Therefore, only the CO_2 peak was expected to appear in the scan with any macroscopic percentage, while no CO_2 was detected at all in the MS scan.

conventional IR signature of CO_2, exactly as expected, thus confirming the hypothesis of new internal bonds as submitted in Fig. 11.12.

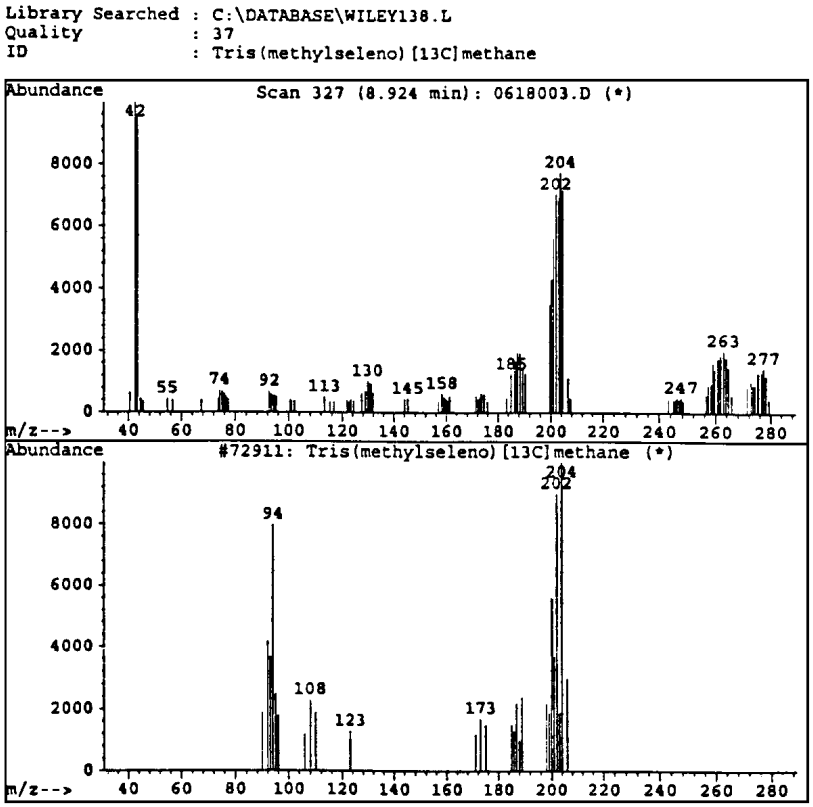

Figure 11.22. A representation of *the first experimental evidence at NTS that the peaks of Fig. 11.12 are "unknown."* The peak at the top is at 8.924 minutes, and that at the bottom shows the lack of its identification by the computer search. Note that the best fit identified by the computer does not match the peak considered. Moreover, the identified substance (methylseleno) cannot possibly exist in magnegas because of the impossible presence of the necessary elements. The same situation occurred for all remaining fifteen peaks of Fig. 11.12.

Note also in Fig. 24 that the computer interprets the IR signature as that belonging to CO which interpretation is evidently erroneous because CO is outside of the selected range of a.m.u.

All remaining small peaks of the IR scan resulted to be "unknown," thus being possible magnecules, following computer search in the database of IR signatures of all known molecules available at the *McClellan Air Force Base*, as illustrated in Fig. 11.25.

Following the removal of magnegas from the GC-MS/IRD, the background continued to show the same anomalous peaks of Fig. 11.21, and reached the

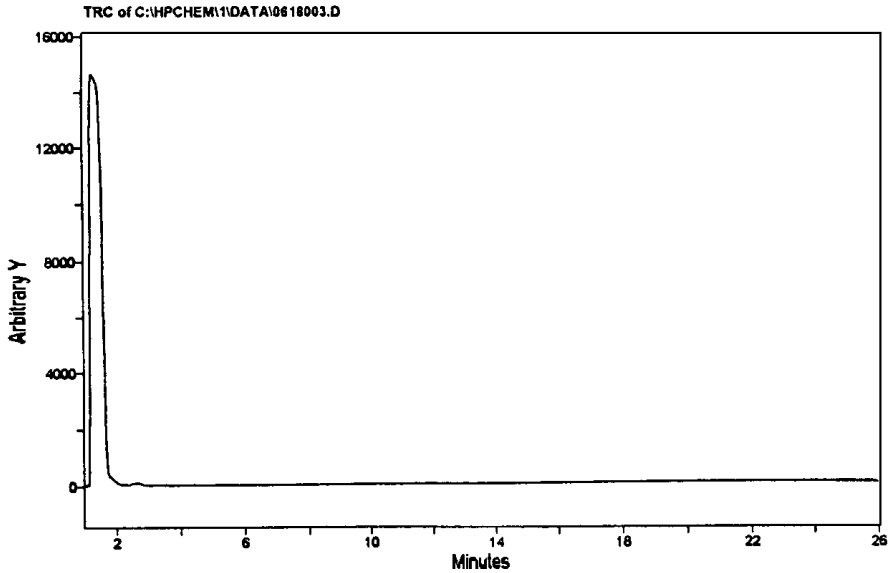

Figure 11.23. The first experimental evidence at NTS of the lack of IR signature of MS peaks. The evidence establishes the existence of large peaks in the MS that have no IR signature at all. The only identified IR signature, that for CO_2, refers to the *constituents* of the peaks of Fig. 11.12. In the above figure only the IR signature of CO_2 appears because the scan was from 40 a.m.u. to 500 a.m.u. and, as such, could not include the IR signatures of other molecules such as O_2 and CO (H_2 has no IR signature).

configuration of Fig. 11.26 only after a weekend bakeout with an inert gas. Note that the latter background is itself anomalous because the slope should have been the opposite of that shown. The background finally recovered the conventional shape only after flushing the instrument with an inert gas at high temperature.

11.4.5 GC-MS/IRD Tests of Magnegas at Pinellas County Forensic Laboratory

Measurements on the same sample of magnegas tested at NTS were repeated on July 25, 1998, via a GC-MS/IRD located at the *Pinellas County Forensic Laboratory* (PCFL) of Largo, Florida, with support from *Toups Technologies Licensing, Inc.*

The equipment consisted of a *HP GC model 5890 Series II, an HP MS model 5970 and an HP IRD model 5965B.* Even though similar to the equipment used at NTS, the PCFL equipment was significantly different inasmuch as the temperature had to be increased from 10°C to 55°C and the ramp time

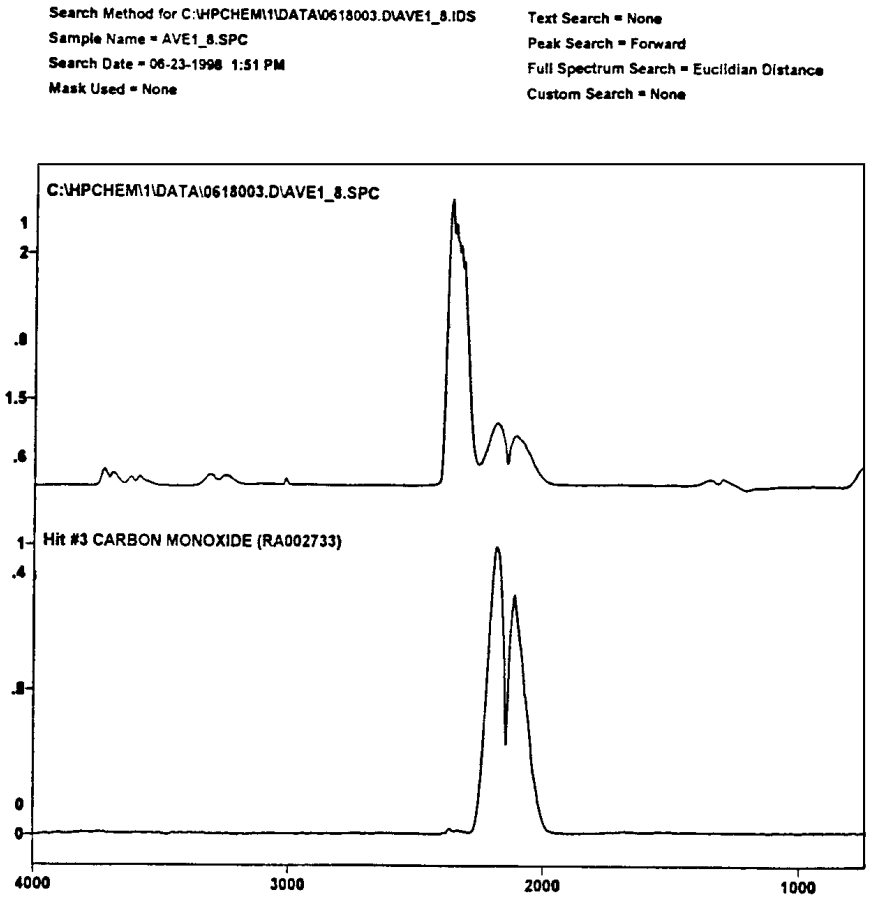

Figure 11.24. The first experimental evidence at NTS on the mutation of the IR signature of magnetically polarized conventional molecules, here referring to the CO_2 (top) compared to the result of the computer search (bottom). Note that the known, double-lobe peak of CO_2 persists in the detected peak with the correct energy, and only with decreased intensity. Jointly, there is the appearance of *two new peaks*, which are evidence of *new internal bonds within the conventional CO_2 molecule.* This evidently implies an increased energy content, thus establishing experimental foundations for the new technology of magnetically polarized fuels such as magnegas [2].*Note that the computer interprets the IR signature as that of CO, which is erroneous since CO is out of the selected range of detection.*

reduced from 26 to 1 minute. The latter reduction implied the cramping of all peaks of Fig. 11.17 into one single large peak, a feature confirmed by all subsequent GC-MS tests with short ramp time.

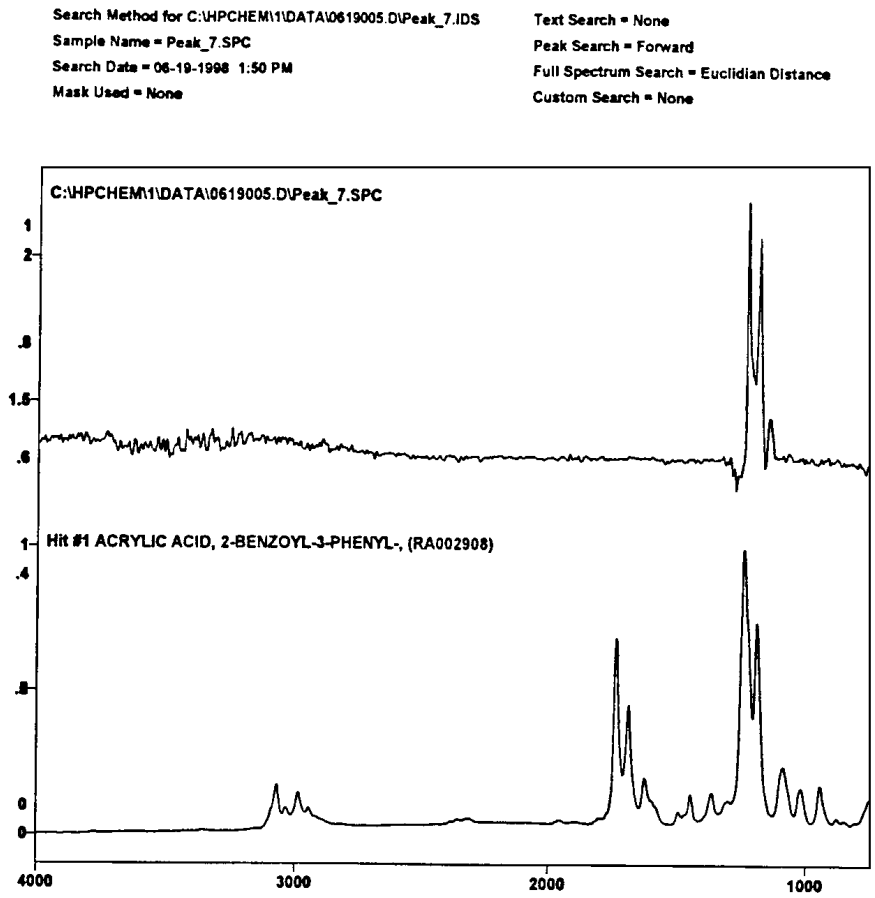

Figure 11.25. A reproduction of the lack of identification in the computer search of small peaks in the IR scan, which can therefore be additional magnecules, or IR signatures of the magnecules appearing in the MS scan.

Despite these differences, the test at PCFL, reported in part via the representative scans of Figs. 8.13 to 8.18, confirmed *all* features of magnecules first detected at NTS. In addition, the tests provided the experimental evidence of additional features.

Following Santilli's request [1], the analysts conducted *two* MS tests of the *same* magnegas at *different times* about 30 minutes apart. As one can see in Figs. 8.13 and 8.14, *the test at PCFL provided the first experimental evidence of mutation in time of the atomic weight of magnecules.* In fact, the peak of Fig. 11.27e is macroscopically different than that of Fig. 11.28.

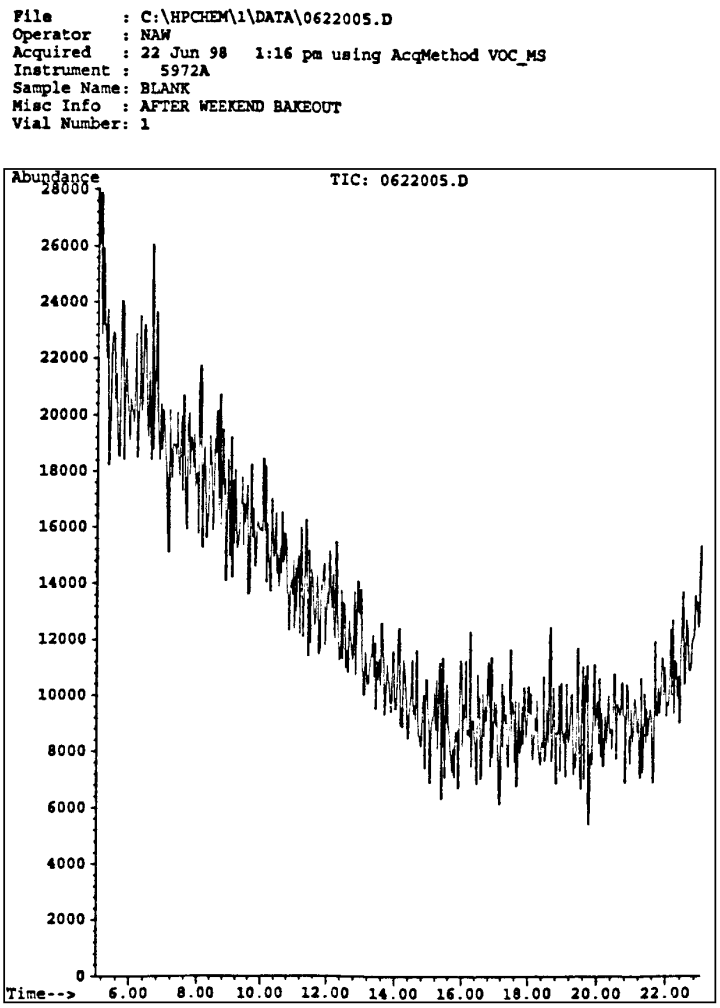

Figure 11.26. A view of the background of the preceding tests following a weekend bakeout.

This difference provides evidence that, when colliding, magnecules can break down into ordinary molecules, atoms, and fragments of magneclusters, which then recombine with other molecules, atoms, and/or magnecules to form new clusters. The same scan provides first experimental evidence of the accretion or loss by magnecules of individual atoms, dimers and molecules, as discussed later on.

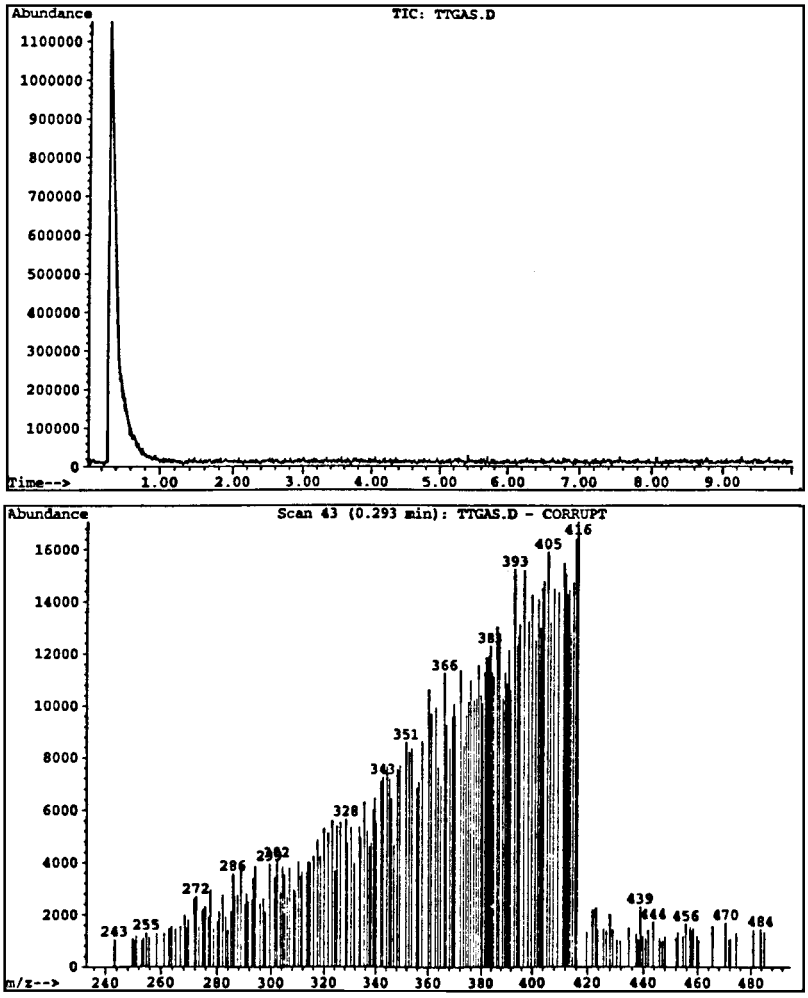

Figure 11.27. A view of the Total Ion Count (top) and MS spectrum (below) of magnegas conducted on July 25, 1998, via a HP GC-MS/IRD at the *Pinellas County Forensic Laboratory* (PCFL) of Largo, Florida, under support from *Toups Technologies Licensing, Inc.* (TTL) also of Largo, Florida. The scan is restricted to the range 40 a.m.u to 500 a.m.u. and confirm all results of the preceding NTS tests.

Figure 8.15 depicts the failure by the GC-MS/IRD to identify the peaks of Figs. 8.13 and 8.14 following a search in the database among all known molecules.

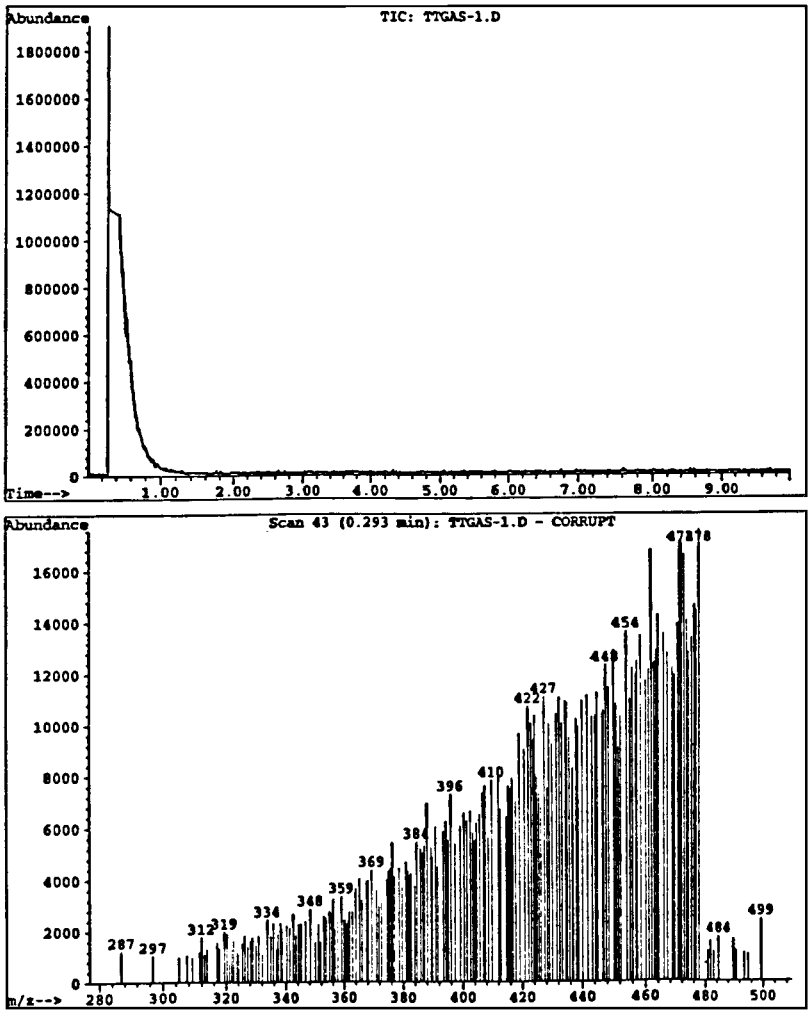

Figure 11.28. A repetition of the scan of the preceding figure conducted at PCFL in the same sample of magnegas on the same instrument and under the same conditions, but 30 minutes later. The scan provides *the first experimental evidence of the mutation of atomic weight of magnecules,* as one can see from the variation of the peaks of this figure compared with that of the preceding figure.

Figure 8.16 provides an independent confirmation that the IR scan of Fig. 11.23, namely, that the MS peaks, this time of Figs. 8.13 and 8.14, have no IR signature except for the single signature of the CO_2. However, the latter was not detected at all in said MS scans. Therefore, the CO_2 detected in said IR scan

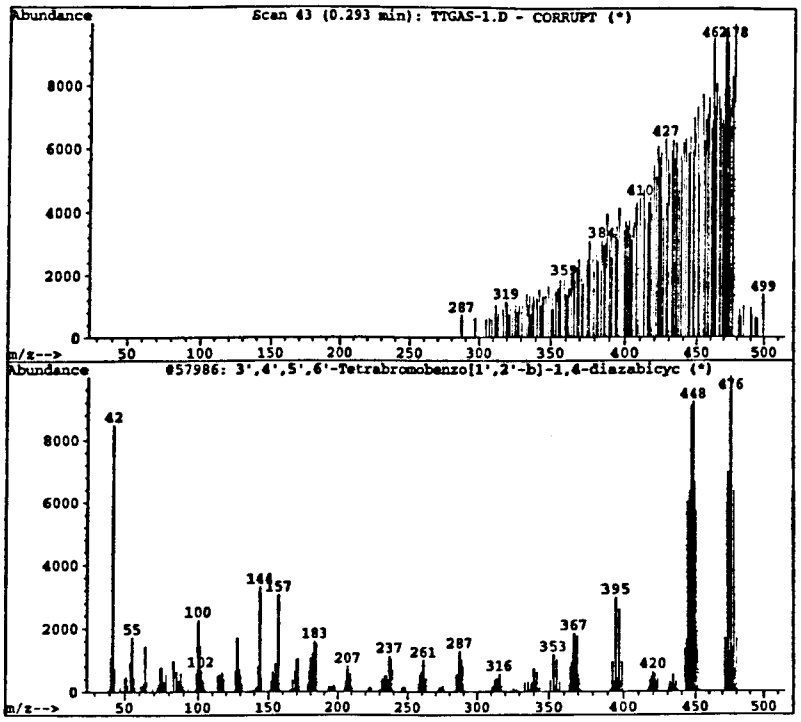

Figure 11.29. Lack of identification by the computer of the GC-MS/IRD at PCFL of the MS peaks of the preceding two scans following search among the database on all available molecules.

is a *constituent* of the new species detected in Figs. 8.13 and 8.14. The lack of IR signature of the MS peaks confirms that said peaks *do not* represent molecules.

Figure 8.17 confirms in full the mutated IR signature of CO_2 previously identified in Fig. 11.24, including the important presence of two new peaks, with the sole difference that, this time, the computer correctly identifies the IR signature as that of carbon dioxide.

Figure 8.18 presents the background of the instrument after routine flushing with an inert gas, which background essentially preserves the peaks of the MS scans, thus confirming the unique adhesion of magnecules to the instrument walls.

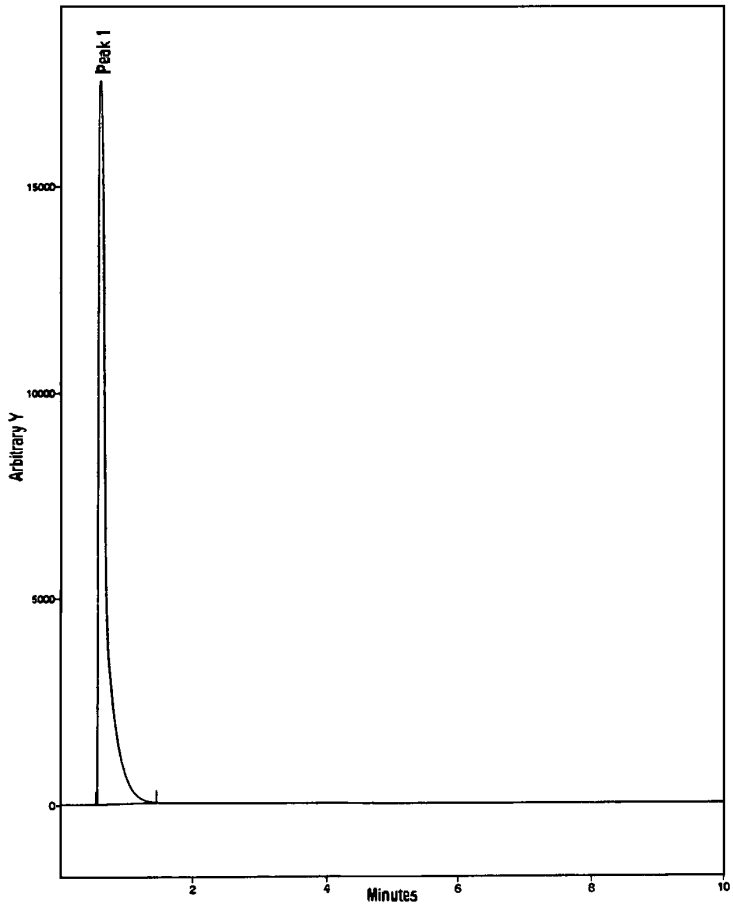

Figure 11.30. A confirmation of the lack of IR signature of the peaks of Figs. 8.13 and 8.14, as occurred for Fig. 11.14, which establishes that the MS peaks of Figs. 8.13 and 8.14 cannot have a valence bond, thus constituting a new chemical species.

11.4.6 Interpretations of the Results

A few comments are now in order for the correct interpretation of the results. First, note in the GC-MS/IRD scans that the CO_2 detected in the IRD has no counterpart in the MS scans, while none of the peaks in the MS have a counterpart in the IR scans. Alternatively, the CO_2 peak detected in the IR scans of Figs. 8.10 and 8.17 *does not* correspond to any peak in the MS scans in Figs. 8.7, 8.13 and 8.14. Therefore, said IR peak identifies a *constituent* of the MS clusters, and not an isolated molecule.

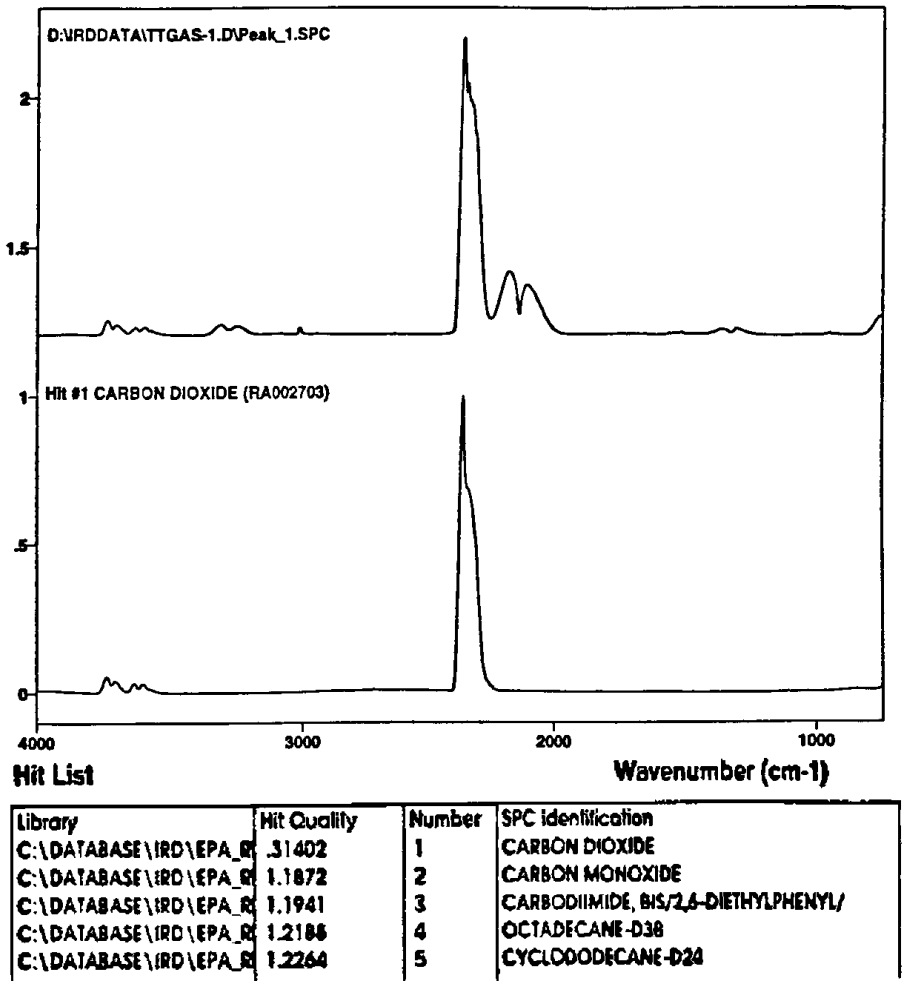

Figure 11.31. The independent confirmation at the PCFL of the NTS finding of Fig. 11.15 regarding the mutated IR signature of the CO_2 in magnegas. Note the identical shapes of the mutated IR peak in the top of the above figure, and that in Fig. 11.15 obtained via a different instrument. Note also the appearance again of two new peaks in the IR signature of CO_2, which indicate the presence of *new internal bonds* not present in the *conventional* molecule. Note finally that the instrument now correctly identifies the signature as that of the CO_2.

Moreover, the IR scan was done for the entire range of 40 to 500 a.m.u., thus establishing that said IR peak is the sole conventional constituent in macroscopic percentage in said a.m.u. range of *all* MS peaks, namely, the single constituent identified by the IRD is a constituent of all MS peaks.

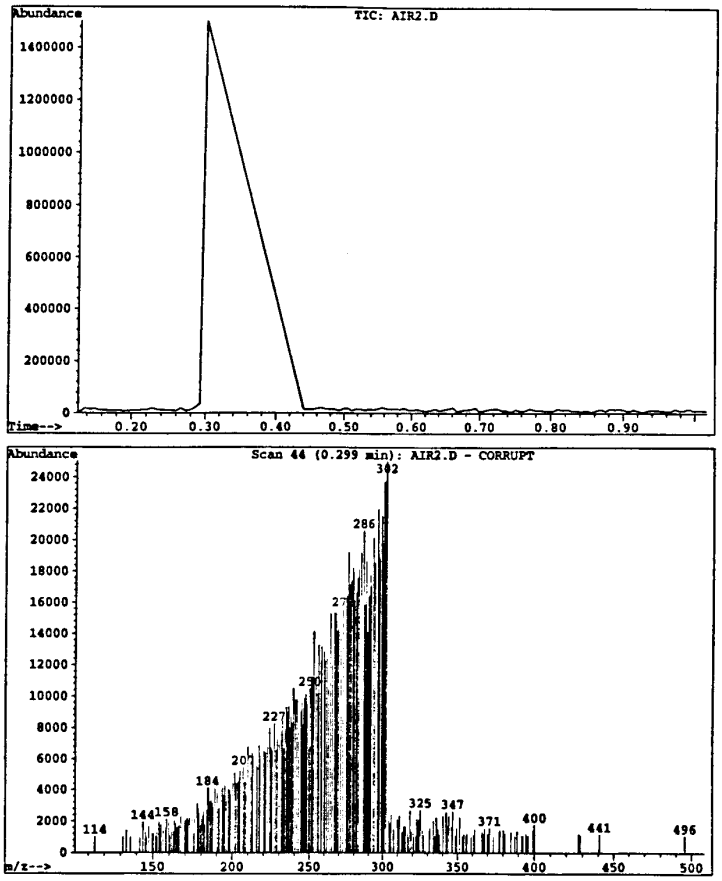

Figure 11.32. The first direct experimental verification at PCFL of the anomalous adhesion of magnecules. The figure reproduces the background of the instrument upon completion of the measurements, removal of magnegas, and conventional flushing. As one can see, the background results in being very similar to the MS scan during the tests, thus establishing that part of the gas had remained in the interior of the instrument. This behavior can only be explained via the induced magnetic polarization of the atoms in the walls of the instrument, with consequential adhesion of magnecules. It should be noted that this anomalous adhesion has been confirmed by all subsequent tests for both the gaseous and liquid states. The removal of magnecules in the instrument after tests required flushing with an inert gas at high temperature.

It should also be noted that, as recalled earlier, the IR only detects *dimers* such as C–O, H–O, *etc.*, and does not detect complete molecules. Therefore, the peak detected by the IRD *is not* sufficient to establish the presence of the complete molecule CO_2 unless the latter is independently identified in the MS.

Yet the MS scan does not identify any peak for the CO_2 molecule, as indicated earlier. Despite that, the presence in the MS peaks of complete molecules CO_2 cannot be ruled out. Therefore, the most plausible conclusion is that the MS peaks represent clusters composed of a percentage of C–O dimers and another percentage of CO_2 molecules, plus other dimers, and/or molecules, and/or atoms with atomic weight smaller than 40 a.m.u., thus outside the range of the considered scans.

As indicated earlier, the presence of dimers and individual atoms in magnegas is essential for a quantitative interpretation of the large excess of energy contained in this new fuel, the order of at least three times the value predicted by quantum chemistry, which energy is released during combustion. The admission of dimers and atoms as constituents of magnecules readily explains this anomalous energy content because said dimers and atoms are released at the time of the combustion, thus being able at that time to form molecules with exothermic reactions of type (8.5). In the event magnecules would not contain dimers and atoms, their only possible constituents are conventional molecules, in which case no excess energy is possible during combustion.

The large differences of MS peaks in the two tests at NTS and at PCFL of exactly the same gas in exactly the same range from 40 to 500 a.m.u., even though done with different GC-MS/IRD equipment, illustrates the importance of having a ramp time of the order of 26 minutes. In fact, sixteen different peaks appear in the MS scan following a ramp time of 26 minutes, as illustrated by Fig. 11.12, while all these peaks collapsed into one single peak in the MS scan of Figs. 8.13 and 8.14, because the latter were done with a ramp time of about 1 minute. Therefore, *the collapse of the sixteen peaks of Fig. 11.12 into the single large peak of Figs. 8.13 and 8.14 is not a feature of magnecules, but rather it is due to the insufficient ramp time of the instrument.*

11.4.7 Anomalous Energy Balance of Hadronic Molecular Reactors

As is well known, the *scientific efficiency* of any equipment is *under-unity* in the sense that, from the principle of conservation of the energy and the unavoidable energy losses, *the ratio between the total energy produced and the total energy used for its production is smaller than one.*

For the case of magnegas production, the total energy produced is the sum of the energy contained in magnegas plus the heat acquired by the liquid, while the total energy available is the sum of the electric energy used for the production of magnegas plus the energy contained in the liquid recycled. Therefore, from the principle of conservation of the energy we have the scientific energy balance

$$\frac{\text{Total energy produced}}{\text{Total energy available}} = \frac{E_{mg} + E_{heat}}{E_{electr} + E_{liq}} < 1. \tag{11.4.13}$$

An important feature of hadronic reactors is that they are *commercially over-unity*, namely, the ratio between the total energy produced and only the electric energy used for its production, is bigger than one,

$$\frac{E_{mg} + E_{liq}}{E_{electr}} > 1. \tag{11.4.14}$$

In this commercial calculation the energy contained in the liquid is not considered because liquid wastes imply an income, rather than costing money.

As a result, Santilli's hadronic molecular reactors can be viewed as reactors capable of tapping energy from liquid molecules, in much of the same way as nuclear reactors can tap energy from nuclei. An important difference is that the former reactors release no harmful radiation and leave no harmful waste, while the latter reactors do release harmful radiations and leave harmful waste.

The energy used for the production of the carbon rod, the steel of the reactors, etc. is ignored in commercial over-unity (7.34) because its numerical value per cubic foot of magnegas produced is insignificant.

The commercial over-unity of hadronic reactors is evidently important for the production of the combustible magnegas or magnetically polarized hydrogen (MagH^{TM}) at a price competitive over conventional fossil fuels.

A first certification of the commercial over-unity (7.34) was done on September 18 and 19, 1998, for the very first, manually operated prototype of hadronic reactors by the independent laboratory *Motorfuelers, Inc.*, of Largo, Florida, and included (see [8]):

1) Calibrating the cumulative wattmeter provided by *WattWatchers, Inc.*, of Manchester, New Hampshire, which was used to measure the electric energy drawn from the power lines per each cubic foot of magnegas produced;

2) The verification of all dimensions, including the volume of the column used for gas production, the volume of the liquid used in the process, etc.;

3) Repetition of numerous measurements in the production of magnegas and its energy content, calculation of the average values, identification of the errors, etc.

During the two days of tests, *Motorfuelers* technicians activated the electric DC generator and produced magnegas, which was transferred via a hose to a transparent plexyglass tower filled up with tap water, with marks indicating the displacement of one cubic foot of water due to magnegas production.

After the production of each cubic foot, the gas was pumped out of the tower, the tower was replenished with water, and another cubic foot of magnegas was produced. The procedure was repeated several times to have sufficient statistics. The electric energy from the electric panel required to produce each cubic foot of magnegas was measured via the previously calibrated cumulative wattmeter.

Figure 11.33. A view of metal cutting via magnegas. Independent certifications by various users have established that: 1) magnegas has a pre-heat time at least half that by acetylene (which is currently used for metal cutting and has an energy content of 2,300 BTU/cf); 2) magnegas cuts metal at least 50% faster than acetylene; 3) the cut produced by magnegas is much smoother without edges as compared to that by acetylene; 4) magnegas exhaust does not contain carcinogenic or other toxic substances, while that of acetylene is perhaps the most carcinogenic and toxic of all fuels; 5) magnegas cutting does not produce the "flash-back" (local explosion of paint over metal) typical of acetylene; 6) magnegas is dramatically safer than acetylene, which is unstable and one of the most dangerous fuels currently used; and 7) magnegas cost about 1/2 that of acetylene.

As a result of several measurements, *Motorfuelers, Inc.* certified [8] that the production of one cubic foot of magnegas with the first prototype required an average electric energy of

$$E_{electr} = 122 \text{ W/cf} = 416 \text{ BTU/cf } \pm 5\%. \tag{11.4.15}$$

It should be stressed that this is the electric energy from the electric panel, thus including the internal losses of the DC rectifier. Alternatively, we can say that the arc is served by only 65% of the measured electric energy, corresponding to

$$E_{electr} = 79.3 \text{ W/cf} = 270 \text{ BTU/cf}. \tag{11.4.16}$$

The energy content of magnegas was measured on a comparative basis with the BTU content of natural gas (1,050 BTU/cf). For this purpose, technicians of *Motorfuelers, Inc.*, used two identical tanks, one of natural gas and one of

magnegas, at the same initial pressure of 110 psi. Both tanks were used for 5 psi pressure decreases, under the same gas flow, to increase the temperature of the same amount of water in the same pot at the same initial temperature. The ratio of the two temperature increases is evidently proportional to the ratio of the respective BTU contents.

Following several measurements, *Motorfuelers, Inc.* certified [8] that magnegas produced from the antifreeze waste used in the reactor has about 80% of the BTU content of natural gas, corresponding to

$$E_{mg} = 871 \text{ BTU/cf } \pm 5\%. \tag{11.4.17}$$

All other more scientific tests of BTU content of magnegas conducted at various academic and industrial laboratories failed to yield meaningful results due to the energy content of magnegas for various reasons. Despite their empirical character, the measurement of BTU content done by *Motorfuelers, Inc.*, remains the most credible one.

It should be noted that the value of 871 BTU/cf is a lower bound. In fact, automotive tests reviewed in Sect. 7.9 have established that the energy output of internal combustion engines powered by magnegas is fully equivalent to that of natural gas, thus yielding a realistic value of about

$$E_{mg} = 1,000 \text{ BTU/cf}. \tag{11.4.18}$$

During the tests, it was evident that the temperature of the liquid waste in the reactor experienced a rapid increase, to such an extent that the tests had to be stopped periodically to cool down the equipment, in order to prevent the boiling of the liquid with consequential damage to the seals.

Following conservative estimates, technicians of *Motorfuelers, Inc.*, certified [8] that, jointly with the production of 1 cf of magnegas, there was the production of heat in the liquid of 285 BTU/cf plus 23 BTU/cf of heat acquired by the metal of the reactor itself, yielding

$$E_{heat} = 308 \text{ BTU/cf}. \tag{11.4.19}$$

In summary, the average electric energy of 122 W = 416 BTU calibrated from the electric panel produced one cf of magnegas with 871 BTU/cf, plus heat in the liquid conservatively estimated to be 308 BTU/cf. These independent certifications established the following *commercial over-unity* of the first, manually operated hadronic reactor within ±5% error:

$$\frac{871 \text{ BTU/cf} + 308 \text{ BTU/cf}}{416 \text{ BTU/cf}} = 2.83. \tag{11.4.20}$$

Note that, if one considers the electric energy used by the arc itself corresponding to 79.3 W/cf = 270 BTU/cf), we have the following commercial

over-unity:

$$\frac{871 \text{ BTU/cf} + 285 \text{ BTU/cf}}{270 \text{ BTU/cf}} = 4.36. \tag{11.4.21}$$

In releasing the above certification, *Motorfuelers, Inc.*, noted that the arc had a poor efficiency, because it was manually operated, thus resulting in large variation of voltage, at times with complete disconnection of the process and need for its reactivation.

Motorfuelers technicians also noted that the BTU content of magnegas, Eq. (11.4.37), is a minimum value, because measured in comparison to natural gas, not with a specially built burner, but with a commercially available burner that had large carbon residues, thus showing poor combustion, while the burner of natural gas was completely clean.

Immediately after the above certification of commercial over-unity, a number of safety and health measurements were conducted on hadronic molecular reactors, including measurements on the possible emission of neutrons, hard photons, and other radiation.

David A. Hernandez, Director of the *Radiation Protection Associates*, in Dade City, Florida conducted comprehensive measurements via a number of radiation detectors placed around the reactor, with particular reference to the only radiations that can possibly escape outside the heavy gauge metal walls, low or high energy neutrons and hard photons.

Under the presence of eyewitnesses, none of the various counters placed in the immediate vicinity of the reactor showed any measurement of any radiation at all. As a result, Radiation Protection Associates released an official Certificate stating that:

> "Santilli's PlasmaArcFlow^{TM} Reactors met and exceed the regulatory regulations set forth in Florida Administrative Code, Chapter 64-E. Accordingly, the reactors are declared free of radiation leakage."

Subsequent certifications of more recent hadronic reactors operating at atmospheric pressure with 50 kW and used to recycled antifreeze waste, this time done on fully automated reactors, have produced the following measurements:

$$E_{mg} = 871 \text{ BTU/cf}, \tag{11.4.22a}$$

$$E_{liq} = 326 \text{ BTU/cf}, \tag{11.4.22b}$$

$$E_{electr} = 100 \text{ W/cf} = 342 \text{ BTU/cf}, \tag{7.42c}$$

resulting in the following commercial over-unity of automatic reactors recycling antifreeze with about 50 kW and at atmospheric pressure:

$$\frac{871 \text{ BTU/cf} + 326 \text{ BTU/cf}}{342 \text{ BTU/cf}} = 3.5. \tag{11.4.23}$$

When ordinary tap water is used in the reactors, various measurements have established a commercial over-unity of about 2.78.

It should be indicated that the commercial over-unity of the hadronic reactors increases nonlinearly with the increase of the kiloWatts, pressure and temperature. Hadronic reactors with 250 kW are under construction for operation at 250 psi and 400° F. The latter reactors have a commercial over-unity considerably bigger than (7.43).

The origin of the commercial over-unity (7.43) is quite intriguing and not completely known at this writing. In fact, conventional chemical structures and reactions have been studied by Aringazin and Santilli [9] and shown not to be sufficient for a quantitative explanation, thus requiring a new chemistry.

Following Aringazin and Santilli [9], our first task is to compute the electric energy needed to create one cubic foot of plasma in the PlasmaArcFlow reactors as predicted by conventional quantum chemistry. Only after identifying the deviations of the experimental data from these predictions, the need for the covering hadronic chemistry can be properly appraised.

For these objectives we make the following assumptions. First, we consider PlasmaArcFlow reactor processing distilled water with the DC arc occurring between a consumable pure graphite cathode and a non-consumable tungsten anode. As indicated earlier, said reactors yield a commercial over-unity also when used with pure water. Therefore, quantum chemical predictions can be more effective studied in this setting without un-necessary ambiguities. We also assume that water and the solid graphite rod are initially at 300° K and that the plasma created by the DC electric arc is at $3{,}300^o$ K.

The electric energy needed to create one cubic foot of plasma must perform the following transitions (see Appendix 7.A for basic units and their conversions):

1) Evaporation of water according to the known reaction

$$\mathrm{H_2O(liquid)} \rightarrow \mathrm{H_2O(vapor)} - 10.4 \text{ Kcal/mole}, \tag{11.4.24}$$

2) Separation of the water molecule,

$$\mathrm{H_2O} \rightarrow \mathrm{H_2} + \frac{1}{2}\mathrm{O_2} - 57 \text{ Kcal/mole}, \tag{11.4.25}$$

3) Separation of the hydrogen molecule,

$$H_2 \rightarrow H + H - 104 \text{ Kcal/mole}, \tag{11.4.26}$$

4) Ionization of H and O, yielding a total of 1,197 Kcal.

We then have the evaporation and ionization of the carbon rod,

$$\mathrm{C(solid)} \rightarrow \mathrm{C(plasma)} - 437 \text{ Kcal/mole}, \tag{11.4.27}$$

resulting in the total 1,634 Kcal for 4 moles of plasma, i.e.

$$\begin{aligned} 408.5 \text{ Kcal/mol} = 0.475 \text{ kWh/mol} = 1621 \text{ BTU/mol} = \\ = 515.8 \text{ Kcal/cf} = 0.600 \text{ kWh/cf} = 2,047 \text{ BTU/cf}, \end{aligned} \tag{11.4.27}$$

to which we have to add the electric energy needed to heat up the non-consumable tungsten anode which is estimated to be 220 BTU/cf, resulting in the total of 2,267 BTU/cf. This total, however, holds at the electric arc itself without any loss for the creation of the DC current from conventional alternative current. By assuming that rectifiers, such as the welders used in PlasmaArcFlow reactors have an efficiency of 70%, we reach the total electric energy from the source needed to produce one cubic foot of plasma

$$\text{Total Electric Energy } = 3,238 \text{ BTU/cf} = 949 \text{ W/cf}. \tag{11.4.28}$$

We now compute the total energy produced by PlasmaArcFlow reactors according to quantum chemistry. For this purpose we assume that the gas produced is composed of 50% hydrogen and 50% carbon monoxide with ignorable traces of carbon dioxide. The latter is indeed essentially absent in PlasmaArcFlow reactors, as indicated earlier. In addition, CO_2 is not combustible. Therefore, the assumption of ignorable CO_2 in the gas maximizes the prediction of energy output according to quantum chemistry, as desired.

Recall that the glow of underwater arcs is mostly due to the combustion of hydrogen and oxygen back into water which is absorbed by the water surrounding the arc and it is not present in appreciable amount in the combustible gas bubbling to the surface. Therefore, any calculation of the total energy produced must make an assumption of the percentage of the original H and O which recombine into H_2O (the evidence of this recombination is established by the production of water during the recycling of any type of oil by the hadronic reactors).

In summary, the calculation of the energy produced by the PlasmaArcFlow reactors requires: the consideration of the cooling down of the plasma from 3,300^o K to 300° K with consequential release of energy; the familiar reactions

$$\text{H} + \text{H} \rightarrow \text{H}_2 + 104 \text{ Kcal/mole}, \tag{11.4.29a}$$

$$\text{H}_2 + \frac{1}{2}\text{O}_2 \rightarrow \text{H}_2\text{O} + 57 \text{ Kcal/mole}, \tag{11.4.29b}$$

$$\text{C} + \text{O} \rightarrow \text{CO} + 255 \text{ Kcal/mole}. \tag{11.4.29c}$$

Under the assumption of 100% efficiency (that is, no recombination of water), the total energy produced is given by

$$398 \text{ Kcal/mole} = 1,994 \text{ BTU/cf}. \tag{11.4.30}$$

By assuming that the entire energy needed to heat up the non-consumable tungsten is absorbed by the liquid surrounding the electric arc in view of its continuous cooling due to the PlasmaArcFlow, we have the total heat energy of 2,254 BTU/cf.

In addition, we have the energy content of the combustible gas produced. For this purpose we recall the following known reactions:

$$\mathrm{H_2(mg)} + \frac{1}{2}\mathrm{O_2(atm)} \rightarrow \mathrm{H_2O} + 57 \text{ Kcal/mole}, \tag{11.4.31a}$$

$$\mathrm{CO(mg)} + \frac{1}{2}\mathrm{O_2(atm)} \rightarrow \mathrm{CO_2} + 68.7 \text{ Kcal/mole}. \tag{11.4.32b}$$

Consequently, the 50%-50% mixture of conventional gases H_2 and CO has the following

$$\text{Conventional energy content of magnegas produced from water} =$$

$$= 62.8 \text{ Kcal/mole} = 249.19 \text{ BTU/mole} = 315 \text{ BTU/cf}. \tag{11.4.33}$$

Therefore, the total energy output of the PlasmaArcFlow Reactors is given by

$$E(\text{mg}) + E(\text{heat}) = 315 \text{ BTU/cf} + 2,254 \text{ BTU/cf} = 2,569 \text{ BTU/cf}. \tag{11.4.34}$$

It then follows that the energy efficiency of the PlasmaArcFlow reactors is under-unity for the case of maximal possible efficiency,

$$\text{Energy efficiency predicted by quantum chemistry} =$$

$$= \frac{\text{Total energy out}}{\text{Electric energy in}} = \frac{E_{mg} + E_{heat}}{E_{electr}} = \frac{2,569 \text{ BTU/cf}}{3,238 \text{ BTU/cf}} = 0.79. \tag{11.4.35}$$

It is possible to show that, for the case of 50% efficiency (i.e., when 50% of the original H and O recombine into water) the total energy output evidently decreases. For detail, we refer the interested reader to Aringazin and Santilli [9].

11.4.8 Cleaning Fossil Fuel Exhaust with Magnegas Additive

Electric power plants continue to attempt the cleaning of their atmospheric pollution (see Figure 11.1) via the cleaning of their exhaust. Since the related equipment is very expensive and notoriously inefficient, these are attempts literally belonging to the past millennium. Nowadays, the exhaust of fossil fueled electric power plants can be cleaned via cost competitive improvement of the combustion.

It is known that, whether burning petroleum or coal, about 60% of the energy in the original fuel is literally thrown through the fluke, and so is the relates cost, due to the notoriously poor combustion.

It is also known in chemistry that hydrogen is the best additive to improve combustion, with consequential improvement of the environmental quality of the exhaust. In fact, hydrogen has the biggest flame temperature and speed among all known fuels. Consequently, the injection of hydrogen as an additive in the flame of fossil fuels burns the uncombusted component of the exhausts in a way proportional to the used percentage of hydrogen. A reason hydrogen as currently available has not (and cannot) be used as additive in fossil fueled electric power plants is its prohibitive cost (that in the U.S.A. is of the order of 50 times the cost of natural gas per same energy content, as recalled in Section 11.1.3).

Magnegas is the best additive for the cleaning of fossil fuel exhaust known to the author[9] because:

1) When produced from the recycling of water-base liquid wastes, magnegas contains about 65% hydrogen, thus qualifying as an effective additive to improve fossil fuel combustion;

2) The remaining components of magnegas are internally rich in oxygen, thus helping to alleviate the large oxygen depletion caused by fossil fuel combustion (Section 11.1); and

3) The cost of magnegas is competitive over that of fossil fuel, particularly when produced by the electric power plants themselves, because of the grossly reduced cost of electricity plus the possibility of producing magnegas from the recycling of city sewage, with a consequential income that covers most of the operating costs of PlasmaArcFlow Recyclers. Un der these conditions, the percentage of magnegas additive to be injected in the flame of fossil fuels becomes a corporate, rather than technical or financial decision.

Besides incontrovertible environmental advantages, the increase of profits for electric power plants in the use of magnegas additive are substantial, such as: the utilization of at least half of the fuel and related cost literally thrown through the fluke due to poor combustion; the capability of producing green electricity that notoriously brings bigger income; and the gaining of the so-called *Kyoto Credits* that, alone, bring millions of dollars of additional income.

Despite these trans[parent gains and numerous solicitations as well as the international exposure of the website [5b], no electric power plant nowhere in the world has expressed interest to this day (fall 2005) interest in at least inspecting the use of magnegas additive. This behavior was expected by the author because, as stated in the opening sentences of this chapter, profits are

[9]The documented indication of other additives comparable to magnegas would be sincerely appreciated.

no longer the dominant drive in the contemporary corporate world. Politics is the dominant drive. Lack of interest for major environmental and financial gains is then another confirmation of the lack of political will toward serious environmental actions in all developed countries (for more details, visit the website [5b]).

11.4.9 Hy-Gasoline, Hy-Diesel, Hy-Ethanol, Hy-NG, Hy-Coal

Fossil fuels are sold in a disproportionate daily volumes recalled in Section 11.1, and we should expect that they will continue to be sold in ever increasing disproportionate volumes until the extinction of all petroleum reserves.

Rather than dreaming of eliminating fossil fuels from the market, scientists in general, and chemists in particular, have the ethical duty to seek additives to clean fossil fuel combustion in automotive use, namely, an usage logistically and technically different than the combustion of fossil fuels in power plants furnaces of the preceding section.

It is at this point where the irreconcilable conflict between academic interest on pre-existing theories and the societal need for new theories emerges in its full light. In fact, the best additive to clean fossil fuel combustion is, again, hydrogen (see the preceding section). However, hydrogen is a gas, while gasoline, diesel, ethanol and other fuels are liquids. Consequently, quantum chemistry provides no possibility of achieving new fuels characterized by a stable mixture of liquid fuels and gaseous hydrogen.

However, the abandonment of quantum chemistry in favor of the covering hadronic chemistry permits indeed the possible resolution of the problem. In fact. magnecular bonds are completely insensitive as to whether the constituents of a magnecular cluster partially originated from liquids and part from gases, trivially, because the bond occurs at the level of individual atoms.

The above principle has permitted the formulation of basically new *liquid* fuels known as Hy-Gasoline^{TM}, Hy-Diesel^{TM}, Hy-Ethanol^{TM}, $HyCoal^{TM}$, etc. (patented and international patents pending [5]), where the prefix "Hy" is used to denote a high hydrogen content. These new fuels are essentially given by ordinary fossil fuels as currently produced, subjected to a bond with magnegas or hydrogen from magnegas (see next section) via the use of special PlasmaArcFlow Reactors.

As predicted, no petroleum company has expressed to date any interest at all in even inspecting the evidence, let alone take serious initiative in these new fuels despite numerous solicitations and the transparent environmental and, therefore, financial gains, because of the origin of the current environmental problems threatening mankind: the lack of serious political will in all developed countries to this day (fall 2005), and actually the subservience of current

political will to the petroleum cartel, as denounced in the opening words of this chapter (for more details, visit the website [5b]).

11.4.10 Catastrophic Inconsistencies of Quantum Mechanics, Superconductivity and Chemistry for Submerged Electric Arcs

In Chapter 9 we identified the *approximate* yet still applicable character of quantum mechanics and chemistry for molecular structures.

The analysis of this section has confirmed the content of section 1.2.11 to the effect that the divergences between submerged electric arcs and the predictions of conventional disciplines are so huge to be called "catastrophics inconsistencies" such as:

1) **Inability by quantum chemistry to identify the chemical composition of magnegas.** This occurrence is due to the fact that quantum chemistry predicts that magnegas produced via a electric arc between pure graphite electrodes submerged within distilled water is composed primarily of the molecule $H - H$ with 2 a.m.u and $C - O$ with 28 a.m.u, with traces of H_2O with 18 a.m.u. and CO_2 with 44 a.m.u. No additional species is predicted by quantum chemistry. By comparison , magnegas is composed of fully identifiable peaks in the MS ranging from 1 a.m.u to $1,000$ a.m.u. *none* of which is identifiable with the preceding molecules, resulting in catastrophic divergences in the sense that the application of quantum chemistry to magnegas would have no scientific sense, not even approximate.

2) **Inability by quantum superconductivity to represent submerged electric arcs.** Distilled water is known to be dielectric. In fact, the electric resistance between electrodes submerged within distilled water at large distance (open arc) can be of the order of 100 Ohms or so. However, when the electric arc is initiated the resistance collapses to fractional Ohms, resulting in a very high temperature kind of "superconductor" (since the arc has about $5,000^oC$). Such a collapse of electric resistance is beyond any hope of representation by quantum superconductivity. in reality, as studied in preceding chapters, the collapse is due to the basic inapplicability of Maxwell' s equations for submerged electric arcs , thus implying the basic inapplicability of the Lorentz and Poincaré symmetry, special relativity and all that in favor of covering theories.

3) **A ten-fold error in defect in the prediction of the CO_2 content of magnegas exhaust.** In fact, quantum chemistry predicts the presence of about 50% of CO in magnegas from distilled water resulting in about 40%CO_2 in the exhaust,, while magnegas has about 1/10-th that value;

4) **A ten fold error in excess in the prediction of heat generated by carbon combustion by the arc.** In fact, in the preceding subsection we showed that quantum chemistry predicts about $2,250$ Kcal/scf of magnegas,

while the measured amount is of the order of 250 for water as feedstock. Note that the latter error confirms the preceding one.

5) **A fourteen-fold error in the prediction of oxygen in the exhaust of magnegas.** In fact, quantum chemistry predicts that, under full combustion in atmosphere, there is no oxygen in the exhaust, while magnegas shows up to 14% breathable oxygen in the exhaust.

an additional large inconsistency of quantum chemistry will be shown in the next section in regard to the hydrogen content of magnegas.

However, the most catastrophic inconsistencies are given by the fact that *magnegas has a variable energy content, a variable specific weight, and a variable Avogadro number.* The first two features are established by the fact that the energy content and density of magnegas produced from the same reactor with the same liquid feedstock increases nonlinearly with the sole increase of the operating pressure, trivially, because bigger pressures produce heavier magnecules.

The all important variation of the Avogadro number is established by the fact, verified every day in the magnegas factories around the world when compressing magnegas in high pressure bottles according to which the same increase of pressures. For instance, the transition from 20 to 120 psi requires about 40 scf, while the transition from $3,500$ psi to $3,600$ psi may require 70 scf of magnegas, an occurrence that can only be explained via the *decrease of the Avogadro number with the increase of pressure.*

The latter anomaly is necessary for gases with magnecular structure for the evident reason that the increase of pressure bonds different magnecules together, thus reducing the Avogadro number. Alternatively, the magnecular structure can be also interpreted as an unusual form of "semi-liquid" in the sense that the magnecular bond is much closer to the so called "h-bridges" of the liquid state of water. the increase of pressure evidently brings magnegas progressively closer to the liquid state, which continuous process can only occur for a variable Avogadro number.

on historical grounds, it should be recalled that *Avogadro conceived his celebrated number as being variable with physical characteristics of pressure and temperature,* a conception clearly stated on the expectation that the gaseous constituents can break down into parts due to collision and subsequent recombinations.

Subsequently, the chemistry of the time believed for decades that the Avogadro number was variable. In fact, the first measurements of the constancy of the Avogadro number maed by Canizzaro also in Italy, were initially very controversial until verified numerous times. Today we know that *the constancy of the Avogadro number for gases wit molecular structure is due to the strength of the valence bond under which no breaking of molecules is possible*

under increasing temperature and pressure, resulting in a constant number of constituents per mole.

For over one century chemistry was restricted to the study of gases with molecular structure and Avogadro original conception was forgotten until resumed by the author with his gases with magnecular structure that verify all original intuition by Avogadro.

11.4.11 Concluding Remarks

The first important experimental evidence presented in this section is the independent certification of hadronic reactors of molecular type as being "commercially over-unity", that is, the ratio between the total energy produced and the electric energy needed for its production can be much bigger than one, Eq. (11.4.14).

This occurrence establishes that said hadronic reactor are based on a *a new combustion of carbon* realized via the electric arc, which combustion is much cleaner and more efficient than the combustion of carbon in a conventional furnace. In fact, the new combustion of carbon occurs in the plasma surrounding the electric arc due to the presence of oxygen originating from the liquid feedstock.

Rather than producing highly polluting exhaust, as for the combustion of carbon in a furnace, the plasma combustion produced a clean burning fuel and heat without pollution. Consequently, the plasma combustion of carbon is much more efficient than conventional combustion because pollutants in the exhaust are uncombusted fuel.

The third experimental evidence presented in this section is that establishing the existence of the new chemical species of Santilli magnecules. More specifically, said experimental evidence, plus additional tests not reported here for brevity, confirm the following features of Definition 11.4.1:

I) Magnecules have been detected in MS scans at high atomic weights where no molecules are expected for the gas considered. In fact, the biggest molecule in macroscopic percentages of the magnegas tested, that produced from tap water with conventional chemical composition (8.20), is CO_2 with 44 a.m.u., while peaks in macroscopic percentages have been detected with *ten times* such an atomic weight and more.

II) The MS peaks characterizing magnecules remain unidentified following a computer search among all known molecules. This feature has been independently verified for *each* of the sixteen peaks of Fig. 11.12, for all peaks of Figs. 8.13 and 8.14, as partially illustrated in Figs. 8.8 and 8.15, as well as for all additional MS scans not reported here for brevity.

III) The above MS peaks characterizing magnecules admit no IR signature, thus confirming that they do not have a valence bond. In fact, none of the peaks here considered had any IR signature as partially illustrated in Figs. 8.9

and 8.16, thus confirming the achievement of an essentially pure population of magnecules.

IV) The IR signature of the only molecule detected in macroscopic percentage, that of the CO_2, is mutated precisely with the appearance of two additional peaks, as shown in Fig. 11.15 and independently confirmed in Fig. 11.22. Since any peak in the IR signature represents an internal bond, the mutation here considered confirms the creation by the PlasmaArcFlow technology of new internal magnetic bonds within conventional molecules, as per Fig. 11.11.

V) The anomalous adhesion of magnecules is confirmed in both tests from the evidence that the background (blank) at the end of the tests following conventional flushing continued to show the presence of essentially the same magnecules detected during the tests, as illustrated in Figs. 8.12 and 8.18.

VI) The atomic weight of magnecules mutates in time because magnecules can break down into fragments due to collisions, and then form new magnecules with other fragments. This feature is clearly illustrated by the macroscopic differences of the two scans of Figs. 8.13 and 8.14 via the same instrument on the same gas under the same conditions, only taken 30 minutes apart.

VII) Magnecules can accrue or lose individual atoms, dimers or molecules. This additional feature is proved in the scans of Figs. 8.13 and 8.14 in which one can see that: the peak at 286 a.m.u. of the former becoming 287 a.m.u. in the latter, thus establishing the accretion of one hydrogen *atom*; the peak at 302 a.m.u. in the former becomes 319 a.m.u. in the latter, thus establishing the accretion of the H–O dimer; the peak at 328 a.m.u. in the former becomes 334 a.m.u. in the latter, thus establishing the accretion of one O_2 molecule; the peak at 299 a.m.u. in the former become 297 a.m.u. in the latter, thus exhibiting the loss of one H_2 molecule; *etc.* It should be indicated that these features have been confirmed by all subsequent GC-MS/IRD scans not reported here for brevity.

The other features of Definition 11.4.1 require measurements other than those via GC-MS/IRD and, as such, they will be discussed in the next section.

A most forceful implication of the experimental evidence presented in this section is that it excludes valence as the credible origin of the attractive force characterizing the detected clusters. This feature is forcefully established by the detection of peaks all the way to 1,000 a.m.u. in a gas solely composed of H, C and O atoms that are combined at the $10,000^oF$ of the electric arc, thus excluding hydrocarbons and other standard molecules. Even more forceful experimental evidence on new non-valence bonds will be presented in the next sections.

It is easy to predict that the emergence of "new" non-valence bonds, we have called magnecular, will inevitably imply a revision of a number of current views in chemistry, the first case coming to mind being that of the so-called *H-bridges* in the liquid state of water.

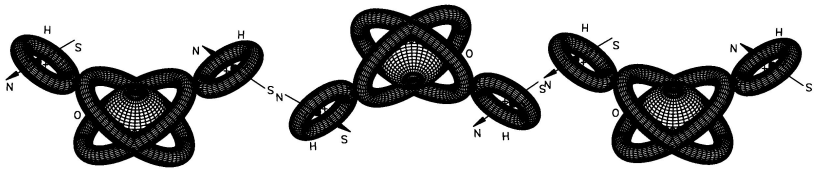

Figure 11.34. A schematic view of the magnecular interpretation of the liquid state of water. Such a state requires an ATTRACTIVE FORCE between the water molecules. But the latter are electrically neutral, diamagnetic and no unbounded electron available for valance bonds. hence, a basically new, non-valence force is needed to represent the water liquid state. Quantum chemistry suggests that such liquid state is due to the so-called "H-bridges" although the latter are pure nomenclature because they do not identify at all explicitly and numerically the attractive force among water molecules. The new chemical species of Santilli magnecules resolves the problem because the H atoms in the H_2O molecule have a polarization in a plane perpendicular to the $H-O-H$ plane, that is precisely a toroidal polarization permitting attractive forces among different H atoms identified in their attractive as well as numerical character in this section. In summary, the main hypothesis here submitted apparently for the first time is that *the liquid state of water, as well as any other liquid state, is a magnecule*, by illustrating in this way the prediction that magnecules can acquire macroscopic dimensions (see additional studies on magnecules in liquids later on in this chapter).

As recalled in Chapter 9, this author never accepted quantum chemistry as "the final theory" for molecular structure because *quantum chemistry lacks the explicit and numerical identification of the attractive force in valence bonds, besides the fact that, according to quantum mechanics, two identical electrons should repel, rather than attract each other, as a consequence of which the name "valence" is a mere nomenclature without sufficient scientific content.*

This was essentially the situation in molecular structures such as the water molecule H_2O. Hadronic mechanics and chemistry have resolved this insufficiency by identifying explicitly and numerically the ATTRACTIVE force between IDENTICAL ELECTRONS that is responsible for the water and other molecules.

In this section we have learned that molecules admit non-valence bonds originating from toroidal polarizations of the orbitals. The magnecular origin of the H-bridges in the liquid state of water is then inevitable because, as recalled in Chapter 9, the orbitals of the H atoms in H_2O *do not* have a spherical distribution, but a distribution that is perpendicular to the $H-O-H$ plane, thus being precisely of the toroidal type underlying magnecules (see Fig. 11.34 for details).

In closing the author would like to stress that the above findings, even though independently confirmed numerous times, should be considered preliminary and in need of additional independent verifications, which are here solicited under the suggestion that:

1) Only peaks in macroscopic percentages should be initially considered to avoid shifting issues of primary relevance into others of comparatively marginal importance at this time;

2) The internal *attractive* force necessary for the very existence of cluster is identified in clear numerical terms without vague nomenclatures deprived of an actual physical reality, or prohibited by physical laws; and

3) The adopted terminology is identified with care. The word "magnecule" is a mere name intended to denote a chemical species possessing the specifically identified characteristics I) to XV) of Definition 11.4.1 which are distinctly different than the corresponding characteristics of molecules. Therefore, the new species can not be correctly called molecules. The important features are these distinctly new characteristics, and not the name selected for their referral.

11.5 THE NEW MAGNECULAR SPECIES OF HYDROGEN AND OXYGEN WITH INCREASED SPECIFIC WEIGHT

11.5.1 Resolution of Hyrogen Problems Permitted by the Magnegas Technology

In Section 11.1.3 we have pointed out serious problematic aspects caused by large scale use of hydrogen, including its large oxygen depletion, vast pollution caused by its current production methods, threat to the ozone layer, seepage and excessive costs due to the need of liquefaction. It is important to note that the new chemical species of magnecules permits the resolution, or at least the alleviation of these problems.

As indicated in Section 11.3, magnegas is synthesized from liquids that are very rich in hydrogen, such as water-base or oil-base liquid wastes. Consequently, magnegas generally contains about 66% hydrogen, not in a valence bond with other atoms as it is the case for CH_4, but *in a magnecular mixture* with other gases, thus permitting simple methods of molecular or other separations without the need of large energies to break valence bonds. Hence, the Magnegas Technology [5b] offers the following possibilities:

A) **Reduction of oxygen depletion caused by hydrogen combustion.** As indicated in the preceding sections, the new magnecular bond has been developed to achieve full combustion as well as to permit the inclusion of oxygen when prohibited by valence bonds, resulting in a fuel that is internally rich in oxygen originating not from the atmosphere, but from liquid wastes.

in fact, magnegas exhaust routinely contains up to 14% of breathable oxygen, and such a percentage can be increased following suitable development. It then follows that *the combustion of hydrogen produced via its separation from magnegas causes dramatically less oxygen depletion than that of hydrogen originating from reformation or electrolysis,* since none of the latter processes release oxygen in the atmosphere.

B) **Reduction of environmental pollution in hydrogen production.** Admittedly, the production of magnegas currently requires the use of commercially available electricity that is polluting because of generally fossil origin. However, PlasmaArcFlow Recyclers release no solid, liquid or gaseous contaminant in the environment; the electric energy used by the arc is about 1/20-th the operating energy (since the rest is given by a very clean carbon combustion via the arc); and the efficiency of PlasmaArcFlow Recyclers can be up to twenty times that of electrolysis. Consequently, the production of hydrogen from magnegas is dramatically less polluting then conventional methods, with the understanding that, when the new clean energies presented in the next chapter achieve industrial maturity, hydrogen production from magnegas will release zero environmental pollutants.

C) **Reduction of the threat to the ozone layer caused by hydrogen seepage and leaks.** Besides a basically new production method, a necessary condition for hydrogen to be a really viable fuel for large scale use is that of achieving a *new magnecular form of hydrogen* consisting of clusters sufficiently large to avoid seepage, as well as to prevent that, in case of leaks, hydrogen quickly rises to the ozone layer. This new species in studied in the next subsections.

D **Elimination of the need for liquefaction of hydrogen.** This objective is related to the preceding one. In fact, the achievement of a magnecular form of hydrogen automatically implies an increase of the specific weight over the standard value of 2.016 a.m.u. that, in turn, automatically implies the reduction of container volumes, with consequential possibility of using hydrogen in a compressed form without any need for its liquefaction. Note that, lacking such heavier form, hydrogen has no realistic possibility of large scale use due to the extreme costs and dangers of changes of state from liquid to gas.

E) **Dramatic reduction of hydrogen cost.** Magnegas produced in volumes is cost competitive with respect to fossil fuels such as natural gas. Consequently, the biggest contribution of the Magnegas Technology to the hydrogen industry is the dramatic reduction of current hydrogen production costs down to values compatible with fossil fuels costs, as shown in more details in the next subsection. Additional advantages over conventional hydrogen are permitted by its magnecular structure as shown below.

11.5.2 The Hypothesis of the New Chemical Species of MagneHydrogen and MagneOxygen

In paper [18] the author submitted, apparently for the first time, the hypothesis that conventional hydrogen H_2 and oxygen O_2 gases can be turned into a new species with magnecular structure here called *MagneHydrogen*^{TM} and *MagneOxygen*^{TM} 9as well as of other gases), with suggested chemical symbols MH and MO, respectively (patented and international patents pending).

The foundations of the above hypothesis are essentially those given in preceding sections. As recalled earlier, the hydrogen molecule is diamagnetic and, therefore, it *cannot* acquire a total net magnetic polarity. Nevertheless, the orbits of the *individual H atoms* can acquire a toroidal polarization under a sufficiently strong external magnetic field. The opposite magnetic moments of the two H atoms then explain the diamagnetic character of the hydrogen molecule as illustrated in Figure 11.7.

The aspect important for the hypothesis of MH and MO is that the toroidal polarization of the orbits of the electrons of the individual H atoms, plus the polarization of the intrinsic magnetic moments of nuclei and electrons in the H_2 molecule is sufficient for the creation of the desired new chemical species with bigger specific weight, because the new bonds can occur between pairs of individual H atoms, as illustrated in Figures 11.10 and 11.11.

The creation of MO is expected to be considerably simpler than that of MH because oxygen is paramagnetic, thus having electrons free to acquire an overall magnetic polarity which is absent for the case of MH. Nevertheless, the achievement of a significant increase of the specific weight of the oxygen will require the toroidal polarization of at least some of the peripheral atomic electrons, in addition to a total magnetic polarization.

The primary technological objective is, therefore, that of achieving physical conditions and geometries suitable for the joint polarization of *atoms*, rather than molecules, in such a way to favor their coupling into chains of opposing magnetic polarities. In the final analysis, the underlying principle here is similar to the magnetization of a ferromagnet, that is also based on the polarization of the orbits of unbounded electrons. The main difference (as well as increased difficulty) is that the creation of MH requires the application of the same principle to a *gaseous*, rather than a solid substance.

Under the assumption that the original gases are essentially pure, MH can be schematically represented

$$(H_\uparrow - H_\downarrow) \times H_\uparrow, \tag{11.5.1a}$$

$$(H_\uparrow - H_\downarrow) \times (H_\uparrow - H_\downarrow), \tag{11.5.1b}$$

$$(H_\uparrow - H_\downarrow) \times (H_\uparrow - H_\downarrow) \times H_\uparrow, etc. \tag{11.5.1c}$$

while MagneO can be schematically represented

$$(O_\uparrow - O_\downarrow) \times O_\uparrow, \tag{11.5.2a}$$

$$(O_\uparrow - O_\downarrow) \times (O_\uparrow - O_\downarrow), \tag{11.5.2b}$$

$$(O_\uparrow - O_\downarrow) \times (O_\uparrow - O_\downarrow) \times O_\uparrow .etc. \tag{11.5.3c}$$

where the arrows now indicate possible polarizations of more than one electron orbit.

By keeping in mind the content of the preceding sections, the achievement of the above magnecular structure does imply that MH and MO have specific weight and energy content greater than the corresponding values for unpolarized gases. The numerical values of these expected increases depend on a variety of factors discussed in the next subsections, including the intensity of the external magnetic field, the pressure of the gas, the time of exposure of the gas to the external field, and other factors.

A first important feature to be subjected to experimental verification (reviewed below) is the expected increase of specific weight. By recalling that the *gasoline gallon equivalent for hydrogen* is about 366 scf, the achievement of a form of MH with five times the specific weight of conventional hydrogen would reduce the prohibitive volume of $7,660$ scf equivalent to 20 g of gasoline to about $1,500$ scf. This is a volume of MH that can be easily stored at the pressure of $4,500$ psi in carbon fiber tanks essentially similar in volume and composition to that of a natural gas tank. As a result, the achievement of MH with sufficiently high specific weight can indeed eliminate the expensive liquefaction of hydrogen in automotive use, with consequential reductions of costs.

Another basic feature to be subjected to experimental verification (reviewed below) is that the combustion of MH and MO releases more energy than the combustion of conventional H and O gases. It then follows that

I) The use for internal combustion engines of MH with a sufficiently high specific weight is expected to eliminate liquefaction, yield essentially the same power as that produced with gasoline, and permit a dramatic decrease of operating costs;

II) The use of MH and MO in fuel cells is expected to yield a significant increase of voltage, power and efficiency; and

III) The use of liquefied MH and MO as fuels for rocket propulsion is expected to permit an increase of the payload, or a decrease of the boosters weight with the same payload.

Moreover, recent studies scheduled for a separate presentation have indicated that the *liquefaction of MH and MO appears to occur at temperatures bigger than those for conventional gases,* thus implying an additional reduction of costs. This expectation is due to the fact that magnecules tend to

aggregate into bigger clusters with the increase of the pressure, evidently due to their magnetic polarizations, which feature evidently favors liquefaction.

It is evident that the same principles outlined above also apply for other gases, and not necessarily to H and O gases alone. In fact, the processing of any gaseous fossil fuel via the principles here considered permits the increase of its specific weight as well as of its energy output, thus permitting a consequential decrease of storage volume, increase of performance and decrease of costs.

Note that the hypothesis of MH and MO is an extension of H_3 and O_3 to arbitrary values H_n and O_m as permitted by local values of pressure and temperature. Alternatively, the experimental evidence on MH and MO reviewed later on in this section confirms the magnecular structure of H_3 and O_3 presented in Section 11.3.4.

11.5.3 Industrial Production of MagneHydrogen and MagneOxygen.

As indicated earlier, the magnetic polarization of the orbits of peripheral atomic electrons requires extremely strong magnetic fields of the order of billions of Gauss. These values are of simply impossible realization in our laboratories with current technologies, that is, at distances of the order of inches or centimeters. These magnetic fields cannot be realized today even with the best possible superconducting solenoids cooled with the best available cryogenic technology.

The only possible, industrially useful method of achieving magnetic fields of the needed very high intensity is that based on direct current (DC) electric arcs with currents of the order of thousands of Amperes (A) when considered at atomic distances, i.e., of the order of 10^{-8} cm. As illustrated in Fig. 11.9, the magnetic field created by a rectilinear conductor with current I at a radial distance r is given by the well known law

$$B = kI/r, \tag{11.5.4}$$

where k = 1 in absolute electromagnetic units. It then follows that, for currents in the range of 10^3 A and distances of the order of the size of atoms r = 10^{-8} cm, the intensity of the magnetic field B is of the order of 10^{13} Oersted, thus being fully sufficient to cause the magnetic polarization of the orbits of peripheral atomic electrons.

Under the above conditions schematically represented in Fig. 11.9, atoms with the toroidal polarization of their orbits find themselves aligned one next to the other with opposing polarities which attract each other, thus forming magnecules. The electric arc decomposes the original molecule, thus permitting the presence of isolated atoms or radicals in the magnecular structure as needed to increase the energy output (Section 3).

In this way, the process transforms the original gas with its conventional molecular structure into a new chemical species consisting of individual atoms, radicals and complete molecules all bonded together by attractive forces among opposite magnetic polarities of the toroidal polarization of the orbits of peripheral atomic electrons.

In the event the original gas has a simple diatomic molecular structure, such as H_2, the magnecular clusters are composed of individual polarized H atom and ordinary polarized molecules H_2 as in Fig. 11.11. In the event the original gas has the more complex diatomic structure of O_2, the magnecular clusters are composed of individual polarized O atoms, O-O single bonds, and O_2 molecules with additional internal bonds as in Fig. 11.12. In the event the original gas has the more complex diatomic structure CO with triple valence bonds, the magnecular clusters are more complex and are generally composed of individual C and O atoms, single bonds C-O, double bond C=O, conventional molecules CO and O_2 with internal new bonds as in Fig. 11.12, plus possible C-complexes. Original gases with more complex conventional molecular structure evidently imply more complex magnecular clusters with all possible internal atomic arrangements.

It is evident that the resulting new species is not composed of all identical magnecules, and it is composed instead of a variety of magnecules from a minimum to a maximum number of atomic components, which have been measured to reach 1,000 a.m.u. and even more. The specific weight of the magnecular gas is then given by the average weight of all different magnecules, as indicated earlier.

Needless to say, a number of alternative methods for the industrial production of MH and MO are possible as identified in the existing patent applications. An alternative method worth mentioning here is the use of solenoids. The reader should however be aware that the latter cannot decompose molecules. Therefore, the MagneGases produced via the use of electric discharges and solenoids are different.

Another type of MH important for this study is that obtained from MagneGas [5]. When MagneGas is produced from a hydrogen rich liquid feedstock (such as water or liquids of fossil origin), it may contain up to 60% hydrogen in a form already polarized by the electric arc used for its production. Therefore, the hydrogen content of MagneGas is indeed a particular form of MH which can be separated via a variety of available technologies, such as filtration, cryogenic cooling and other processes.

This particular form of MH (whose features are identified in the next subsection) is particularly suited as fuel for internal combustion engines, rather than for fuel cells. This is due to the expected presence of very small C and O impurities which do not permit their use in fuel cells.

This particular type of MH derived from MagneGas has already been tested for automotive usage and proved to have a performance essentially similar to that of gasoline without any need of liquefaction, as needed instead by hydrogen vehicles currently tested by BMW, GM and other automakers. The tests were conducted via the conversion of two Honda and one Ferrari cars to operate on the new fuels (see [5] for brevity).

Above all, this particular type of MH has resulted to be cost competitive with respect to fossil fuels, of course, when produced in sufficiently large volumes. This cost competitiveness is due to a variety of factors, including (see [5] for detail):

1) the use of hydrogen rich wastes as liquid feedstock, such as city and farm sewage, antifreeze and or oil waste, etc., which implies an *income*, rather than a cost;

2) the possible utilization of steam at 400° produced by the cooling of the highly esoenergetic processes of the reactors, which steam can be used for other *income producing applications*, such as desalting seawater via evaporation, production of electricity via turbines, heating of buildings, and other income producing uses; and

3) the unusually high efficiency of Santilli Hadronic Reactors of molecular types used for the process which brings the cost of electricity down to $0.005/scf$.

Specific equipment and designs for the industrial production of MH, MO, and other magnetically polarized gases are available on request.

11.5.4 Experimental Evidence on MagneHydrogen and MagneOxygen

It is now important to review the experimental evidence supporting the existence of MH and MO.

The first tests were conducted with MH produced from MagneGas as indicated in the preceding subsection. MagneGas was first produced by using antifreeze waste as liquid feedstock. The combustible gas was then passed through 5 Armstrong zeolite filters, which essentially consist of a microporous molecular sieve selecting a gas via the so-called "molecular sieving," or molecular size exclusion.. The filtered gas was then subjected to the following three measurements:

1) This type of MH was first subjected to analytic measurements by a laboratory via Gas Chromatography (CG) and independent tests for confirmation were conducted via Fourier Transform Infrared Spectroscopy (FTIS). All measurements were normalized, air contamination was removed, and the lower detection limit was identified as being 0.01%. The results are reported in Fig. 11.35. As one can see, these measurements indicate that this particular

ADSORPTION RESEARCH INC.
ARI
6175-D Shamrock Court
Dublin, OH 43016

Gas	Molecular Weight (g/mol or amu/molecule)
MagneGas™ [Feed]	15.60
MagneHydrogen™ [Product]	15.06
Ordinary Hydrogen [for comparis	2.016

Figure 11.35. A view of the main results on the measurement of specific weight on a specific form of MH produced from magnegas released by Adsorptions Research Laboratory, in Ohio, under signature by its laboratory director. It should be stressed that the high value of specific weight was due to a specific treatment not expected to be possible on a industrial basis. Therefore, the specific weight ofg MH industrially production from magnegas is expected to have about three times the specific weight of H_2, thus sufficient to render MH equivalent to natural gas as far as energy content is concerned (because natural gas contains about $1,000$ BTU/scf, $H2$ contains about 300 BTU/scf, consequently $MH = 3H_2$ would contain BTU/scf close to those of natural gas)

type of MagneH is composed of 99.2% hydrogen and 0.78% methane, while no carbon monoxide was detected.

2) The average specific weight of this type of MH was measured by two independent laboratories as being 15.06 a.m.u., while conventional pure hydrogen has the specific weight of 2.016 a.m.u., thus implying a 7.47 fold increase of the specific weight of conventional hydrogen.

3) The same type of MH used in the preceding tests was submitted to CG-MS scans via the use of a HP GC 5890 and a HP MS 5972 with operating conditions specifically set for the detection of magnecules (Section 5 and Ref. [5]). The results of these third tests are reproduced in Fig. 11.37. As one can see, by keeping in mind the results of GC-FTIS of Fig. 11.36, the GC-MS measurements should have shown only two peaks, that for hydrogen H_2 at about 2 a.m.u., and that for methane CH_4 at about 16 a.m.u. On the contrary, these GC-MS tests confirm the existence of a large peak at about 2 a.m.u. evidently representing hydrogen, but do not show any peak at 16 a.m.u. proportional to the 0.78% of methane, and exhibit instead the presence of a considerable number of additional peaks in macroscopic percentages all the way to 18 a.m.u. This GC-MS scan establishes the existence beyond credible doubt of a magnecular structure in the type of MH here studied. Note, in particular, *the existence of well identified peaks in macroscopic percentage with atomic weight of 3, 4, 5, 6, 7, 8 and higher values which peaks, for the gas under consideration here, can only be explained as magnecules composed of individual H atoms as well as H molecules in increasing numbers.*

SPECTRALAB

6349 82nd Avenue North
Pinellas Park, Florida 33781
Phone: (727) 545-2297 • Fax (727) 547-8024

Component	Gas
Hydrogen	99.2
Carbon monoxide	None detected
Carbon dioxide	None detected
Methane	0.78
Ethane	None detected
Ethene (ethylene)	None detected
Ethyne (acetylene)	None detected

Figure 11.36. A summary view of the spectroscopic analyses conducted by Spectra lab of largo, Florida, showing 99.2% hydrogen in the species of MH here considered. Note the "experimental belief" that the species here considered contains 0.78% methane. MH produced from magnegas cannot possibly contain methane since magnegas is formed at about $10,000^oF$ of the electric arc at which methane cannot possibly survive. in reality, the analytic instrument has detected a magnecular species with 16 a.m.u and identified that species with methane due to lack of info in the computer data banks.

The above measurements 1), 2) and 3) confirm the capability to produce hydrogen with a multiple value of their standard specific weight, and consequential increased energy content.

Next, to test MO in fuel cells, the author had constructed by technicians in Florida a rudimentary apparatus based on the use of automotive sparks powered by an ordinary car battery, the system operating at about 15 psi. Two types of MO, denoted by MO_1 and MO_2, were produced from pure oxygen for comparative purposes.

This type of MO was tested in lieu of ordinary oxygen in a 2-cell Proton Exchange Membrane (PEM) fuel cell operated with conventional high pu-

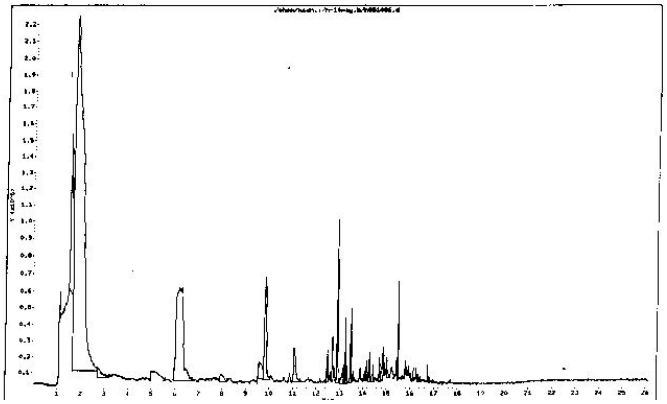

Figure 11.37. A view of one of the numerous GC-MS scans conducted at the Toxic Analytic Laboratory in California establishing in a final form the magnecular character of the species here studied. In fact, the molecular seeving process used by Adsorption Research Laboratory could only allow the separation of hydrogen and definitely not the numerous heavy clusters identified in this scan. Since hydrogen has only one electron and, consequently can only form under valence bond H_2, the heavy species of hydrogen here considered establishes the existence of a *non-valence* bond beyond any possible or otherwise credible doubt.

rity hydrogen. The membrane material was Nafion 112; the catalyst in the electrodes was platinum acting on carbon; the plates for heat transfer were given by two nickel/gold plated material; the temperature of the fuel cell was kept constant via ordinary cooling means; the current was measured via a HP 6050A electronic load with a 600 W load module; a flow rate for oxygen and hydrogen was assigned for each current measurement; both oxygen and hydrogen were humidified before entering the cell; the measurements reported herein were conducted at 30 degrees C.

The results of the measurements are summarized in Figs. 11.38, 11.39 and 11.40 that report relative measurements compared to the same conditions of the cell when operated with ordinary pure oxygen. As one can see, these measurements show a clear increase of the voltage, power and efficiency of the order of 5% when the cell was operated with MO_1 and MO_2. The increase was consistent for both samples except differences within statistical errors.

To appraise these results, one should note that the types of MO used in the test were produced via rudimentary equipment based on intermittent sparks operated with an ordinary automotive battery, and with the pressure limited to 15 psi. By comparison, the industrial production of MO should be done with an array of arcs each operated with continuous currents of thousands of Amperes, and at pressures of thousands of psi. It is evident that the latter conditions are expected to imply a significant increase of the performance of

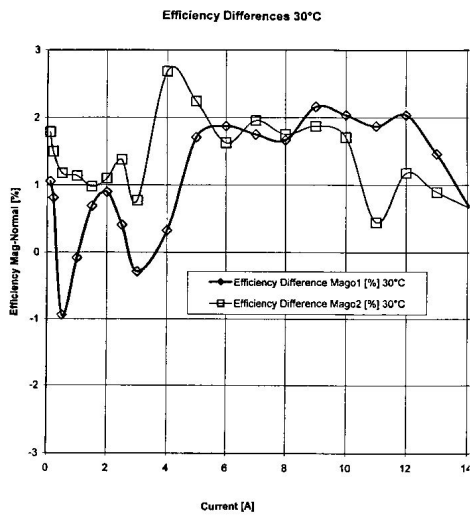

Figure 11.38. A schematic view of the voltage increase in a test fuel cell operated with ordinary pure hydrogen and the two samples of MO produced by rudimentary equipment.

the fuel cells when operated with MO. Still bigger increases in voltage, power and efficiency occur when the fuel cells are operated with both MO and MH for the reasons discussed in Section 3. These latter tests are under way and are contemplated for reporting in a future research..

In summary, the systematic character of the experimental results, combined with the limited capabilities of the used equipment, appear to confirm the hypothesis of new forms of hydrogen and oxygen with magnecular structure capable of producing an industrially significant increase in voltage, power and efficiency of fuel cells. Independent measurements are here solicited for the finalization of these issues.

11.5.5 Conclusions

Despite the known uneasiness created by novelty, the rather vast experimental evidence, only partially reproduced in this section to avoid a prohibitive length, supports the following results:

1) The *existence of a new chemical species whose bonding force is not of valence type* (from the absence of infrared signature and various other evidence as in Figs. 6 and 7), which has been interpreted by this author as being due to the only fields available in a molecular structure, the electric and magnetic fields, and called *electromagnecules* in general, the name *Santilli magnecules*

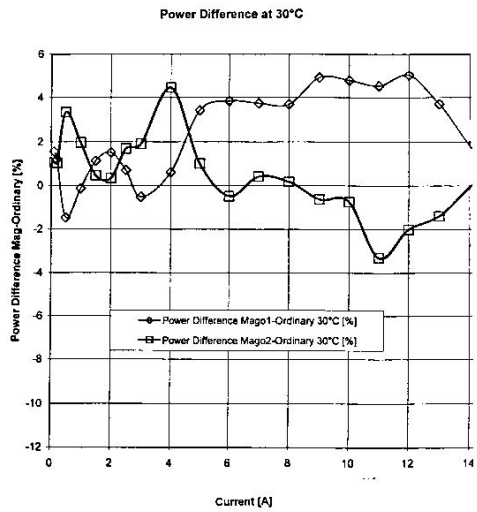

Figure 11.39. A schematic view of the power increase in a test fuel cell operated as in Fig. 11.38 confirming the results of the latter.

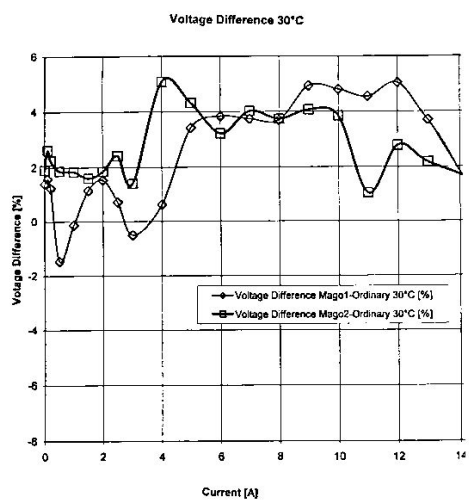

Figure 11.40. A schematic view of the efficiency increase in a test fuel cell operated as in Fig. 11.38, which provide additional confirmation of the latter results.

being used to denote the dominance of magnetic over electric effects (Section 2). Other researchers may prefer different nomenclatures and search for esoteric fields other than the electric and magnetic fields, with the understanding that the *non-valence novelty* of the new species is outside scientific debate.

2) The *existence of a form of hydrogen with about seven times the atomic weight of molecular hydrogen which eliminates the need for liquefaction in automotive use, while having a power output essentially similar to that of gasoline, and being cost competitive with respect to fossil fuel when produced in large scale.* This is the new species of hydrogen, called by this author MagneH^{TM} (patented and international patents pending) which is derived via filtering, cryogenic separation or other means from the new combustible fuel called *Santilli MagneGas*^{TM} (international patents pending). The latter gas s is produced via DC electric arcs between carbon-base consumable electrodes submerged within a hydrogen rich liquid feedstock, such as fresh or salt water, antifreeze or oil waste, city or farm sewage, crude oil, etc.

3) The *industrial capability of turning conventional hydrogen and oxygen into new species with bigger atomic weight and energy content for use in fuel cells with increased voltage, power and efficiency.*

4) The *existence of new forms of liquid hydrogen and oxygen for rocket propulsion with increased trust, and consequential increased payload or decreased boosters' weight with the same payload.*

5) The *experimental evidence of dramatic departures from quantum chemistry in support of the covering hadronic chemistry* [5].

Evidently, these studies are in their infancy and much remains to be done, both scientifically and industrially. Among the existing intriguing open problems we mention:

A) The identification of *new analytic equipment specifically conceived for the detection of magnecules.* In fact, researchers in the field know well the dramatic insufficiency for tests on magnecular substances of currently available analytic equipment specifically conceived for molecular substances.

B) The *identification of the possible frequency at which magnecules may have an infrared signature.* For instance, the detection of methane in the MH tests of Fig. 11.36 has a mere indicative value, rather than being an actual experimental fact. In any case, the detection of methane is not confirmed by at least one second independent test to achieve final scientific character. Also, a peak at 16 a.m.u. which is necessary in the GC-MS scans of Fig. 11.27 to confirm the presence of methane (CH_4), is missing. Finally, the original MagneGas is created in the 10,000^o F of electric arcs at which temperature no methane can survive. In view of the above, a more plausible possibility is that the "methane" detected by the analyses of Fig. 11.37 is, in reality, the infrared signature of a magnecule.

C) The *study of the liquefaction of MagneGases* on a comparative basis with the liquefaction of the same gases with conventional molecular structure. This study is recommended particularly for rocket propulsion, due to the expected new species of *liquid magnecules* [5], the liquefaction itself at a temperature bigger than the conventional ones, the increase in trust and the reduction in liquefaction costs.

D) The *study of the possible storage of energy in inert gases* via the mechanism of internal magnetic polarization and resulting new molecular bonds illustrated in Figs. 5 and 8. In fact there exist patents as well as reported test engines operating on inert gases which are generally dismissed by academia because of the believed "inert" character of these cases. Perhaps, a more open mind is recommendable for truly basic advances.

E) The *study of nonlinear deviations from the perfect gas law and the Avogadro number* which are inherent in magnecular clustering since they can break down into fragments due to collision and then have different recombinations, resulting in a population with generally varying number of constituents, while keeping constant statistical averages.

Needless to say, the author solicits the independent verification of all results presented in this section without which no real scientific advance is possible.

11.6 HHO, THE NEW GASEOUS AND COMBUSTIBLE FORM OF WATER WITH MAGNECULAR STRUCTURE

11.6.1 Introduction

Studies on the electrolytic separation of water into hydrogen and oxygen date back to the 19-th century (for a textbook on the water molecule see, e.g., Ref. [20a] and for an account on its electrolytic separation see, e.g., Ref. [20b]). More recently, there has been considerable research in the separation of water into a mixture of hydrogen and oxygen gases. These studies were initiated by Yull Brown in 1977 via equipment generally referred to as electrolyzers and the resulting gas is known as "Brown gas" (see patents [21]).

In accordance with these patents as well as the subsequent rather vast literature in the field, the Brown gas is defined as a combustible gas composed of conventional hydrogen and conventional oxygen gases having the exact stochiometric ratio of 2/3 (or 66.66% by volume) of hydrogen and 1/3 (or 33.33% by volume) of oxygen.

In this section the author (a physicist) presents to the chemistry community for its independent verification various measurements on an apparently new mixture of hydrogen and oxygen hereon referred to as the HHO gas (international patent pending) developed by Hydrogen Technology Applications, Inc., of Clearwater, Florida (www.hytechapps.com). The new HHO gas is regularly

produced via a new type of electrolyzer and has resulted to be distinctly different in chemical composition than the Brown gas, even though both gases share a number of common features.

The main scope of this section is to report, apparently for the first time, new clusters of hydrogen and oxygen atoms contained in the HHO gas, which clusters appear to escape the traditional valence interpretation and constitute one of the novelties of the HHO gas over the Brown gas.

Another objective of this sec tion is to initiate quantitative studies on the rather unique features of the HHO gas that do not appear to be representable via the conventional quantum chemistry of hydrogen and oxygen gases.

Yet another objective of this section is to present a working hypothesis to initiate the understanding of the capability by the HHO electrolyzers to perform the transition of water from the liquid to a gaseous state via a process structurally different than evaporation or separation, due to the use of energy dramatically less than that required by said evaporation or separation.

The final objective of this section is the submission, apparently for the first time, of it a new form of the water molecule created by the removal of its natural electric polarization and consequential collapse of the two HO dimers, from their conventional configuration with 105° to a new configuration in which the two dimers are collapsed one against the other due to strongly attractive opposing magnetic polarizations (see below for details and pictures).

Due to the loss of electric polarization, polymerization and other features, the above new form of the water molecule permits a plausible representation of the creation of the HHO gas from liquid water without the evaporation energy. Its unstable character also permits a plausible interpretation on the experimental measurements of all anomalous features of the HHO gas.

Independent verification by interested chemists of the various measurements reported in this section are solicited, jointly with the conduction of additional much needed tests. Samples of the HHO gas can be obtained at any time by contacting Hydrogen Technology Applications, Inc. at their website www.hytechapps.com.

11.6.2 Experimental Measurements on the New HHO Gas

Under visual inspection, both the HHO gas results to be odorless, colorless and lighter than air, as it is also the case for the Brown gas. Their first remarkable feature is the efficiency E of the electrolyzer for the production of the gas, here simply defined as the ratio between the volume of HHO gas produced and the number of Watts needed for its production. In fact, the electrolyzers rapidly convert water into 55 standard cubic feet (scf) of HHO gas at 35 pounds per square inch (psi) via the use of 5 Kwh, namely, an

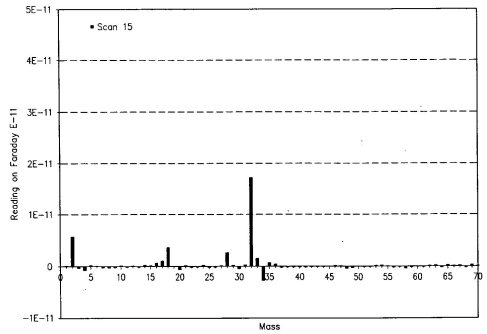

Figure 11.41. A view of one of the GC scans on the HHO gas conducted by Adsorption Research Laboratories showing conventional as well as anomalous peaks.

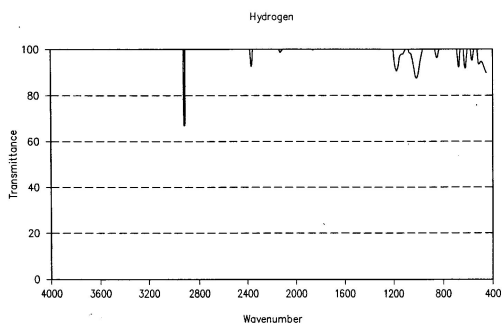

Figure 11.42. The IR signature of a conventional H_2 gas made by the PdMA laboratory.

efficiency that is at least ten times the corresponding efficiency of conventional water evaporation, thus permitting low production costs.

The above efficiency establishes the existence of a transition of water from the liquid to the gaseous state that is not caused by evaporation. By keeping in mind the combustible character of the HHO gas compared to the noncombustible character of water vapor, the above efficiency suggests the existence of new chemical processes in the production of the gas that deserve quantitative studies.

A second important feature is that the HHO gas does not require oxygen for combustion since the gas contains in its interior all oxygen needed for that scope, as it is also the case for the Brown gas. By recalling that other fuels (including hydrogen) require atmospheric oxygen for their combustion, thus

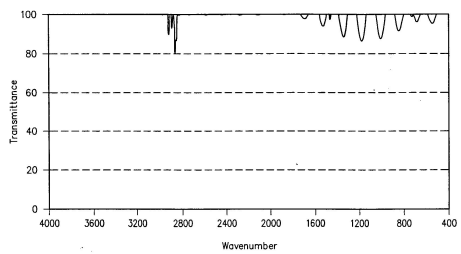

Figure 11.43. The IR signature of a conventional O_2 gas made by the PdMA laboratory.

causing a serious environmental problem known as oxygen depletion, the capability to combust without any oxygen depletion (jointly with its low production cost) render the gas particularly important on environmental grounds.

A third feature of the gas is that it does not follow the PVT of gases with conventional molecular structure, since the gas reacquires the liquid water state at a pressure of the order of 150 psi, while conventional gases acquire the liquid state a dramatically bigger pressures. This feature suggests that the gas here considered does not possess a conventional molecular structure, namely, a structure in which the bond is of entire valence type.

A fourth feature of the gas is its anomalous adhesion (adsorption) to gases, liquids and solids, as verified experimentally below, thus rendering its use particularly effective as an additive to improve the environmental quality of other fuels, or other applications. This feature is manifestly impossible for conventional gases H_2 and O_2, thus confirming again a novel chemical structure.

A fifth feature of the gas is that it exhibits a widely varying thermal content, ranging from a relatively cold flame in open air at about 150^oC, to large releases of thermal energy depending on the substance to which the flame is applied to, such as the instantaneous melting of bricks requiring up to $9,000^oC$.

The measurements conducted by the author at various independent laboratories on the HHO gas can be summarized as follows.

On June 30, 2003, Adsorption Research Laboratory of Dublin, Ohio, measured the specific weight of the HHO gas and released a signed statement on the resulting value of 12.3 grams/mole. The same laboratory repeated the measurement on a different sample of the gas and confirmed the result.

The released value of 12.3 grams/mole is anomalous. In fact, the conventional separation of water into H_2 and P_2 produces a mixture of 2/3 HBN_2 and 1/3 O_2 that has the specific weight $(2 + 2 + 32)/3 = 11.3$ grams/mole.

Therefore, we have the anomaly of 12.3 - 11.2 = 1 gram/mole, corresponding to 8.8% anomalous increase in the value of the specific weight. Rather than

the predicted 66.66% of H_2 the gas contains only 60.79% of the species with 2 atomic mass units (amu), and rather than having 33.33% of O_2 the gas contains only 30.39% of the species with 32 amu.

These measurements provide direct experimental evidence that the HHO gas is not composed of a sole mixture of H_2 and O_2, but has additional *heavier* species.

Moreover, the HHO gas used in the tests was produced from distilled water. Therefore, there cannot be an excess of O_2 over H_2 to explain the increased specific weight. The above measurement establishes the presence in HHO of 5.87% of hydrogen and 2.94% oxygen bonded together into species heavier than water, as identified below via mass spectroscopy and other analytic measurements.

Adsorption Research Laboratory also conducted scans of the HHO gas via a Gas Chromatographer (GC) reproduced in Fig. 11.41 establishing the presence in the HHO gas of the following species here presented in order of their decreasing percentages:

1) A first major species with 2 amu expectedly representing gaseous hydrogen;

2) A second major species with 32 amu expectedly representing gaseous oxygen;

3) A large peak at 18 amu expectedly representing water vapor;

4) A significant peak with 33 amu expectedly representing a new species expectedly of non-molecular nature;

5) A smaller yet clearly identified peak at 16 amu expectedly representing atomic oxygen;

6) Another small yet fully identified peaks at 17 amu expectedly representing the radical OH whose presence in a gas is also anomalous;

7) A small yet fully identified peak at 34 amu expectedly representing the bond of two dimers HO that is also anomalous for a gas;

8) A smaller yet fully identified peak at 35 amu that cannot be identified in any known molecule;

9) Additional small peaks expected to be in parts per million.

It should be added that the operation of the GC detector was halted a few seconds following the injection of the HHO gas, while the same instrument was operating normally with other gases. This anomalous behavior can be best interpreted via an anomalous adhesion of the gas to the walls of the feeding line as well as of the column and other parts of the instruments, an anomalous adhesion confirmed by additional tests reviewed below.

On July 22, 2003, the PdMA Corporation in Tampa, Florida, conducted InfraRed (IR) scans reported in Figures 2, 3 and 4 via the use of a Perkin-Elmer IR scanner model 1600 with fixed point/single beam. The reported

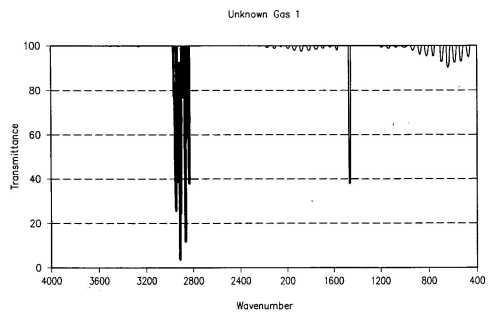

Figure 11.44. The IR signature of the HHO gas made by the PdMA laboratory. When compared to the IR scans of Figures 2 and 3, this scan shows that the HHO gas is not a mixture of H_2 and O_2 gases.

scans refer to a conventional H_2 gas (Fig. 11.42), a conventional O_2 gas (Fig. 11.43), and the HHO gas Fig. 11.44).

Inspection of these scans shows a substantial differences between HHO gas and H_2 and O_2 gases. In fact, the latter gases are symmetric molecules, thus having very low IR peaks, as confirmed by scans 2 and 3. The first anomaly of HHO is that of showing comparatively much stronger resonating peaks. Therefore, the indicated IR scans establish that the HHO gas has an asymmetric structure, which is remarkable since the same feature is absent for the conventional mixture if H_2 and O_2 gases.

Moreover, H_2 and O_2 gases can have at most two resonating frequencies each, one for the vibrations and the other for rotations. Spherical distributions of orbitals and other features imply that H_2 has essentially only one IR signature as confirmed by the scan of Fig. 11.42, while O_2 has one vibrational IR frequency and three rotational ones, as also confirmed by the scans of Fig. 11.43.

Inspection of the IR scans for the HHO gas in Fig. 11.44 reveals additional novelties. First, the HHO scan show the presence of at least nine different IR frequencies grouped around wavenumber 3000, plus a separate distinct frequency at around wavenumber 1500.

These measurements provide experimental evidence that the species with 18 amu detected in the GC scans of Fig. 11.41 is not water vapor, but a yet unknown bond of two hydrogen and one oxygen atoms.

In fact, water vapor has IR frequencies with wavelengths 3756, 3657, 1595, their combination and their harmonics (here ignored for simplicity). The scan for the HHO gas in Fig. 11.44 confirms the presence of an IR signature near 1595, thus confirming the molecular bond HO, but the scan shows no presence

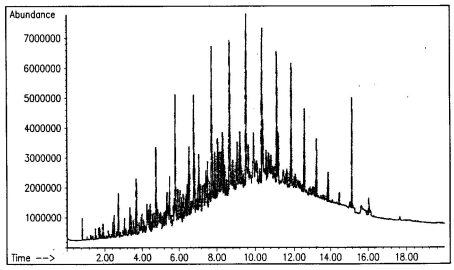

Figure 11.45. A TIC of the GC-MS scans of conventionally sold diesel fuel made by Southwest Research Institute.

of the additional very strong signatures of the water molecules at 3756 and 3657, thus establishing the fact that the peak at 18 amu is not water as conventionally understood in chemistry.

On July 22, 2003, the laboratory of the PdMA Corporation in Tampa, Florida measured the flash point, first on commercially available diesel fuel, detecting a flash point of 75^oC, and then of the same fuel following the bubbling in its interior of the HHO gas, detecting the flash point of 79^oC.

The latter measurement too is anomalous because it is known that the addition of a gas to a liquid fuel *reduces* its flash point generally by half, rather than *increasing* it as in the above measurement, thus implying the expected flash value of about 37^C for the mixture of diesel and HHO gas. Therefore, the anomalous increase of the flash point is not of 4^oC, but of about 42^oC.

Such an increase cannot be explained via the assumption that HHO is contained in the diesel in the form of a gas (otherwise the flash point would decrease), and requires the occurrence of some type of anomalous bond between the gas and the liquid that cannot possibly be of valence type.

An experimental confirmation of the latter bond was provided on August 1, 2003, by the Southwest Research Institute of Texas, that conducted mass spectrographic measurements on one sample of ordinary diesel as used for the above flash point measurements, here reported in Fig. 11.45, and another sample of the same diesel with HHO gas bubbled in its interior, here reported in Fig. 11.46.

The measurements were conducted via a Total Ion Chromatogram (TIC) and Gas Chromatography Mass Spectrometry GC-MS manufactured by Hewlett Packard with GC model 5890 series II and MS model 5972. The TIC was obtained via a Simulated Distillation by Gas Chromatography (SDGC).

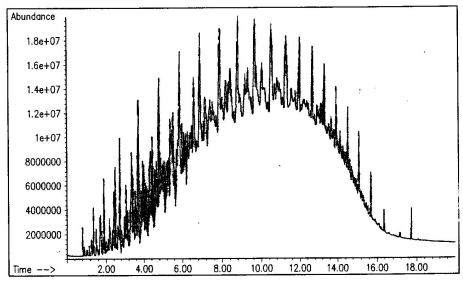

Figure 11.46. A TIC of the GC-MS scans made by Southwest Research Institute on the same diesel fuel of Figure 5 in which the HHO gas had been bubbled through, showing the alteration of the TIC both in shape as well as increased mass, thus indicating a new bond between diesel and HHO that cannot be of valence type (since HHO is gaseous and diesel is liquid. In any case, all valence electrons in both the gas and the liquid are used by conventional molecular bonds.

The column was a HP 5MS $30 \times 0,25$ mm; the carrier flow was provided by helium at 50^oC and 5 psi; the initial temperature of the injection was 50^oC with a temperature increase of 15^oC per minute and the final temperature of 275^oC.

The chromatogram of Fig. 11.45 confirmed the typical pattern, elusion time and other feature of commercially available diesel. However, the chromatograph of the same diesel with the HHO gas bubbled in its interior of Fig. 11.46 shows large structural differences with the preceding scan, including a much stronger response, a bigger elusion time and, above all, a shift of the peaks toward bigger amu values.

Therefore, the latter measurements provide additional confirmation of the existence of an anomalous bond between the diesel and the HHO gas, precisely as predicted by the anomalous value of the flash point and the clogging up of GC feeding lines. In turn such a bond between a gas and a liquid cannot possibly be of valence type, since all valence electrons are expected to be coupled in both the liquid and the gas.

Further mass spectrographic measurements on the HHO gas were done on September 10, 2003, at SunLabs, of the University of Tampa, Florida, via the use of a very recent GC-MS Clarus 500 by Perkin Elmer, one of the most sensitive instruments currently available to detect hydrogen.

Even though the column available at the time of the test was not ideally suited for the separation of all species constituting the HHO gas, the latter measurements confirmed the preceding results.

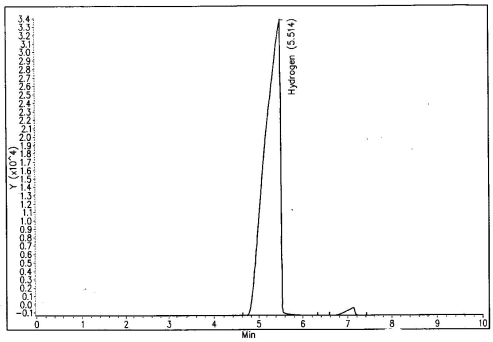

Figure 11.47. A TIC of the GC-MS scans on the HHO gas made by Toxic LTD Laboratories showing the H_2 content of the HHO gas.

In fact, the scan of Fig. 11.50 confirms the presence in the HHO gas of a basic species with 2 amu representing hydrogen, plus a species with 5 amu that cannot admit any valence or molecular interpretation for the HHO gas even if the species is formed by the spectrometer.

In conclusion, the experimental measurements of the flash point and of the scans of Figs. 5 and 6 establish beyond doubt the capability by the HHO gas to have an anomalous bond with liquid fuels, that is, a bond that is not of valence type.

Additional analyses on the chemical composition of the HHO gas were done by Air Toxic LTD of Folsom, California, via the scans reproduced in Figs. 7, 8 and 9. These scans confirmed that H_2 and O_2 are the primary constituents of the HHO gas. However, the same measurements identify the following anomalous peaks:

a) A peak in the H_2 scan at 7.2 minutes elusion times (Fig. 11.47);

b) A large peak in the O_2 scan at 4 minutes elusion time (Fig. 11.48); and

c) An anomalous blank following the removal of the HHO gas (Fig. 11.49), because said blank shows the preservation of the peaks of the preceding scans, an occurrence solely explained via anomalous adhesion of the HHO gas to the interior walls of the instrument.

The scan of Fig. 11.51 provides evidence of a species with mass 16 amu that can only be interpreted as atomic oxygen, thus providing additional indication of the presence in the HHO gas of atomic hydrogen as expected from its capabilities, although the species, again, could be separated by the spectrometer due to the expected weak nature of the bond. The latter could not be detected in the preceding scan due to the impossibility of the instrument here considered to detect a species with 1 amu. The same scan of Fig. 11.51

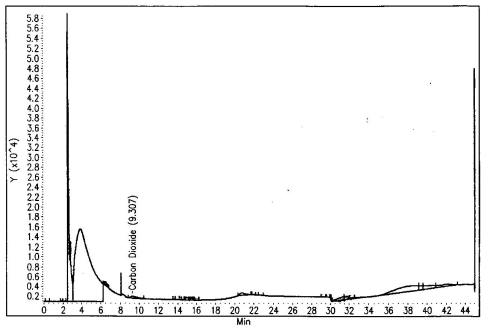

Figure 11.48. A TIC of the GC-MS scans on the HHO gas made by Toxic LTD Laboratories showing the peaks belonging to H_2 and O_2 , plus anomalous peaks.

confirms the presence in the HHO gas of a species with 17 amu and a species with 18 amu detected in earlier tests.

The scan of Fig. 11.52 establishes the presence in the HHO gas of species with 33 and 34 amu, while the species with 35 amu detected in preceding measurements was confirmed in other scans here not reported for brevity.

The tests also confirmed the blank anomaly, namely, the fact that the blank of the instrument following the removal of the gas continues to detect the basic species constituting the gas, which blank is not reproduced here for brevity, thus confirming the anomalous adhesion of the HHO gas to the interior walls of the instrument.

In summary, the above analytic measurements establish the following properties of the HHO gas:

I) An anomalous increase in specific weight of 1 gram/mole (or 8.8% in volume) establishing the presence in the HHO gas of species heavier than the predicted mixture of H_2 and O_2, thus establishing the presence in the HHO gas of new species composed of H and O atoms that cannot possibly have valence bonds.

II) The GC scans done by Adsorption Research (Fig. 11.41) confirm the presence of chemical species in the HHO gas that cannot have a valence interpretation, such as the species with 17 amu, 33 amu, 34 amu, and 35 amu, besides conventional species with 2 amu, 16 amu and 18 amu, all species independently confirmed by other tests, such as the scans of Figs. 10, 11 and 12

III) The halting of the GC instrument in the scans of Fig. 11.41 after a few seconds following the injection of the HHO gas, while the same instrument works normally for conventional gases, is experimental evidence for an

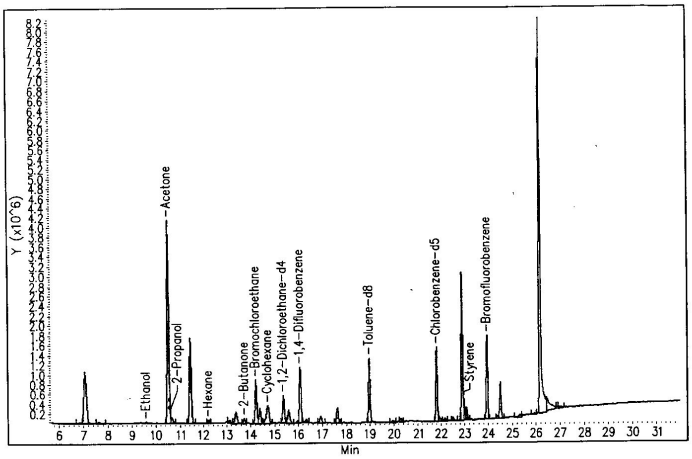

Figure 11.49. One of the anomalous blanks of the GC-MS scans made by Toxic LTD Laboratories following the tests of the HHO. The blank is firstly anomalous because only the background should have been detected, thus indicating a bond between the HHO gas and the walls of the instrument, whose most plausible explanation is the magnetic polarization by induction of said walls by a form of magnetic polarization of the species composing the HHO gas. the second reasons for the anomalous nature of the blank is that the substances detected cannot possibly exist in the HHO gas produced from distilled water, thus showing an accretion of bonds to the instrument walls.

anomalous adhesion by the HHO gas to the internal walls of the instrument, to such a level of occluding the column and causing the shut down of the scan;

IV) The large increase of the flash point of diesel fuel following inclusion of the HHO gas also constitutes experimental evidence of anomalous adhesion by the HHO gas, this time, to a liquid fuel that cannot also be of valence type since all valence electrons available in both the liquid and the gas are expected to be paired;

V) The mass spectrometric measurements on the mixture of diesel and HHO (Figs. 5 and 6) provide additional experimental confirmation of an anomalous bond between the HHO gas and diesel;

VI) The additional scans of Figs. 7, 8 and 9 confirm all the preceding results, including the anomalous blank following the removal of the HHO gas, thus confirming the anomalous adhesion of the HHO gas to the internal walls of the instrument;

VII) The capability by the HHO gas to melt instantaneously tungsten and bricks is the strongest evidence on the existence in the HHO gas of basically new chemical species that cannot possibly have a valance bond, since a mixture

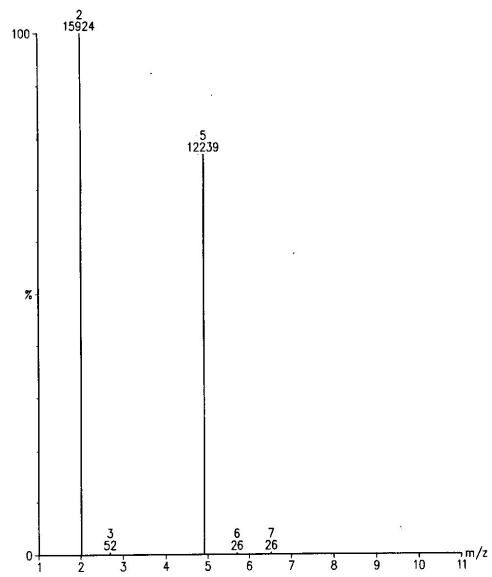

Figure 11.50. The scan conducted by SunLabs on the HHO gas confirming the presence of H_2, plus additional anomalous peaks, such as the species at 5 amu, that cannot possibly admit a molecular interpretation.

of 2/3 H_2 and 1/3 O_2 cannot melt instantly tungsten and bricks , as any interested chemist is encouraged to verify.

It should be indicated that a number of species in the HHO gas, particularly those with higher specific weight, are expected to be unstable and, as such, decomposed by the analytic instrument itself, In different terms, by no means GC, IR and other scans should be expected to detect *all* constituents of the HHO gas, since a number of them are expected to be decomposed or altered by the ionization and other processes connected to the scans themselves.

11.6.3 Magnecular Interpretation of the Measurements

The first experimental evidence supporting the magnecular structure of the HHO gas is its capability of instantly melting tungsten and bricks. In fact, such a capability can only be explained via the presence in the HHO gas, not only of atomic (that is, unbounded) hydrogen as depicted in the top of Fig. 11.9, but also of atomic hydrogen with the toroidal polarization of their orbitals as depicted in the bottom of Fig. 11.10.

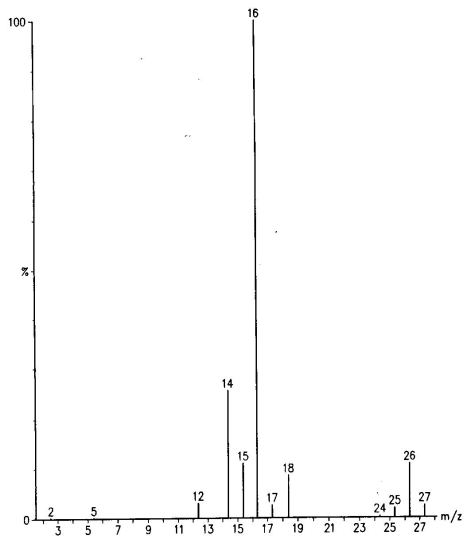

Figure 11.51. The scan conducted by SunLabs on the HHO gas detecting a peak at 16 amu that confirms the presence of atomic oxygen in the HHO gas of Fig. 11.51, plus a peak at 17 amu indicating the presence of traces of the radical $O - H$, a peak at 18 amu indicating the presence of water vapor all three species also detected in the scan of Fig. 11.51, as well as additional anomalous peaks at 12, 14, 25, 26, 27 amu that, for the case of the HHO gas produced from distilled water cannot admit a molecular interpretation.

In fact, no instantaneous melting of bricks is possible without the hydrogen contained in the HHO gas rapidly penetrating within deeper layers of the brick structure. Such a rapid penetration cannot be explained with atomic hydrogen, although it can be readily explained via the polarized hydrogen atom of the bottom of Fig. 11.10.

Besides having a smaller sectional area that favors fast penetration, polarized H-atoms cause an induced polarization of the orbitals of the atoms of the brick, their consequential attraction to the polarized H atoms, and the latter rapid penetration within deep layers of the brick structure. In turn, faster penetration within the lattice of solids implies a bigger reactivity that, in turn, causes a bigger melting temperature.

Moreover, polarized atomic hydrogen as well as oxygen are needed to explain the anomalous adhesion of the HHO gas to internal walls of detection instruments as well as to other substances.

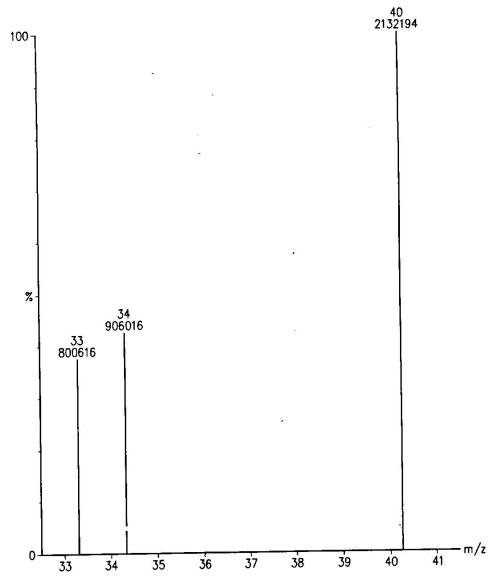

Figure 11.52. A sample of various additional scans conducted by SunLabs on the HHO gas detecting anomalous peaks at 33, 34 and 40 amu that cannot possibly have a consistent molecular interpretation. Intriguingly, the peak at 35 amu detected in other tests did not appear sequentially in this scan, and appeared instead in other scans here not reported for brevity, thus indicating that the peaks of this and of the preceding scans conducted by SunLabs are, in actuality, the constituents of the clusters composing the HHO gas, and not the actual constituents themselves.

Note that the studies of the Brown gas [2] have indicated the need for *atomic hydrogen.* Therefore, the presence of *atomic and polarized hydrogen* is a novelty of the HHO gas.

Evidently, individual hydrogen atoms cannot maintain their polarization as in Fig. 11.9 in view of motions caused by temperature, as well known. The only known possibility for maintaining said polarization is that polarized H atoms bond themselves with opposing magnetic polarities as depicted in Fig. 11.11. In fact, rotations and vibrations due to temperature occur for such bonded H atoms as a whole, while individually preserving said polarization.

In turn, bonds of polarized atomic hydrogen constitute the very basic bond of magnecules, thus supporting the hypothesis of the magnecular structure of the HHO gas.

Note that a conventional hydrogen gas cannot acquire any magnetic polarization because the conventional hydrogen molecules is diamagnetic. However, as established in Refs. [21], the diamagnetic character refers to the hydrogen

molecule as a whole, because quantum mechanics establishes that each individual hydrogen *atom* of a hydrogen molecule can indeed acquire a magnetic polarization under sufficiently strong external magnetic fields.

The diamagnetic character of the hydrogen molecules, as depicted in Fig. 11.10, is due to the fact that the individual magnetic polarizations of its H atoms are opposite to each other, and are at such a close mutual distances to cancel each other when inspected at sufficiently large distances.

Needless to say, the above hypothesis on the polarization of atomic hydrogen also applies to oxygen, the latter being known to be paramagnetic, resulting in atomic oxygen with the spherical distribution of orbitals, polarized atomic oxygen with the polarization of at least the valance electrons, and pairs of bonded polarized oxygen atoms as depicted in Fig. 11.11.

The first prediction of the magnecular structure of the HHO gas is that the species at 2 amu and 32 amu detected by mass spectroscopy could, in actuality, be constituted by a mixture of the conventional molecules H_2 and O_2 and a percentage of the same atoms although with the magnecular bond, since the latter are expected to have essentially the same atomic weight than the former.

The separation of hydrogen molecules and magnecules is possible via instruments based on magnetic resonance techniques because the conventional hydrogen molecule is diamagnetic (Fig. 11.9) while the hydrogen magnecule has a distinct magnetic polarity (Fig. 11.11).

It is easy to see that the magnecular hypothesis on the chemical structure of the HHO gas permits a quantitative interpretation of all anomalous species reported in the preceding section.

As now familiar, let us denote the conventional valence bond with the usual symbol "-" and the magnecular bond with the symbol "$\times$". According to this notation, $H_2 = H - H$ represents the molecule of Fig. 11.10 while $H \times H$ represents the magnecule of Fig. 11.11. Molecular bonds are notoriously restricted to valence pairing, in the sense that no additional atom can be bonded when all available valence pairs are coupled. By contrast, magnecular bonds do not have such a restriction, in the sense that atoms can indeed be added to a magnecule under the sole condition of the availability of opposite magnetic polarizations.

Needless to say, for the HHO gas at ambient temperature and pressure, the stability of the magnecular clusters is inversely proportional to the number of their constituents. As a result, magnecular clusters with relatively low atomic weight are expected to exist in significant percentages, while those with large atomic weight are expected to be present at best in parts per millions.

The magnecular hypothesis permits the following interpretations of the species composing the HHO gas: the species with 3 amu is interpreted as a combination of the magnecules $H \times H \times H$ or $(H - H) \times H$; the species with

4 amu is interpreted as a combination of $(H-H)\times(H-H$, $(H-H)\times H\times H$, or $H\times H\times H\times H$, heavier magnecular bonds solely of hydrogen atoms being unstable due to collisions; the species with 17 amu is interpreted as a combination of the traditional dimer $H-O$ and the magnecular bond $H\times O$; the species with 33 amu is interpreted as a mixture of $(O-O)\times H$, $(H-O)\times O$ and $O\times O\times H$; the species with 34 amu is interpreted as a mixture of $(H-H)\times(O-O)\times(H-H)\times H$ and similar configurations; the species with 35 amu is interpreted as a mixture of $(O-O)\times(H-H)\times(H-H)\times H$ and equivalent configurations (see Fig. 11.11); and other magnecular species in progressively smaller percentages.

11.6.4 the New Gaseous and Combustible Form of Water

Besides a quantitative interpretation of the chemical structure of all species contained in the HHO gas, as well as of its anomalous thermal content and adhesion, perhaps the biggest contribution of the magnecular hypothesis is a quantitative interpretation of the formation of the HHO gas despite the lack of evaporation or separation energy.

Recall that nature has set the water molecule $H_2O = H-O-H$ in such a way that its H atoms do not have the spherical distribution, and have instead precisely the polarized distribution of Fig. 11.10 along a toroid whose symmetry plane is perpendicular to that of the $H-O-H$ plane, as depicted in Fig. 153, and established in the technical literature (see, e.g., Ref. [1=20a]).

It is also known that the H-O-H molecule at ambient temperature and pressure, even though with a null total charge, has a high electric polarization (namely, a deformation of electric charge distributions) with the predominance of the negative charge density localized in the O atom and the complementary predominant positive charge density localized in the H atoms [1a]. This feature causes a repulsion of the H atoms due to their predominantly positive charges, resulting in the characteristic angle of (about) 105° between the $H-O$ and $O-H$ dimers as depicted in Fig. 11.54.

It is well established in quantum mechanics that toroidal polarizations of the orbitals of the hydrogen atom as in the configuration of Fig. 11.11 create very strong magnetic fields with a symmetry axis perpendicular to the plane of the toroid, and with a value of said magnetic field sufficient for the creation of the new chemical species of magnecules [3].

It then follows that, in the natural configuration of the $H-O-H$ molecule, the strong electric polarization caused by the oxygen is such to weaken the magnetic field of the toroidal polarization of the H-orbital resulting in the indicated repulsion of the two H-atoms in the $H-O-H$ structure.

However, as soon as the strong electric polarization of the molecule $H-O-H$ is removed, the strong attraction between opposite polarities of the

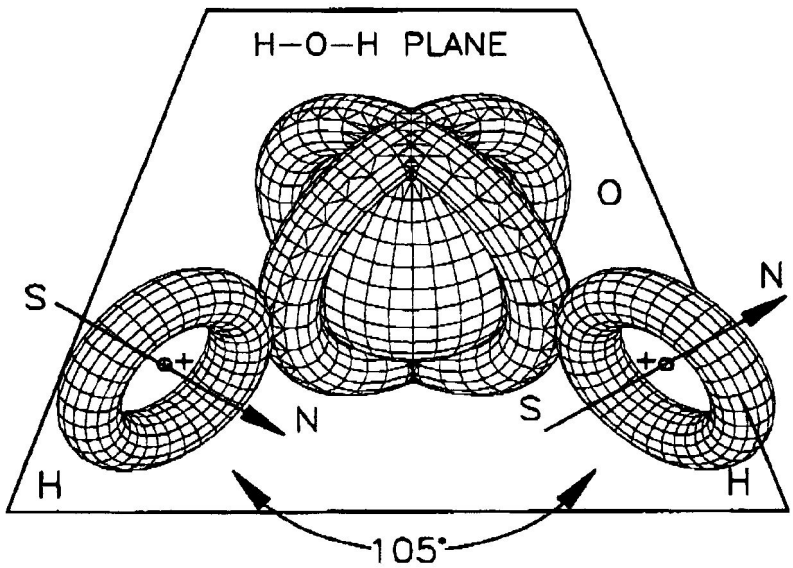

Figure 11.53. A conceptual rendering of the conventional water molecule without any electric polarization. This rendering is primarily intended to illustrate the experimentally established feature that the orbitals of the two hydrogen atoms do not have a spherical distribution as in Fig. 11.413, but have instead a distribution essentially perpendicular to the $H-O-H$ plane (see Refs. [20] for details) here conceptually represented with a toroid. The strong valence bond needed to achieve the first known exact representation of the experimental data of the water molecule achieved in Ref. [21] requires that the corresponding orbitals of the valence electrons of the oxygen have a corresponding polarized distribution here also conceptually depicted with toroids perpendicular to the $H-O-H$ plane around the spherical core of the remaining electrons of the oxygen atom.

magnetic fields of the polarized H atoms become dominant over the Coulomb repulsion of the charges, resulting in a new configuration of the water molecule depicted in Figs. 19 and 20 apparently presented in this section for the first time.

Therefore, a central hypothesis of this section is that the electrolyzer developed by Hydrogen Technology Applications, Inc., is such to permit the transformation of the water molecule from the conventional $H-O-H$ configuration of Fig. 11.54 to the basically novel configuration of Fig. 11.55.

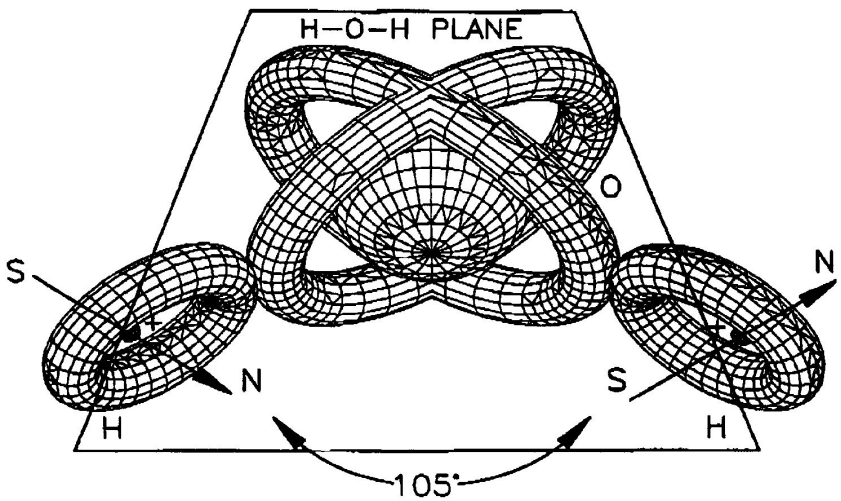

Figure 11.54. A conceptual rendering of the conventional water molecule of Fig. 16, this time with the electric polarization as occurring in nature. Note the consequential the predominance of a positive charge in the two hydrogen atoms that is responsible in part for the angle of 105° between the two $H - O$ radicals.

By using the above identified symbols for molecules and magnecules, the conventional water molecule is represented by $H - O - H$ while the new configuration of Fig. 11.55 is represented by $(H \times H) - O$, where the symbol "-" evidently denotes double valence bond.

The plausibility of the new form of water is supported by the fact that, when $H - O - H$ is liquid, the new species $(H \times H) - O$ is expected to be gaseous. This is due to various reasons, such as the fact that the hydrogen is much lighter than the oxygen in the ratio 1 to 16 amu. As a result, the new species $(H \times H) - O$ is essentially equivalent to ordinary gaseous oxygen in conformity with conventional thermodynamical laws, since the transition from the liquid to the gas state implies the increase of the entropy, as well known.

Alternatively, the loss of electric polarization in the transition from $H - O - H$ to $(H \times H) - O$ is expected to cause the loss of the processes permitting the very existence of the water molecule, such as the hydrogen bridges between dimers $O - H$ of different molecules. Transition to a gaseous form is then consequential, thus confirm the plausibility of the new form of water $(H \times H) - O$ proposed in this section.

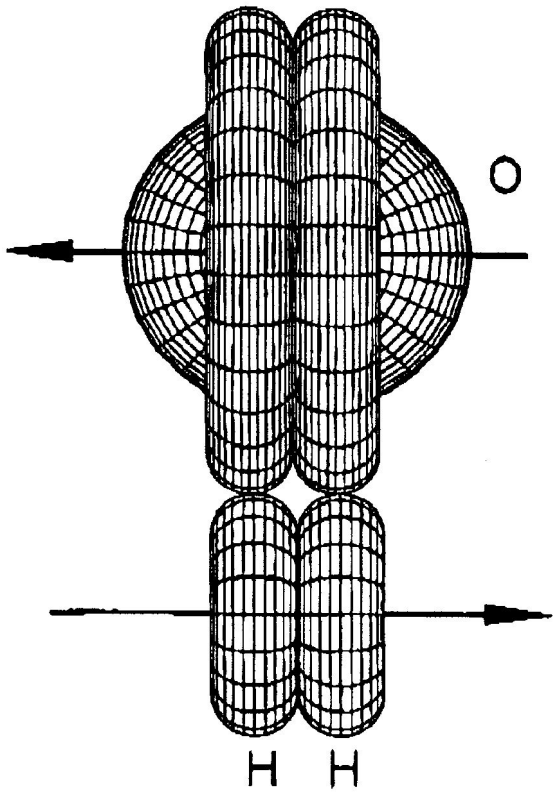

Figure 11.55. A conceptual rendering of the central hypothesis submitted for the first time in this section, namely, the $H-O-H$ molecule in which all electric polarizations have been removed, with the consequential collapse of the two polarized H-atoms one into the other due to their neutral charge and strongly attractive opposing magnetic polarities. This hypothesis permits a quantitative interpretation of the transition of state from liquid to gas achieved by the HHO electrolyzers via processes structurally different than evaporation energy. In fact, unlike the configuration of Fig. 11.11, that of this figure can only exist at the gaseous state due to the loss of the processes permitting the liquid state, such as hydrogen bridges between pairs of water molecules. It should be noted that the configuration here depicted is unstable and decomposes into atomic oxygen, as detected in the HHO gas, plus the new magnecular species $H \times H$ that has indeed been detected but it is generally interpreted as $H - H$.

However, it can also be seen that the new form of water $(H \times H) = O$ is *unstable,* and decomposes in $H \times H$ and O. This decomposition is supported by the clear evidence in the HHO gas of atomic oxygen, as well as of the species

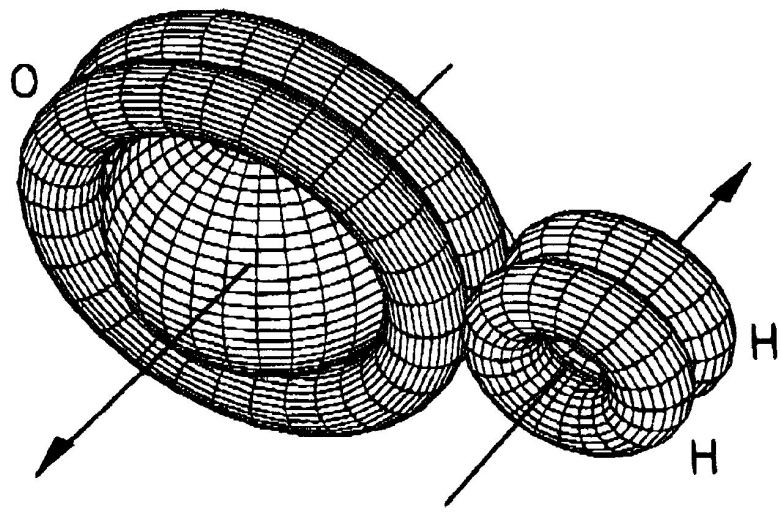

Figure 11.56. A conceptual rendering of a perspective view of the central hypothesis submitted for the first time in this section via Fig. 11.55, better illustrating the bond via opposing magnetic polarities of the two H-atoms, as well as the unstable character of the configuration due to collision with other species and intrinsic instabilities to be studied in a forthcoming section.

with 2 amu that is normally interpreted as being $H - H$, while we suggest the additional possibility that such a species is, at least in part, $H \times H$.

11.6.5 Contributions of Hadronic Chemistry Toward the Future Understanding of the Complexities of Water

There is no doubt that, being the foundation of life, water is by far the most complex chemical structure in nature. Any chemist who believes to have achieved a final understanding of water via quantum chemistry should be removed from the scientific community because of either mental or ethical problems, and the same holds for chemists using hadronic chemistry.

It is merely hoped that the efforts presented in this section have achieved another step in the study of water beyond those permitted by quantum chemistry, with the understanding that a serious understanding of water may well require efforts throughout this third millennium.

Recall that quantum chemistry was unable to achieve an exact and invariant representation of the main characteristics of the water molecule from unadul-

terated first principles despite efforts over the past century. In fact, a historical 2% has been missing in the representation of the water binding energy, while the representation of its electric and magnetic moments was embarrassingly wrong even in the signs.

An improvement of the numerical representation was achieved via the so-called "screening of the Coulomb law", that is, the multiplication of the Coulomb potential by an arbitrary function of unknown physical or chemical origin, $\frac{q_1 \times q_2}{r} \rightarrow f(r) \times \frac{q_1 \times q_2}{r}$. However, as indicated since Chapter 1, this type of screening implies the abandonment of the notion of "quantum" of energy, trivially, due to the loss of all quantized orbits, as well as the exiting from the basic axioms of quantum mechanics, because the transition from the Coulomb potential to its screened form requires nonunitary transforms.

Independently from these basic shortcomings, the fundamental problem of quantum chemistry, whether with or without screening processes, remains the fact that the name "valence" is a pure nomenclature, since it does not identify in explicit and numerical terms the *attractive force* needed for two hydrogen atoms to be bounded to the oxygen atom in the structure $H - O - H$, and electrons repel each other in any case for quantum mechanics and chemistry.

Besides fundamental insufficiencies in a numerically exact and invariant representation of the main characteristics of the water molecules, additional vast insufficiencies exist for the liquid and solid state of water. As an example, the use of the "H-bridges" to represent the liquid state of water is another case of basically ascientific nomenclature because, again, of the lack of any identification of the *attractive force* needed to explain the bond of neutral and diamagnetic water molecules in their liquid state.

When water becomes part of biological organisms, the open problems became so great to be beyond our imagination at this writing (also because most chemists believe that the water molecule remains the same).

As shown in Chapter 9, the *isotopic branch of hadronic chemistry,* or *isochemistry* for short, was first and most fundamentally focused in the identification of the *attractive force* in the singlet coupling of two valence electrons, which identification required a necessary nonunitary theory since the valence force resulted to have a contact, thus non-Hamiltonian character.

Thanks to this basic advance, the isochemistry permitted, for the first time in scientific history, the numerically exact and invariant representation not only of the binding energy but also of the electric and magnetic moments of the water molecules (Section 9.3).

Subsequently, in Section 11.5 we indicated that the liquid state of water appears to be of magnecular character since the H-atoms in the H_2O structure have by nature a toroidal polarization in a plane perpendicular to the $H-O-H$ plane, thus permitting the magnecular bond between two H atoms of different water molecules $H_\uparrow \times H \downarrow$ that is referred to as "H-bridges" (see Figure 11.34.

In this section, we have shown that water admits a previously unknown gaseous and combustible state achievable from the liquid state *without* the evaporation energy believed to be necessary by quantum chemistry. In turn, such a feature indicates our basic lack of understanding of the conventional water evaporation itself, trivially, because of the lack of conventional identification of the force responsible for the liquid state.

To understand the limited character of the advances permitted by isochemistry, it is important to recall that they have been achieved via a lifting of quantum chemistry that is strictly reversible in time as the original theory.

Consequently, *isochemistry is strictly inapplicable (rather than violated) for any irreversible process involving the water molecule,* such as the very creation of the molecule itself

$$2 \times H + \frac{O_2}{2} \quad \rightarrow \quad H_2O + 57 Kcal/mole. \tag{11.6.1}$$

Any insistence in the use of a reversible theory, whether quantum chemistry of its isotopic covering, for the above irreversible process may imply severe scientific drawbacks. As one example among many, it is generally believed in chemistry that the above process is unique and immutable.

On the contrary, the use of the *genotopic branch of hadronic chemistry,* or *genochemistry* for short, establishes that the rate of the above process depends on the distribution of the orbitals.

Recall that the H atoms in the H_2 molecule have a spherical distribution. Consequently, to achieve reaction (11.6.1), nature has to first break down the H_2 molecule and then polarize the orbitals of the individual H atoms from their spherical to the above indicated toroidal polarization.

Genochemistry then predicts that basically new advances over reaction (1.6.xx) can be achieved with the combustion of H and O, firstly, if we start from *atomic* H and/or O atoms (because in this case there is no need to separate atoms prior to their new bond) and, secondly, via the use of *atomic and polarized* H and O atoms, that is, by preparing them in the form as appearing in the $H-O-H$ molecule. Similar basic advances can be obtained in various other chemical reactions.

Despite these possibilities, genochemistry remains basically insufficient for further advances in the study of the water molecule because the theory is indeed irreversible but single-valued. It is an easy prediction that further advances in the study of water, particularly when a member of a biological structure, will require the *hyper-structural branch of hadronic chemistry,* or *hyperchemistry* for short, due to its multi-valued character. In turn, the latter broadening will inevitably require the notion of *hypermagnecule* (Definition 11.2.1).

At that point the complexities of water and its role as the basis of life appear in their full light, e.g., because of the joint need of all four directions of time (Section 2.1), each time being multivalued (Chapter 5).

In summary, water is perhaps the best illustration of the fact that the human adventure in science will never end.

11.7 EXPERIMENTAL EVIDENCE OF MAGNECULES IN LIQUIDS AND SOLIDS

11.7.1 Preparation of Liquid Magnecules used in the Tests

In early 1998 Santilli [1] obtained a number of samples of *fragrance oils* from *Givaudan-Roure Corporation* (GR) with headquarters in Teaneck, New Jersey. About 50 cc of various samples of perfectly transparent fragrance oils were placed in individual glass containers. One polarity of an alnico permanent magnet with 12,000 G and dimension $1/2'' \times 1'' \times 2''$ was immersed within said oils.

Starting with a perfect transparency, after a few days a darkening of the oils became visible, jointly with a visible increase of the viscosity, with changes evidently varying from oil to oil. Subsequently, there was the appearance of granules of dark complexes in the interior of the oil which were visible to the naked eye. Both the darkening and the viscosity increased progressively in subsequent days, to reach in certain cases a dark brown color completely opaque to light. The viscosity increased to such an extent that the oil lost all its fluidity.

It should be stressed that the above visible effects are of pure magnetic origin because of the lack of any other contribution, *e.g.*, the complete absence of any additives. After the immersion of the permanent magnets, all samples were left undisturbed at ordinary room conditions. The indicated effects remain unchanged to this day, thus showing that the changes were stable at ordinary conditions of temperature and pressure.

Santilli's [1] main hypothesis on the darkening of the oils is that their molecules acquire a magnetic polarization in the orbits of at least some of their atomic electrons (called in chemistry *cyclotron resonance orbits*), by therefore bonding to each other according to Definition 11.2.1 in a way similar to the corresponding occurrence for gases.

It should also be indicate that the immersion of one polarity of a permanent magnet in fragrance oils is, evidently, a rudimentary way to create magnecules in detectable percentage although not an essentially pure population of magnecules as requested for a new chemical species (see Sect. 11.2). A number of more sophisticated magnetic polarization techniques are now available with

rather complex geometries. Also, as indicated in Sect. 11.6, an essentially pure population of liquid magnecules can be reached via the PlasmaArcFlow reactors described in Section 11.4.

11.7.2 Photographic Evidence of Magnecules in Liquids

The above alteration of the structure of fragrance oils was confirmed by photographs taken by the GR Research Laboratory in Dubendorf, Switzerland, via a microscope with minimal magnification, as illustrated in the pictures of Figs. 8.19 and 8.20.

The pictures of Fig. 11.57 refer to the GR fragrance oil received under the code "ING258AIN, Text 2" subjected to the rudimentary magnetic polarization indicated in the preceding section under the respective magnification 10X and 100X.

As one can see, these photographs establish that, under the indicated magnetic treatment, the oil has acquired a structure of the type of "brick layering" which is visible under only 10X magnification, and is per se highly anomalous for a liquid that was originally fully transparent. Note that the magnecules are not constituted by the individual "bricks," but rather by the dark substance which interlock said "bricks." This point is important to understand the size of the magnecule here considered which covers the entire 50 cc of the liquid.

The photographs in Figs. 8.20 were taken at the University of South Florida in St. Petersburg via a microscope with the same magnifications 10X and 100X, but refer to a different GR fragrance oil received under the code "Mixture 2" and magnetically treated to such a point of completely losing transparency and fluidity. As one can see, the latter picture provides confirmation that, following exposure to a 12,000 G magnetic field, fragrance oil molecules bond together into rather large clusters estimated to be well in excess of 10,000 a.m.u., that is, with an atomic weight which is dramatically bigger than that of the largest molecule composing the oil, as per Feature I) of Definition 11.2.1.

Inspection of the various photographs shows a variety of sizes of magnecules, thus establishing their lack of unique characteristics for any given liquid. This evidently confirms the *lack* of a valence bond. Inspection of the samples also show the magnecules capability of increasing their size via the accretion of further oil molecules.

Other photographic documentations of various magnecules in liquids were done, by confirming the findings of Figs. 8.19 and 8.20.

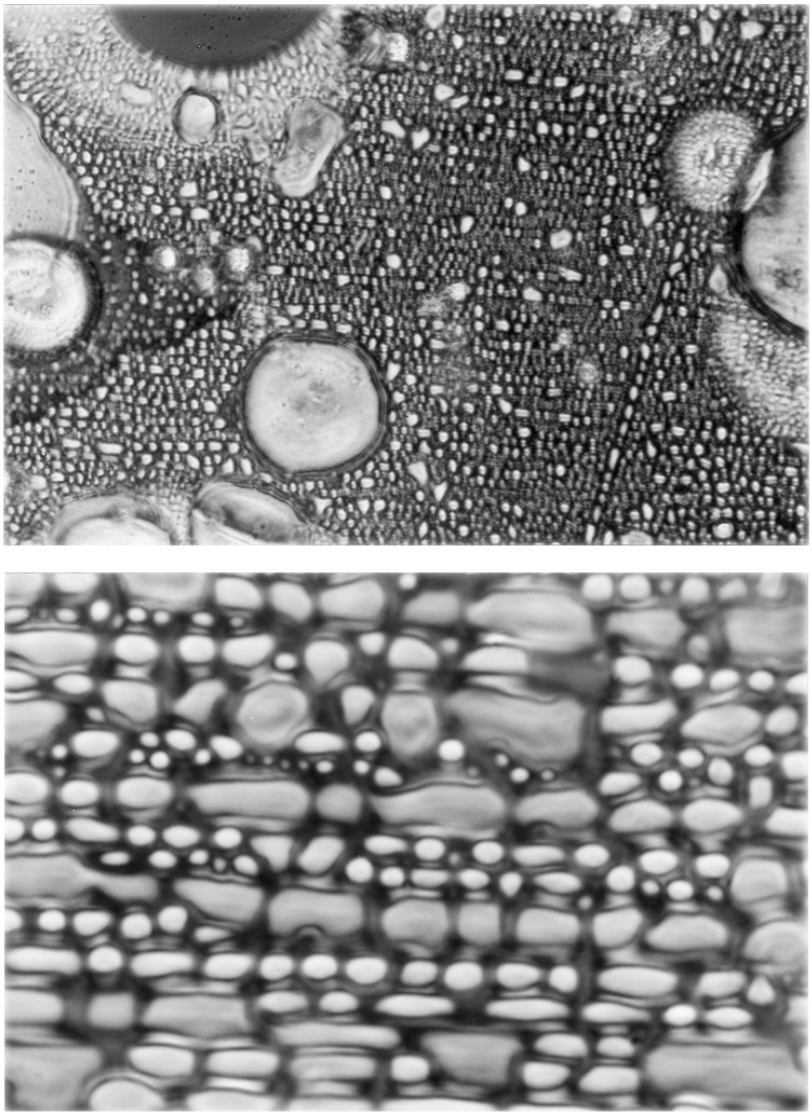

Figure 11.57. A photographic evidence of magnecules in liquids obtained at the *Givaudan-Roure Research Laboratory* in Dubendorf, Switzerland, in the GR fragrance oil "ING258IN Test 2" under magnifications 10X and 100X [1].

11.7.3 Spectroscopic Evidence of Liquid Magnecules at the Tekmar-Dohrmann Corporation

The first experimental evidence of magnecules in liquids was established on May 5, 1998, by analysts *Brian Wallace* and *Mia Burnett* at *Tekmar-*

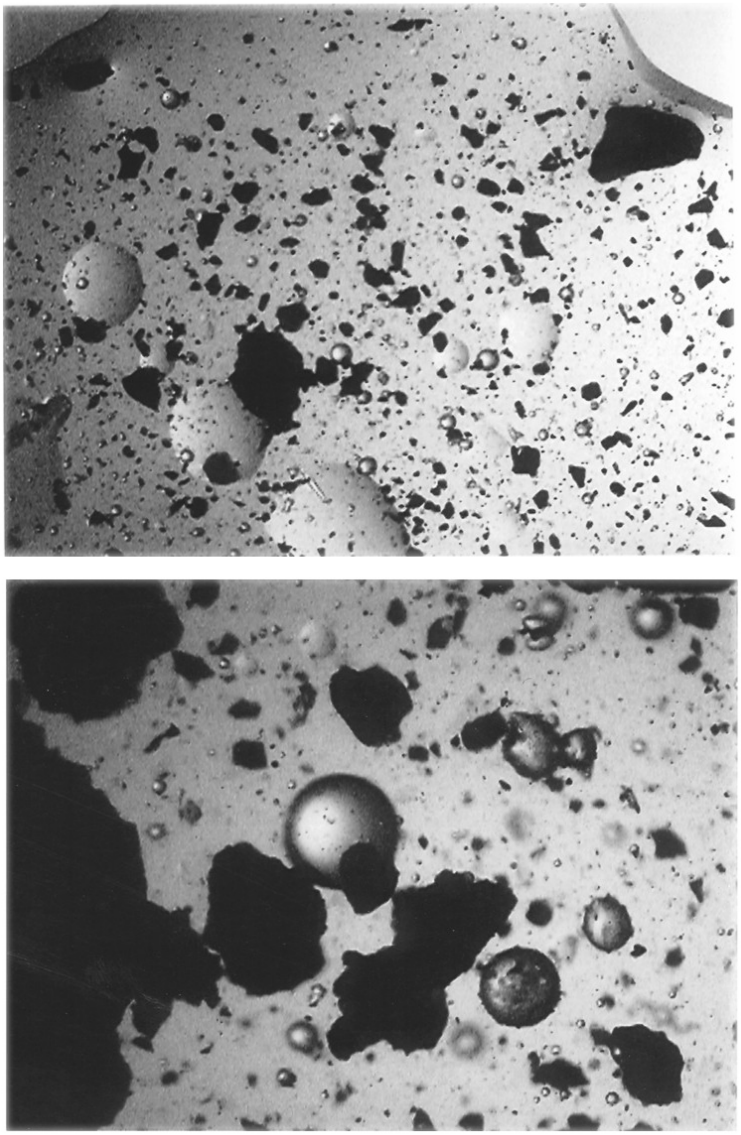

Figure 11.58. Confirmation of magnecules in GR fragrance oil "Mixture 2" under 10X and 100X obtained at the University of South Florida in St. Petersburg. Note the difference in sizes of the magnecules and their difference with those of Fig. 11.57 [1].

Dohrmann Corporation (TDC) in Cincinnati, Ohio, operating a *Tekmar 7000 HT Static Headspacer Autosampler* equipped with a Flame Ionization Detector (FID). The tests were repeated on May 8 and 11, 1998, by confirming the preceding results. It should be noted that the Tekmar equipment lacks the computer search as well as the UV scan. Also, the instrument had limited capability in atomic weight. Finally, the FID was permitted in this case because the liquids were not combustible.

The measurements were done on: Sample 1, pure (magnetically untreated) GR "Fragrance Oil 2"; Sample 2, magnetically untreated tap water; and Sample 3, a magnetically treated mixture of the two.

Despite these limitations, *the results of the Tekmar tests provided the first direct spectroscopic evidence of the existence of magnecules in liquids, including the first direct experimental evidence of water magneplexes* as per Definition 11.2.1. In particular, these tests established that magnecules in liquids have the same main features of the magnecules in gases.

To avoid a prohibitive length we reproduce only a few representative scans in Figs. 8.21 to 8.25 [1]. Figure 8.21 reproduces the origin test of the fragrance oil without magnetic treatment. Note the dominance of three molecules denoted "Peak 1" with 24.28%, "Peak 2" with 3.19% and "Peak 3" with 70.00%. Figure 8.22 depicts the background which is shown to be correct. Figure 8.23 represent the scan of magnetically treated water with a large "unknown 1" with 64.24% and "unknown 2" with 33.53% totaling 97.78%. This is evidence of the creation of magnecules in water, also called magneplexes according to Definition 11.2.1. Figure 8.24 represents a scan of the magnetically treated combination of water and fragrance oil with "unknown 1" 1.75% and "unknown 2" with 0.45%. An important information of this scan is that the original Peak 1 of Fig. 11.59 with 24.28% and Peak 3 with 70.00% have been decreased to the values 5.33% and 68.71%, respectively. This is evidence that the missing percentages of these molecules have been used in the formation of magnecules. Figure 8.25 reproduces the background following the tests and routine flushing. As one can see, the scan preserves macroscopic percentages of the preceding scans, thus confirming the anomalous adhesion also existing in gas magnecules.

11.7.4 Spectroscopic Evidence of Liquid Magnecules at Florida International University

Additional comprehensive tests via a modern equipment for LC-MS equipped with UVD were conducted on the GR fragrance oil "ING258IN Test 2" of Figs. 8.19 on December 1, 1998, at the chemistry laboratory of *Florida International University* (FIU) in Miami, Florida. The tests were then repeated on December 17 and 18 by confirming the preceding results.

Software Version: 4.0<4J28>
Date: 5/5/98 08:18 AM
Sample Name : 500ul Perfume Oil ID#1
Data File : C:\TC4\HP210\MY04003.RAW Date: 5/4/98 04:44 PM
Sequence File: C:\TC4OLD\HP210\MY04.SEQ Cycle: 3 Channel : B
Instrument : 772_-_2 Rack/Vial: 0/0 Operator: mb
Sample Amount : 1.0000 Dilution Factor : 1.00

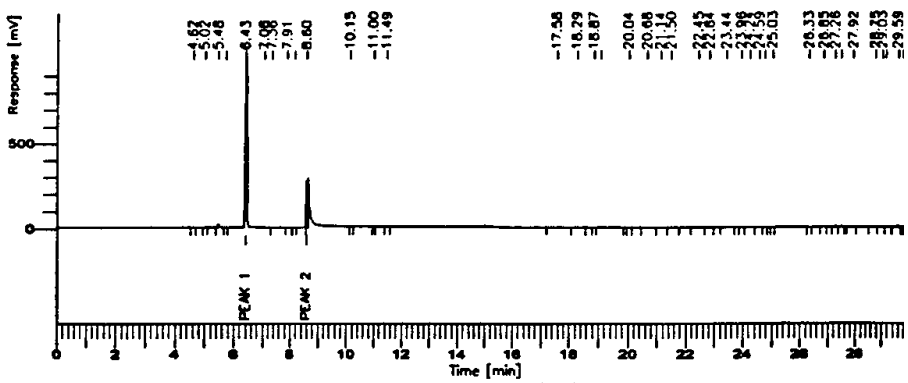

DEFAULT REPORT

Peak #	Component Name	Time [min]	Area [µV·s]	Area [%]
1		4.620	2106.00	0.01
2		5.022	432.00	0.00
3		5.479	68060.38	0.43
4		5.731	1320.12	0.01
5	peak 1	6.430	3894142.72	24.38
6		7.077	23106.00	0.14
7		7.355	8426.86	0.05
8		7.911	1549.62	0.01
9		9.163	190.00	0.00
10	peak 2	8.604	509716.00	3.19
11		10.146	829.00	0.01
12		10.999	338.00	0.00
13		11.485	798.00	0.00
14		17.582	9646.00	0.06
15		18.294	814.50	0.01
16		18.871	748.51	0.00
17		19.082	12390.99	0.08
18		20.043	582.50	0.00
19		20.679	4000.46	0.03
20		21.139	654.15	0.00
21		21.500	716.38	0.00
22		22.452	4196.12	0.03
23		22.837	1128.08	0.01
24		23.437	10546.00	0.07
25		23.958	1292.73	0.01
		24.241	5968.77	0.04
		24.587	980.85	0.01
		24.764	700.15	0.00
29		25.034	221.00	0.00
30		26.330	189.00	0.00
31		26.849	7912.00	0.05
32		27.264	19913.14	0.12
33		27.461	10844.36	0.07
34		27.918	1332.00	0.01
35		28.753	751.69	0.00
		29.026	3094.14	0.02
		29.163	2312.68	0.01
		29.589	30846.00	0.19
39		29.750	383.00	0.00
40		30.320	6254.00	0.04
41		31.370	3617.37	0.02
42		31.720	51605.63	0.32
43		32.296	268.00	0.00
44		32.519	87913.29	0.55
45	Peak 3	32.742	11181133.21	70.00
			15973772.00	100.00

Figure 11.59. A first scan done on May 5, 1998, 8.18 a.m. at *Tekmar Dohrmann Company* (TDC) in Cincinnati, Ohio, via a Tekmar 7000 HT Static Headspacer Autosampler with a Flame Ionization Detector (FID).

The tests were conducted under a number of technical characterizations specifically selected to detect magnecules, among which include:

1) Total Ion Chromatogram (TIC) collected under the positive ion atmospheric pressure electrospray ionization (ESI+) mode;

Software Version: 4.0<4J28>
Date: 5/5/98 08:19 AM
Sample Name : Blank vial
Data File : C:\TC4\HP210\MY04004.RAW Date: 5/4/98 05:25 PM
uence File: C:\TC4OLD\HP210\MY04.SEQ Cycle: 4 Channel : B
nstrument : 772_-_2 Rack/Vial: 0/0 Operator: mb
Sample Amount : 1.0000 Dilution Factor : 1.00

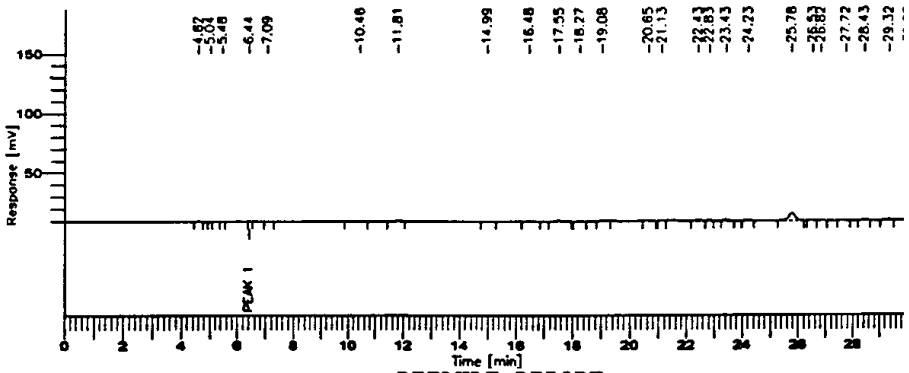

DEFAULT REPORT

Peak #	Component Name	Time [min]	Area [µV·s]	Area [%]
1		4.620	2225.00	0.14
2		5.035	243.50	0.02
3		5.483	664.00	0.04
4	peak 1	6.435	1182.00	0.07
5		7.090	493.50	0.03
6		10.463	1636.00	0.10
7		11.807	1495.00	0.09
8		14.988	790.00	0.05
9		16.482	1491.00	0.09
10		17.547	9839.00	0.61
11		18.270	912.50	0.06
12		19.076	7533.00	0.47
13		20.653	4130.00	0.26
14		21.133	670.50	0.04
15		22.430	5150.00	0.32
16		22.828	983.50	0.06
17		23.428	10284.00	0.64
18		24.228	5984.00	0.37
19		25.777	93506.00	5.82
20		26.530	2279.19	0.14
21		26.822	3216.81	0.20
22		27.720	857.00	0.05
23		28.426	4520.50	0.28
24		29.321	9393.42	0.59
25		30.017	7103.93	0.44
		30.302	6186.65	0.39
		31.654	1421071.00	88.50
--	Peak 3	32.674	1842.00	0.11
			1605703.00	100.00

Figure 11.60. The scan at TDC on 5/5/98 at 8.19 a.m. to check that the background is correct.

2) Integrated TIC with retention times and areas for the most abundant peaks;

3) Raw mass spectra for all peaks identified in item 2;

```
Software Version: 4.0<4J28>
Date: 5/5/98  08:20 AM
Sample Name   : 500ul H2O ID#2
Data File     : C:\TC4\HP210\MY04005.RAW   Date: 5/4/98  06:06 PM
   uence File: C:\TC4OLD\HP210\MY04.SEQ    Cycle: 5   Channel : B
Instrument    : 772_-_2   Rack/Vial: 0/0   Operator: mb
Sample Amount     : 1.0000                 Dilution Factor  : 1.00
```

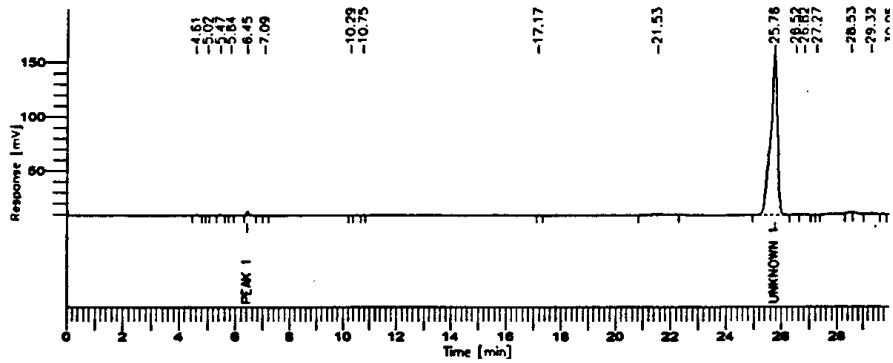

DEFAULT REPORT

Peak #	Component Name	Time [min]	Area [µV·s]	Area [%]
1		4.614	2904.00	0.07
2		5.024	375.50	0.01
3		5.469	1328.00	0.03
4		5.844	322.00	0.01
5	peak 1	6.446	17310.50	0.43
6		7.088	390.00	0.01
7		10.288	164.00	0.00
8		10.746	189.00	0.00
9		17.171	970.50	0.02
10		21.527	32334.00	0.81
11	unknown 1	25.763	2565644.21	64.24
12		26.522	2794.13	0.07
13		26.821	3354.66	0.08
14		27.271	184.00	0.00
15		28.534	3914.50	0.10
16		29.315	9941.00	0.25
17		30.048	1062.00	0.03
18		30.981	1916.00	0.05
19	unknown 2	31.653	1339095.00	33.53
20	Peak 3	32.680	9951.00	0.25
			3994144.00	100.00

Figure 11.61. The scan at TDC on 5/5/98 at 8.19 a.m. on the magnetically treated water which constitutes experimental evidence of magnecules in water given by the large unknown peak.

4) HP LC chromatograms collected at fixed wavelength of 254 cm; and

5) UV-visible spectra form the HPLC diode array detector with 230–700 mm.

The tests were conducted on the following samples:

I) Sample GR331, the magnetically untreated, fully transparent GR fragrance oil "ING258IN Test 2";

Software Version: 4.0<4J28>
Date: 5/5/98 08:21 AM
Sample Name : 500ul Oil&H2O ID#3
Data File : C:\TC4\HP210\MY04009.RAW Date: 5/4/98 08:50 PM
Sequence File: C:\TC4OLD\HP210\MY04.SEQ Cycle: 9 Channel : B
Instrument : 772_-_2 Rack/Vial: 0/0 Operator: mb
Sample Amount : 1.0000 Dilution Factor : 1.00

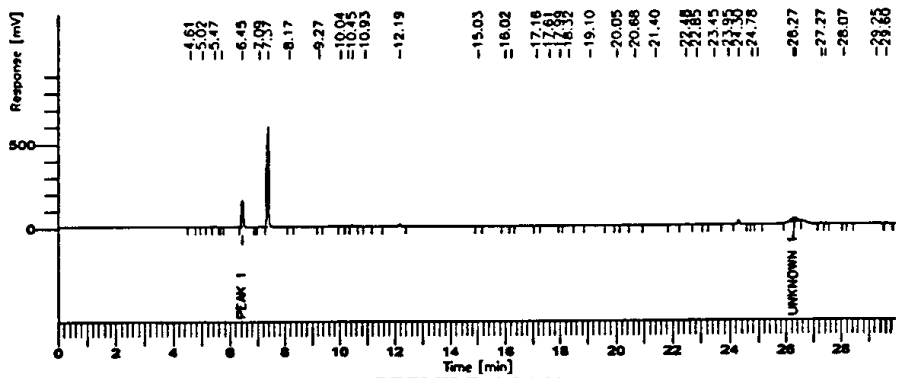

DEFAULT REPORT

Peak #	Component Name	Time [min]	Area [µV·s]	Area [%]
1		4.612	2960.00	0.02
2		5.021	482.50	0.00
3		5.466	14446.00	0.11
4		5.716	302.00	0.00
5	peak 1	6.449	700997.00	5.33
6		7.085	17702.00	0.13
7		7.373	2463631.95	18.74
8		8.174	1041.55	0.01
9		9.273	398.50	0.00
10		10.038	693.50	0.01
11		10.287	407.59	0.00
12		10.454	32776.91	0.25
13		10.932	455.00	0.00
14		12.185	45046.00	0.34
15		15.029	735.50	0.01
16		16.018	363.50	0.00
17		16.215	289.50	0.00
18		17.163	405.10	0.00
19		17.607	8138.75	0.06
20		17.989	258.64	0.00
21		18.323	773.50	0.01
22		19.101	7936.00	0.06
23		20.050	1513.00	0.01
24		20.684	3329.49	0.03
25		21.403	6640.01	0.05
--		22.477	3617.00	0.03
		22.848	1399.00	0.01
		23.453	8746.50	0.07
29		23.945	5373.77	0.04
30		24.296	89748.23	0.68
31		24.777	1228.40	0.01
32		24.964	2011.60	0.02
33	unknown 1	26.272	229566.61	1.75
34		26.347	152811.39	1.16
35		27.273	23098.00	0.18
		27.410	13015.00	0.10
		28.070	324.00	0.00
		29.254	52774.58	0.40
39		29.599	19904.00	0.15
40		30.345	65596.75	0.50
41		30.880	2408.67	0.02
42		31.387	6170.93	0.05
43	unknown 2	31.491	59456.07	0.45
44		32.089	664.00	0.01
45		32.526	64277.94	0.49
46	Peak 3	32.758	9034646.06	68.71
			13148362.00	100.00

Figure 11.62. The scan on 5/5/98 at 8.21 a.m. on the magnetically treated mixture of water and fragrance oil of scan 8.21 which constitutes evidence of magnecules given by two unknown peaks.

II) Sample GR332, magnetically treated "ING258IN Test 2" with 10% Dipropylene Glycol (DPG);

III) Sample GR332S, bottom layer of the preceding sample;

```
Software Version: 4.0<4J28>
Date: 5/5/98  02:06 PM
Sample Name  : Blank
Data File    : C:\TC4\HP210\MY05001.RAW   Date: 5/5/98  09:08 AM
Sequence File: C:\TC4OLD\HP210\MY05.SEQ   Cycle: 1   Channel : B
Instrument   : 772_-_2   Rack/Vial: 0/0   Operator: mb
Sample Amount    : 1.0000                 Dilution Factor  : 1.00
```

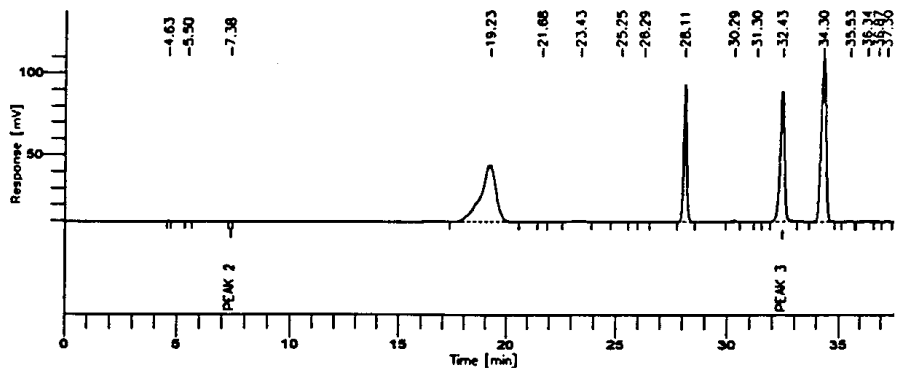

DEFAULT REPORT

Peak #	Component Name	Time [min]	Area [uV·s]	Area [%]
1		4.633	2621.00	0.05
2		5.496	695.50	0.01
3	peak 2	7.379	293.00	0.01
4		19.227	1795761.00	33.57
5		21.679	1071.00	0.02
6		23.432	18393.00	0.34
7		25.247	6824.50	0.13
8		26.290	2393.00	0.04
9		28.110	835986.00	15.63
10		30.291	12877.00	0.24
11		31.296	1435.00	0.03
12	Peak 3	32.425	1135236.50	21.22
13		34.296	1508602.50	28.20
14		35.532	6202.50	0.12
15		36.344	9033.76	0.17
16		36.866	1934.19	0.04
17		37.297	7005.65	0.13
18		37.914	2731.10	0.05
			5349096.00	100.00

Figure 11.63. The scan at TDC on 5/5/98 at 2.26 p.m. on the background with anomalous adhesion confirming the corresponding anomalous background for gas magnecules.

IV) Sample GR335, magnetically treated mixture 4% GR fragrance oil "ING258IN Test 2", 0.4% DPG and 95% tap water; and

V) Sample GR335O, visible dark clusters in the preceding sample.

To avoid a prohibitive length of this presentation, only representative scans are reproduced in Figs. 8.26 to 8.30 [1]. As one can see, these scans provide a second experimental evidence of magnecules in liquids as evident in comparing the peaks of the untreated liquid with those of the treated one.

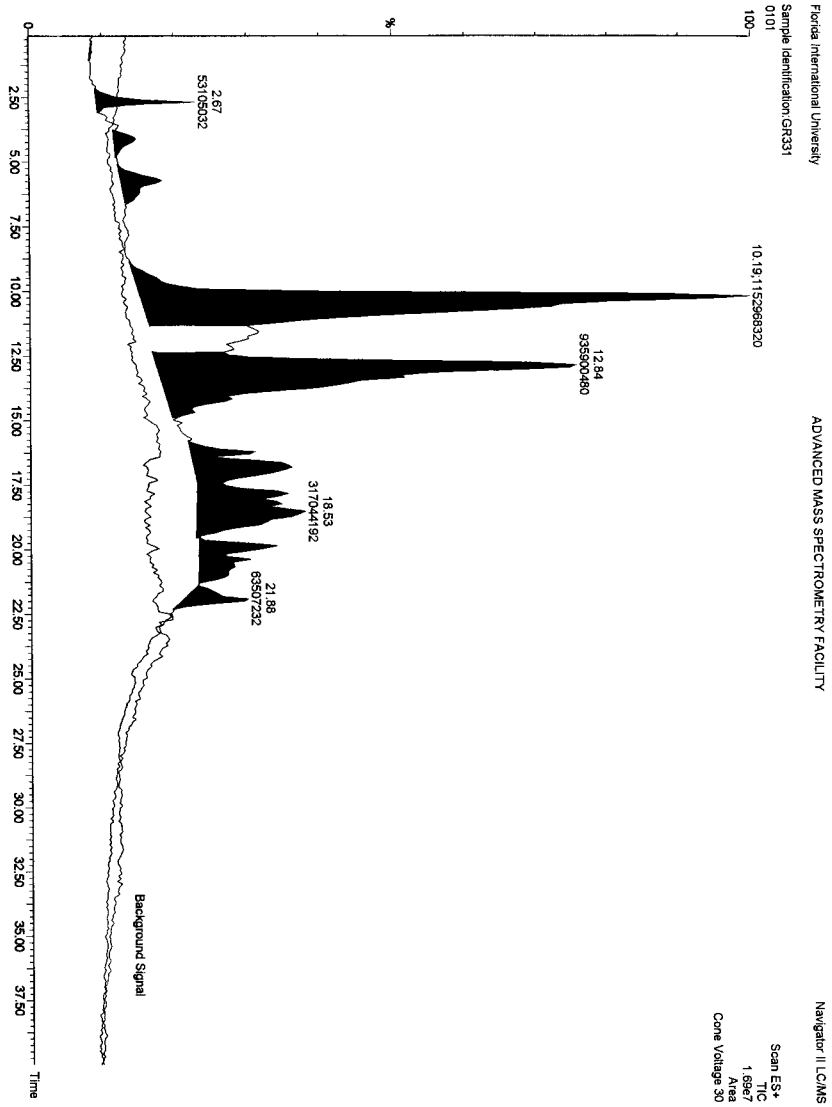

Figure 11.64. Scan on the untreated GR oil "ING258IN Test 2" of Fig. 11.56 (GR331 of the text) conducted at *Florida International University* (FIU).

A few comments are in order. To understand the FIU measurements the reader should keep in mind that the liquid is that of Fig. 11.57. Consequently, *the magnecules to be tested are visible to the naked eye. Therefore, only*

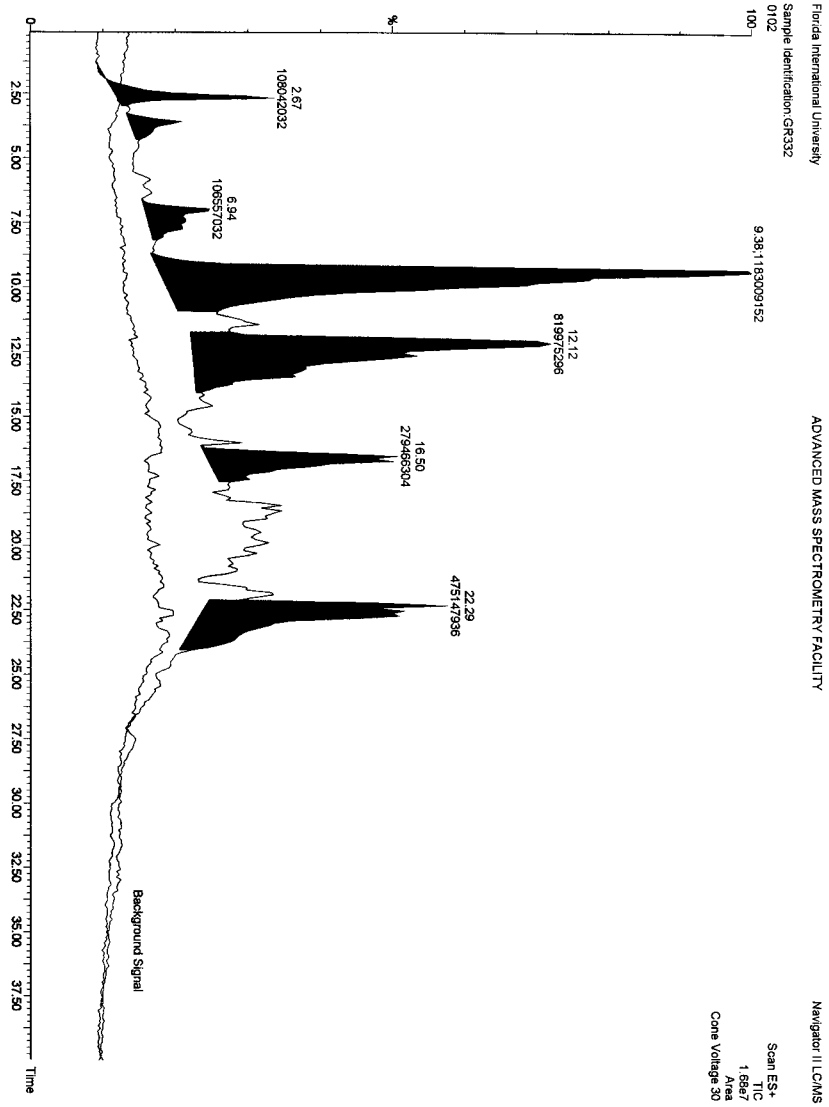

Figure 11.65. Scan at FIU of Sample GR332.

minute fragments entered the capillary feeding lines of the LC-MS/UVD instrument.

Finally, the reader should keep in mind that the magnetic polarization of the test has been minimal, and *the liquid does not constitute a pure population*

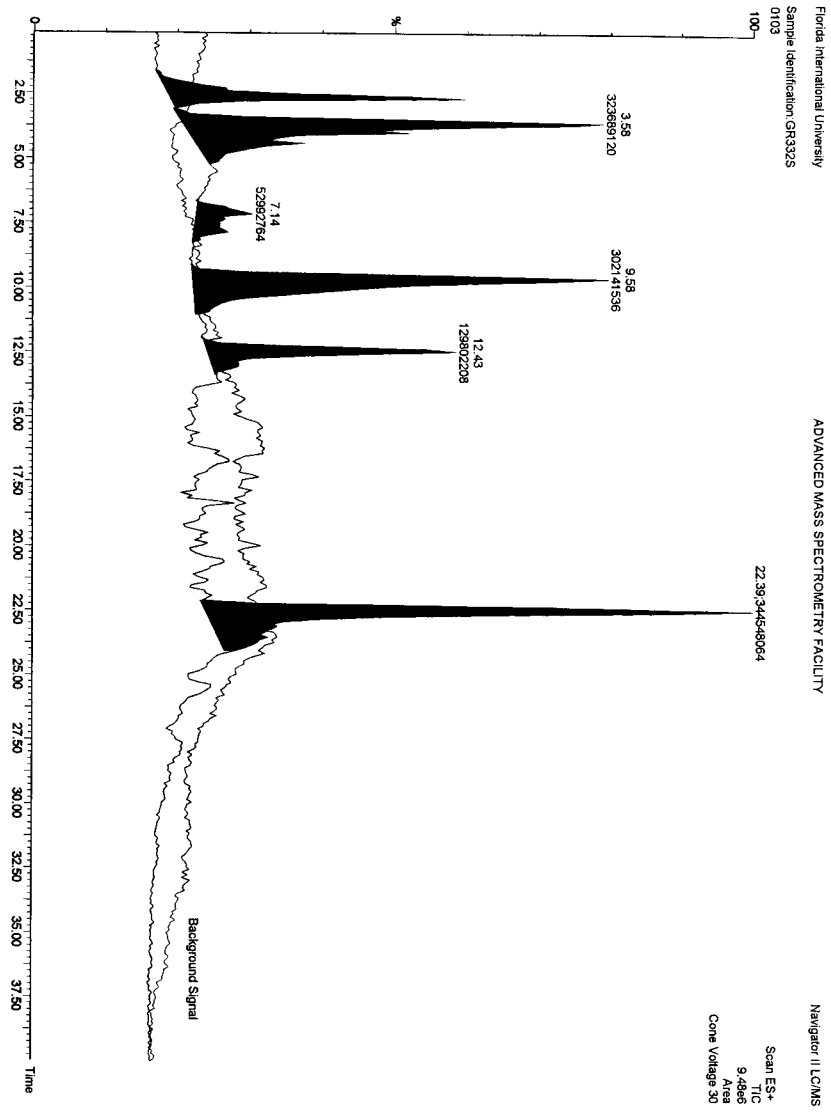

Figure 11.66. Scan at FIU of Sample GR332S.

of liquid magnecules. The latter case is available from the PlasmaArcFlow reactors of Section 11.4 whose study is here omitted.

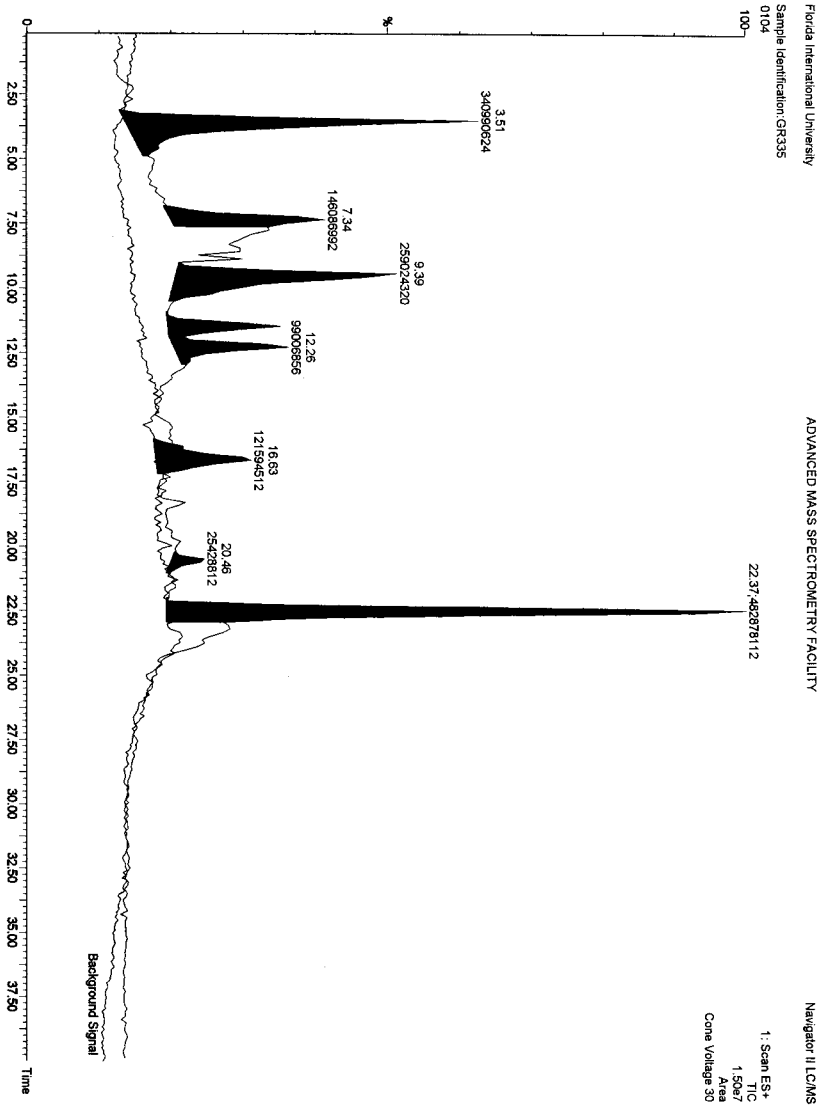

Figure 11.67. Scan at FIU of Sample GR335.

11.7.5 Experimental Verification of Mutated Physical Characteristics

In addition to the preceding *chemical* features, the existence of magnecules implies the mutation of *physical* characteristics, such as increase of the specific

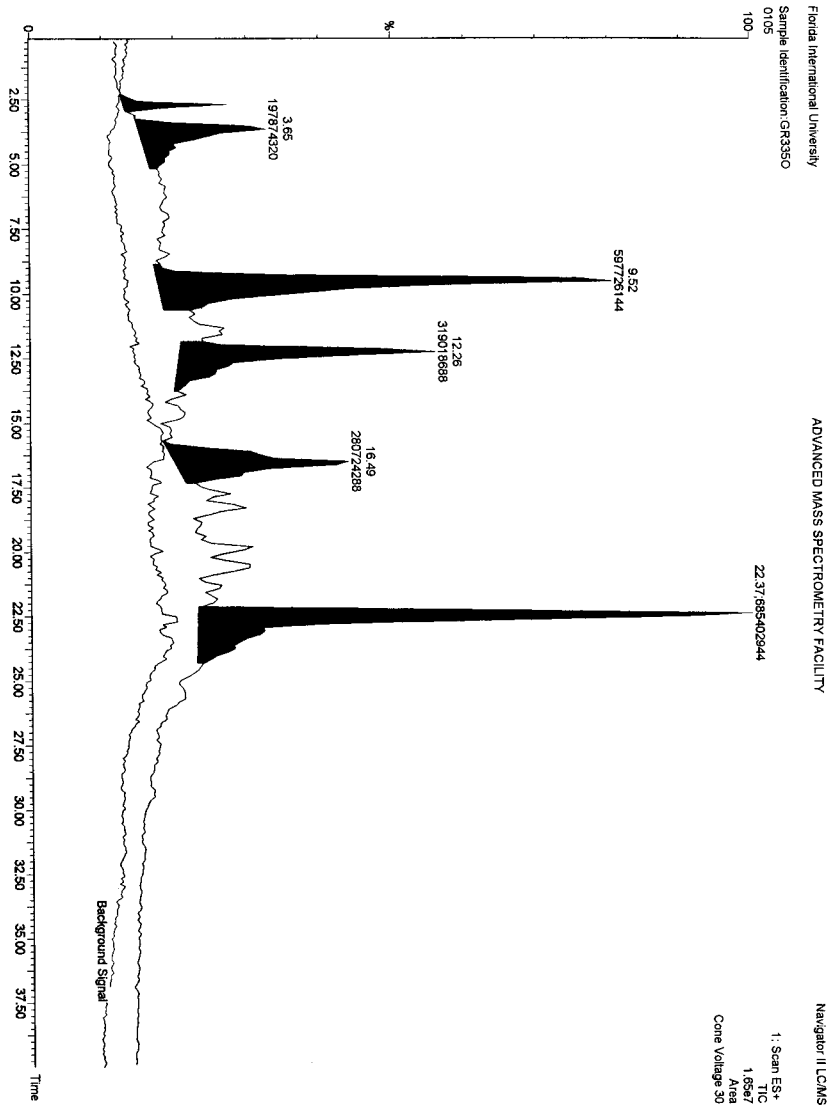

Figure 11.68. Scan at FIU of Sample GR335O.

density and viscosity. This is due to the fact that magnetic bonds among ordinary molecules imply an evident reduction of intermolecular distances, thus resulting in more molecules per unit volume, as compared to the magnetically untreated substance. The increases in density and viscosity are then consequential.

A most intriguing feature of gas magnecules with important scientific and industrial implications is that *the Avogadro number of a gas with magnecular structure is not constant, or, equivalently, the so-called "gas constant" R of a gas with magnecular structure is an (expectedly nonlinear) function of P, V, T, $R = R(P, V, T)$,* resulting in the generalized gas law

$$\frac{PV}{T} = nR(P, V, T), \tag{8.21}$$

where the explicit dependence of R on P, V, and T depends on the magnecular gas considered.

The variation of the Avogadro number for gas with magnecular structure has been proved by routine tests at *USMagnegas, Inc.,* Largo, Florida, establishing that:

1) The number of constituents of a gas with magnecular structure decreases with a sufficient increase of the pressure;

2) Given a fixed and sealed tank with volume V of a gas with magnecular structure at given pressure P and temperature T, after bringing this tank to a sufficiently higher temperature $T' > T$, and then returning it to the original temperature T, the pressure of the tank is not the original pressure P but a generally bigger pressure $P' > P$;

3) The increase of pressure of a gas with magnecular structure requires a volume which generally increases with the pressure itself, that is, if the increase of pressure in a given tank from 100 psi to 200 psi requires V cf of magnecular gas, the same increase of pressure in the same tank via the same gas, this time from 4,000 psi to 4,100 psi at the same temperature does not require the same volume V but a volume V' of the magnecular gas bigger than the original volume, $V' > V$.

The above deviations from the conventional gas law are easily explained by the fact that *the increase of pressure in a gas with magnecular structure generally implies the aggregation of magnecules into bigger clusters, with consequential decrease of the number of constituents.* Similarly, *the increase of temperature generally implies the breaking down of magnecules into smaller clusters, with consequential increase of the number of constituents and resulting anomalous increase of pressure.* It then follows that, if the increase of temperature of a given fixed volume is beyond the Curie Magnecular Point (Definition 8.2.1), all magnetic polarizations are terminated with consequential increase of the number of constituents due to the reduction of magnecules to molecules. This implies that the return of the gas to the original temperature does not restore the original magnecules, and, consequently, the return to the original temperature generally occurs at an increased pressure due to the increased number of constituents.

We now report measurements of specific density, viscosity and other characteristics of fluids with magnecular structure which confirm the above GC-MS/IRD and LC-MS/UVD tests, by providing final evidence on the existence of magnecules as per Definition 8.2.1.

All tests were done via the use of ordinary tap water and a number of GR fragrance oils. All samples here considered were prepared by conventionally mixing tap water and one fragrant oil, and then submitting that mixture to rather weak permanent magnets of 200 G (much weaker than those used for the fragrance oils of Figs. 8.18 and 8.19). All samples resulted in being very stable without any measurable change over a period of about one year, and survived freezing followed by defrosting. The various samples were numbered from 1 to 25.

The measurements of the specific density were conducted on March 9, 1998 by the *U.S. Testing Company, Inc.* (USTC) of Fairfield, New Jersey. The results of the tests are presented in Figs. 8.31 and 8.32.

Sample 1 is ordinary untreated tap water. Sample 2 is ordinary tap water magnetically treated for about 5 minutes. Samples 3 and 4 were tap water treated with other magnetic equipment. Sample 5 was ordinary untreated GR fragrance oil "APC Fragrance." Sample 6 was a mixture of fragrance oil 5 with tap water magnetically treated for about 5 minutes. Mixtures 7 and 8 were the same mixture 5 although treated with other equipment. Sample 17 was a magnetically treated GR oil "Air Freshener 1." Mixture 19 was Fragrance 17 with tap water 16 magnetically treated for 5 minutes. Note that all measurements were done to an accuracy of the fourth digit. Therefore, numerical results up to the third digit can be considered accurate.

In the transition from Sample 1 (untreated water) to Sample 2 (magnetically treated water) there is an increase in the specific density in the macroscopic amount of 0.86%, thus confirming the indicated mutation of the specific density of water under a magnetic treatment. In turn, the increase in density supports the existence of magneplexes in magnetically treated water as per the scan of Fig. 11.65.

As well known, fragrance oils are (generally) *lighter* than water, *i.e.*, the specific density of the untreated fragrance in Sample 5 is *smaller* than that of the untreated water in Sample 1. According to quantum chemistry, the specific density of any mixture of the above two liquids, whether solution, suspension or dispersion, should be *in between* the lighter and heavier specific densities.

On the contrary, as one can see, *the specific density of the magnetically treated mixture of GR fragrance with tap water, Sample 6, resulted in being bigger than that of the densest liquid, the water.* This measurement constitutes additional, rather strong, direct experimental verification of the mutation of physical characteristics in liquids under magnetic fields.

REPORT OF TEST

SGS U.S. Testing Company Inc.

291 Fairfield Avenue
Fairfield, NJ 07004-3833
Tel: 973-575-5252
Fax: 973-244-1694

Report Number: 103947
Date: 03/09/98
Page: 1 of 1

Millennium Results

Density of	g/mL	% Change Density vs Ordinary Water
Sample #1	0.9805	0
Sample #2	0.9889	+0.86
Sample #3	0.9804	0
Sample #4	0.9853	+0.49
Fragrant #5	0.9720	NA
Mixture #6	0.9967	+1.65
Mixture #7	0.9982	+1.80
Mixture #8	0.9902	0.99
Treated Water #16	0.9893	0.89
Frag Treated # 17	0.9453	NA
Mixture #18	0.9902	0.99
Mixture #19	0.9929	1.26

Samples were transferred to a separatory funnel. The layers were allowed to separate. The water layer was withdrawn into a funnel with Whatman #4 filter paper. The filtrate was transferred to a preweighed 10 mL volumetric flask. The sample was weighed to 0.0001 grams and the density calculated.

When the samples were pure substances, they were transferred directly to preweighed 10 mL volumetric flasks.

Calculations:

Weight flash with sample - weight flask + volume of flask = g/ mL

Arlyn Sibille, Ph.D.

Figure 11.69. USTC measurements of specific density on magnetically treated liquids.

REPORT OF TEST

SGS U.S. Testing Company Inc.

291 Fairfield Avenue
Fairfield, NJ 07004-3833
Tel: 973-575-5252
Fax: 973-244-1694

Report Number: 103947
Date: 03/09/98
Page: 1 of 1

SUBJECT: Three (3) samples received on 02/09/98 and identified by the client as:

PURPOSE: Determine the density and viscosity of the three samples.

TEST DATE: 02/25/98

PROCEDURE: Three 10 milliliter volumetrtic flasks were pre-weighed. One of the samples was transferred to each of the volumetric flasks with a pipet. The samples were weighed again. The density of each sample was calculated.

The three oil samples were measured for viscosity using a Kinematic viscometer (ASTM D-445).

RESULTS:

Sample Identification	Density, g/mL)	Viscosity (cps)	Increase Viscosity, %
1) Motor Oil, "as is"	0.8682	199.8	0
2) Motor Oil, Treatment Type A	0.8714	288.7	44.5
3) Motor Oil, Treatment Type B	0.8689	302.0	51.2

SIGNED FOR THE COMPANY BY:

James R. Tyminski
Laboratory Supervisor

Arlyn Sibille, Ph.D.
Laboratory Director

/mo

Member of the SGS Group

ANALYTICAL SERVICES · PERFORMANCE TESTING · STANDARDS EVALUATION · CERTIFICATION SERVICES

SGS U.S. TESTING COMPANY INC. REPORTS ARE FOR THE EXCLUSIVE USE OF THE CLIENT TO WHOM THEY ARE ADDRESSED. ANYONE RELYING ON SUCH REPORTS SHOULD UNDERSTAND ALL OF THE DETAILS OF THE ENGAGEMENT. REPORTS REFLECT RESULTS ONLY OF THE STANDARDS OR PROCEDURES IDENTIFIED TO THE TESTS CONDUCTED AND ARE LIMITED TO THE SAMPLES TESTED. TEST RESULTS MAY NOT BE INDICATIVE OF THE QUALITIES OF THE LOT FROM WHICH THE SAMPLE WAS TAKEN. SGS U.S. TESTING COMPANY INC. HAS NOT CONDUCTED ANY QUALITY CONTROL PROGRAM FOR THE CLIENT. NEITHER THE NAME, SEALS, MARKS NOR INSIGNIA OF SGS U.S. TESTING COMPANY INC. MAY BE USED IN ANY ADVERTISING OR PROMOTIONAL MATERIALS WITHOUT THE PRIOR WRITTEN APPROVAL OF SGS U.S. TESTING COMPANY INC. THIS REPORT SHALL NOT BE REPRODUCED EXCEPT IN FULL WITHOUT WRITTEN APPROVAL. SAMPLES NOT REMOVED IN TESTING ARE DISPOSED OF AFTER 30 DAYS.

Figure 11.70. USTC measurements of viscosity on magnetically treated liquids.

A remarkable point is that the *magnetic mutations of density are macroscopically large*. In fact, they were called by an analyst "UPS-type anomalies", meaning that the shipment via UPS of a given volume of a magnetically treated liquid may require an increase of the shipping cost of the same volume of untreated liquid due to the macroscopic increase in the weight.

A further prediction of magnetically polarized liquids is the increase of its viscosity. This is evidently due to the arbitrary size of an individual mag-

necule, as well as the tendency of the same to bond to near-by molecules, resulting in accretions, not to mention the anomalous adhesion to the walls of the container, which has been systematically detected for all magnetically polarized liquids.

As indicated earlier, in certain cases the increase of viscosity is so large as to be first visible to the naked eye, and, when the treatment is sufficiently protracted, the increase in viscosity is such as to lose the customary liquid mobility.

Ordinary engine oils are particularly suited for magnetic treatment because, when properly treated, their increase in viscosity is so dramatic as to be visible to the naked eye jointly with a visible change in visual appearance (color, texture, opacity, *etc.*).

The measurements on viscosity are reported in Fig. 11.70. The selected engine oil was an ordinarily available 30-40 Castrol Motor Oil subjected to a particular type of magnetic treatments via two different kinds of equipment called of Type A and B. All treatments were done at ordinary conditions without any additive or change of any type. As one can see, *measurement 2 shows a dramatic increase in the viscosity in the magnetically treated oil of 44.5%.*

The above experimental results evidently provide additional support for the existence of magnecules.

The tests also provide evidence of the anomalous adhesion of liquids with magnecules, which is established in this case by a dramatic, macroscopic increase of adhesion of the oil to the walls of the glass container.

The same macroscopic anomaly is confirmed at the microscopic level. During the measurement of viscosity there was such an anomalous adhesion of the magnetically treated oils to the walls of the instrument that said oil could not be removed via routine cleaning with acetone and required the use of strong acids.

This anomalous adhesion is further experimental evidence of the existence of magnecules, because of their predicted capability to induce the polarization of the orbits of the valence electrons of the atoms in the walls of the container, thus resulting in anomalous adhesion via magnetic bonds due to induction.

It is evident that the mutations of density and viscosity implies the expected mutation of *all* other physical characteristics of the liquid considered. These measurements are left to the interested researchers.

The existence of mutation of *physical* characteristics then implies the mutation of *chemical* features. At this moment, we can only indicate the visual evidence reported by the analysts of USTC according to whom the reaction of magnetically treated oils with acetone is dramatically different from that with untreated oil, including mutations in color, texture and other appearances.

11.7.6 Concluding Remarks

The theoretical and experimental evidence presented in this Chapter establishes that the chemical species of molecules, defined as stable clusters of atoms under a valance bond, does not exhaust all possible chemical species existing in nature.

This conclusion is proved beyond scientific doubt, for instance, by macroscopic percentage of stable clusters, with atomic weight of several hundreds a.m.u., in light gases without an infrared signature where heaviest possible detected molecule is the CO_2 with 44 a.m.u.; the mutation of transparent oils into a completely opaque substance without fluidity; the joint increase of the specific density for both gaseous and liquid cases; and other evidence.

Needless to say, the final *characterization* and *detection* of the new chemical species submitted in Refs. [1,2] and reviewed in this chapter will require a considerable collegial effort, since the methods presented in this chapter are manifestly preliminary, with the understanding that, again, the *existence* of the new chemical species is outside scientific doubts.

As a matter of fact, the proposed new chemical species of magnecules, which, according to Definition 11.2.1 includes that of molecules, cannot be considered itself as the final chemical species in nature as it is the fate proved by history for all scientific discoveries.

As an example, the reformulation of magnecules via the hyperstructural branch of hadronic chemistry implies the prediction of the broader chemical species of *hypermagnecules* which is apparently more suitable to represent living organisms due to its inherent irreversibility, multidimensional structure compatible with our three-dimensional sensory perception, and other features needed for a more adequate representation of the complexities of living organisms. The *novelty* of this possible species is then an evident consequence of its novel features. Its *need* is established by the fact that current attempts to decipher the DNA code via the numbers used for molecules and magnecules dating back to biblical times have little chance of success, thus mandating the use of broader numbers, such as the hypernumbers and related multi-dimensional structures.

All in all, we can safely conclude that science is a discipline that will never admit final theories.

Appendix 11.A
Aringazin's Studies on Toroidal Orbits of the Hydrogen Atom under an External Magnetic Field

In the main text of this chapter we have presented the theoretical and experimental foundations of the new chemical species of magnecules which is centrally dependent on individual atoms acquiring a generally toroidal configuration of the orbits of at least the peripheral electrons when exposed to sufficiently intense external magnetic fields, as originally proposed by Santilli [1] and reviewed in the main text of this Chapter.

In this Appendix we outline the studies by Aringazin [8] on the Schrödinger equation of the hydrogen atom under a strong, external, static and uniform magnetic field which studies have confirmed the toroidal configuration of the electron orbits so crucial for the existence of the new chemical species of magnecules.

It should be stressed that when considered at orbital distances (i.e., of the order of 10^{-8} cm), atoms and molecules near the electric arc of hadronic reactors (Section 11.4), and in the plasma region, are exposed to a strong magnetic field, whose intensity may be high enough to cause the needed magnetic polarization (see Fig. 11.4.D).

A weak, external, static, and uniform magnetic field B causes an anomalous Zeeman splitting of the energy levels of the hydrogen atom, with ignorably small effects on the electron charge distribution. In the case of a more intense magnetic field which is strong enough to cause decoupling of a spin-orbital interaction (in atoms), $e\hbar B/2mc > \Delta E_{jj'} \simeq 10^{-3}$ eV, i.e., for $B \simeq 10^5$ Gauss, a normal Zeeman effect is observed, again, with ignorably small deformation of the electron orbits.

More particularly, in the case of a *weak* external magnetic field B, one can ignore the quadratic term in the field B because its contribution is small in comparison with that of the other terms in Schrödinger equation, so that the *linear* approximation in the field B can be used. In such a linear approximation, the wave function of electron remains unperturbed, with the only effect being the well known Zeeman splitting of the energy levels of the H atom. In both Zeeman effects, the interaction energy of the electron with the the magnetic field is assumed to be much smaller than the binding energy of the hydrogen atom, $e\hbar B/2mc \ll me^4/2\hbar^2 = 13.6$ eV, i.e., the intensity of the mag-

netic field is much smaller than some characteristic value, $B \ll B_0 = 2.4 \cdot 10^9$ Gauss = 240000 Tesla (recall that 1 Tesla = 10^4 Gauss). Thus, the action of a weak magnetic field can be treated as a small perturbation of the hydrogen atom.

In the case of a *very strong* magnetic field, $B \gg B_0$, the quadratic term in the field B makes a great contribution and cannot be ignored. Calculations show that, in this case, a considerable deformation of the electron charge distribution in the hydrogen atom occurs. More specifically, under the influence of a very strong external magnetic field a magnetic confinement takes place, i.e., in the plane perpendicular to the direction of magnetic field (see Fig. 8.4.D), the electron dynamics is determined mainly by the action of the magnetic field, while the Coulomb interaction of the electron with the nucleus can be viewed as a small perturbation. This adiabatic approximation allows one to separate variables in the associated Schrödinger equation [9]. At the same time, in the direction of the magnetic field the motion of electron is governed both by the magnetic field and the Coulomb interaction of the electron with the nucleus.

The highest intensities of magnetic fields maintained macroscopically at large distances in modern magnet laboratories are of the order of $10^5 - 10^6$ Gauss (~ 50 Tesla), i.e., they are much below $B_0 = 2.4 \cdot 10^9$ Gauss ($\sim 10^5$ Tesla). Extremely intense external magnetic fields, $B \geq B_c = B_0/\alpha^2 = 4.4 \cdot 10^{13}$ Gauss, correspond to the interaction energy of the order of the mass of electron, $mc^2 = 0.5$ MeV, where $\alpha = e^2/\hbar c$ is the fine structure constant. In this case, despite the fact that the extremely strong magnetic field does characterize a stable vacuum in respect to creation of electron-positron pairs, one should account for relativistic and quantum electrodynamics (QED) effects, and invoke Dirac or Bethe-Salpeter equation. These contributions are of interest in astrophysics, for example, in studying the atmosphere of neutron stars and white dwarfs which are characterized by $B \simeq 10^9 \ldots 10^{13}$ Gauss.

Aringazin [8] has focused his studies on magnetic fields with intensities of the order of $2.4 \cdot 10^{10} \leq B \leq 2.4 \cdot 10^{13}$ Gauss, at which value nonrelativistic studies via the Schrödinger equation can be used to a very good accuracy, and the adiabatic approximations can be made.

Relativistic and QED effects (loop contributions), as well as effects related to finite mass, size, and magnetic moment of the nucleus, and the finite electromagnetic radius of electron, reveal themselves even at low magnetic field intensities, and can be accounted for as very small perturbations. Additional effects are related to the apparent deviation from QED of strongly correlated valence bonds as studies in Chapter 4. These effects are beyond the scope of the presented study, while being important for high precision studies, such as those on stringent tests of the Lamb shift.

It should be noted that locally high-intensity magnetic fields may arise in plasma as the result of nonlinear effects, which can lead to the creation of stable self-confined structures having nontrivial topology with knots [10]. More particularly, Faddeev and Niemi [10] recently argued that the static equilibrium configurations within the plasma are topologically stable solitons describing knotted and linked fluxtubes of helical magnetic fields. In the region close to such fluxtubes, we suppose the magnetic field intensity may be as high as B_0. In view of this, a study of the action of strong magnetic field and the fluxtubes of magnetic fields on atoms and molecules becomes of great interest in theoretical and applicational *plasmachemistry*. Possible applications are conceivable for the new chemical species of magnecules.

As a result of the action of a very strong magnetic field, atoms attain a great binding energy as compared to the case of zero magnetic field. Even at intermediate $B \simeq B_0$, the binding energy of atoms greatly deviates from that of the zero-field case, and even lower field intensities may essentially affect chemical properties of molecules of heavy atoms. This occurrence permits the creation of various other bound states in molecules, clusters and bulk matter [9, 11, 12].

The paper by Lai [12] is focused on very strong magnetic fields, $B \gg B_0$, motivated by astrophysical applications, and provides a good survey of the early and recent studies in the field, including studies on the intermediate range, $B \simeq B_0$, multi-electron atoms, and H_2 molecule. Several papers using variational/numerical and/or analytical approaches to the problem of light and heavy atoms, ions, and H_2 molecule in strong magnetic field, have been published within the last years (see, e.g., references in [12]). However, highly magnetized molecules of heavy atoms have not been systematically investigated until Santilli's proposal for the new species of magnecules [1]. One of the surprising implications is that for some diatomic molecules of heavy atoms, the molecular binding energy is predicted to be several times bigger than the ground state energy of individual atom [13].

To estimate the intensity of the magnetic field which causes considerable deformation of the ground state electron orbit of the H atom, one can formally compare Bohr radius of the H atom in the ground state, in zero external magnetic field, $a_0 = \hbar^2/me^2 \simeq 0.53 \cdot 10^{-8}$ cm $= 1$ a.u., with the radius of orbit of a single electron moving in the external static uniform magnetic field $\vec{B}$.

The mean radius of the orbital of a single electron moving in a static uniform magnetic field can be calculated exactly by using Schrödinger's equation, and it is given by

$$R_n = \sqrt{\frac{n + 1/2}{\gamma}}, \tag{11.A.1}$$

where $\gamma = eB/2\hbar c$, B is intensity of the magnetic field pointed along the z axis, $\vec{B} = (0, 0, B)$, $\vec{r} = (r, \varphi, z)$ in cylindrical coordinates, and $n = 0, 1, \ldots$ is the principal quantum number. Thus, the radius of the orbit takes *discrete* set of values (11.A), and is referred to as Landau radius. This is in contrast to well known *classical* motion of electrons in an external magnetic field, with the radius of the orbit being of a continuous set of values.

The energy levels E_n of a single electron moving in said external magnetic field are referred to as Landau energy levels,

$$E_n = E_n^{\perp} + E_{k_z}^{\parallel} = \hbar\Omega(n + \frac{1}{2}) + \frac{\hbar^2 k_z^2}{2m}, \qquad (11.A.2$$

where $\Omega = eB/mc$ is so called cyclotron frequency, and $\hbar k_z$ is a projection of the electron momentum $\hbar\vec{k}$ on the direction of the magnetic field, $-\infty < k_z < \infty$, m is mass of electron, and $-e$ is charge of electron.

Landau's energy levels $E_n^{\perp}$ correspond to a discrete set of round orbits of the electron which are projected to the transverse plane. The energy $E_{k_z}^{\parallel}$ corresponds to a free motion of the electron in parallel to the magnetic field (*continuous* spectrum), with a conserved momentum $\hbar k_z$ along the magnetic field.

In regard to the above review of Landau's results, we recall that in the general case of a *uniform* external magnetic field the coordinate and spin components of the total wave function of the electron can always be separated.

The corresponding coordinate component of the total wave function of the electron, obtained as an exact solution of Schrödinger equation for a single electron moving in the external magnetic field with vector-potential chosen as $A_r = A_z = 0$, $A_\varphi = rB/2$,

$$-\frac{\hbar^2}{2m}\left(\partial_r^2 + \frac{1}{r}\partial_r + \frac{1}{r^2}\partial_\varphi^2 + \partial_z^2 - \gamma^2 r^2 + 2i\gamma\partial_\varphi\right)\psi = E\psi, \qquad (11.A.3$$

is of the following form [9]:

$$\psi_{n,s,k_z}(r, \varphi, z) = \sqrt{2\gamma} I_{ns}(\gamma r^2)\frac{e^{il\varphi}}{\sqrt{2\pi}}\frac{e^{ik_z z}}{\sqrt{L}}, \qquad (II.A.4)$$

where $I_{ns}(\rho)$ is Laguerre function,

$$I_{ns}(\rho) = \frac{1}{\sqrt{n!s!}} e^{-\rho/2}\rho^{(n-s)/2} Q_s^{n-s}(\rho); \qquad (II.A.5)$$

Q_s^{n-s} is Laguerre polynomial, L is normalization constant, $l = 0, \pm 1, \pm 2, \ldots$ is azimuthal quantum number, $s = n - l$ is radial quantum number, and $\rho = \gamma r^2$.

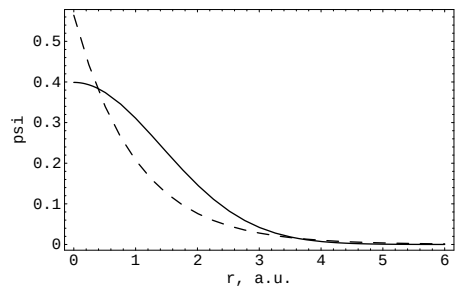

Figure 11.A.1. Landau's ground state wave function of a single electron, ψ_{000} (solid curve), Eq. (11.A), in a strong external magnetic field $B = B_0 = 2.4 \cdot 10^9$ Gauss, as function of the distance r in cylindrical coordinates, and (for a comparison) the hydrogen ground state wave function (at *zero* external magnetic field), $(1/\sqrt{\pi})e^{-r/a_0}$ (dashed curve), as function of the distance r in spherical coordinates. The associated probability densities are shown in Fig. **??**; 1 a.u. $= a_0 = 0.53 \cdot 10^{-8}$ cm.

Spin components of the total wave function are trivially given by

$$\psi(\frac{1}{2}) = \begin{pmatrix} 1 \\ 0 \end{pmatrix}, \quad \psi(-\frac{1}{2}) = \begin{pmatrix} 0 \\ 1 \end{pmatrix}, \tag{II.A.6}$$

with the corresponding energies $E_{spin} = \pm\mu_0 B$, to be added to the energy (11.A); $\mu_0 = e\hbar/2mc$ is Bohr magneton.

For the *ground* Landau level, i.e. at $n = 0$ and $s = 0$, and zero momentum of electron in the z-direction, i.e. $\hbar k_z = 0$, we have from (11.A)

$$E_0^{\perp} = \frac{e\hbar B}{2mc}, \tag{II.A.7}$$

and due to Eq. (11.A) the corresponding normalized ground state wave function is

$$\psi_{000}(r, \varphi, z) = \psi_{000}(r) = \sqrt{\frac{\gamma}{\pi}}\, e^{-\gamma r^2/2}, \tag{II.A.8}$$

$\int_0^\infty \int_0^{2\pi} r dr d\varphi\, |\psi_{000}|^2 = 1$.

The corresponding (smallest) Landau's radius of the orbit of electron is

$$R_0 = \sqrt{\frac{\hbar c}{eB}} \equiv \sqrt{\frac{1}{2\gamma}}, \tag{II.A.9}$$

in terms of which ψ_{000} reads

$$\psi_{000} = \sqrt{\frac{1}{2\pi R_0^2}}\; e^{-\frac{r^2}{4R_0^2}}. \tag{II.A.10}$$

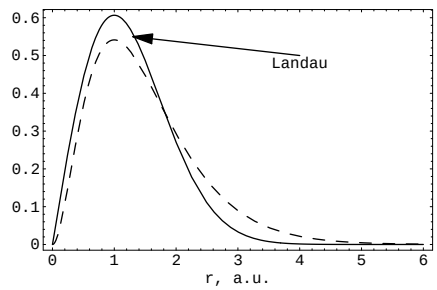

Figure 11.A.2. Probability density for the case of Landau's ground state of a single electron, $2\pi r|\psi_{000}|^2$ (solid curve), Eq. (11.A), in a strong external magnetic field $B = B_0 = 2.4 \cdot 10^9$ Gauss, as a function of the distance r in cylindrical coordinates, and (for a comparison) the probability density of the hydrogen atom ground state (at *zero* external magnetic field), $4\pi r^2|(1/\sqrt{\pi})e^{-r/a_0}|^2$ (dashed curve), as function of the distance r in spherical coordinates. The associated wave functions are shown in Fig. 11.A.1; 1 a.u. $= 0.53 \cdot 10^{-8}$ cm.

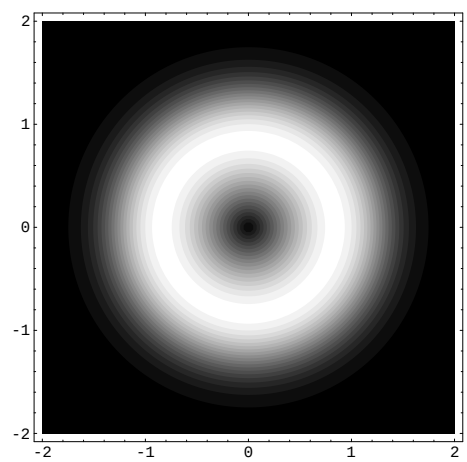

Figure 11.A.3. Contour plot of the (r, φ) probability density for the case of Landau's ground state of a single electron, $2\pi r|\psi_{000}|^2$, Eq. (11.A), in strong external magnetic field $B = B_0 = 2.4 \cdot 10^9$ Gauss, as a function of the distance in a.u. (1 a.u. $= 0.53 \cdot 10^{-8}$ cm). The lighter area corresponds to a bigger probability of finding the electron. The set of maximal values of the probability density is referred to as an "orbit".

Figure 11.A.1 depicts Landau's ground state wave function of a single electron, ψ_{000}, in the strong external magnetic field $B = B_0 = 2.4 \cdot 10^9$ Gauss ($R_0 = 1$ a.u.), and (for a comparison) of the hydrogen ground state wave function, at *zero* external magnetic field, $(1/\sqrt{\pi})e^{-r/a_0}$. Figures 11.A.2 and 11.A.3 display the associated probability density of the electron as a function

of the distance r from the center of the orbit, the radius of which is about 1 a.u.

The condition that Landau's radius is smaller than Bohr's radius, $R_0 < a_0$ (which is adopted here as the condition of a considerable "deformation" of the electron orbit of the H atom) then implies

$$B > B_0 = \frac{m^2 ce^3}{\hbar^3} = 2.351 \cdot 10^9 \text{ Gauss}, \qquad (II.A.11)$$

where m is mass of electron. Equivalently, this deformation condition corresponds to the case when the binding energy of the H atom, $|E_0^{Bohr}| = |-me^4/2\hbar^2| = 0.5$ a.u. $= 13.6$ eV, is smaller than the ground Landau energy $E_0^{\perp}$.

The above critical value of the magnetic field, B_0, is naturally taken as an *atomic unit* for the strength of the magnetic field, and corresponds to the case when the pure Coulomb interaction energy of the electron with nucleus is equal to the interaction energy of the single electron with the external magnetic field, $|E_0^{Bohr}| = E_0^{\perp} = 13.6$ eV, or equivalently, when Bohr radius is equal to Landau radius, $a_0 = R_0 = 0.53 \cdot 10^{-8}$ cm.

It should be stressed here that the characteristic parameters, Bohr's energy $|E_0^{Bohr}|$ and Bohr's radius a_0, of the H atom have the purpose to establish a criterium for the critical strength of the external magnetic field of the hydrogen atom under the conditions here considered. For other atoms the critical value of the magnetic field may be evidently different.

After outlining the quantum dynamics of a single electron in an external magnetic field, Aringazin [8] turns to the consideration of the H atom under an external static uniform magnetic field.

In the cylindrical coordinate system (r, φ, z), in which the external magnetic field is $\vec{B} = (0, 0, B)$, i.e., the magnetic field is directed along the z-axis, Schrödinger's equation for an electron moving around a fixed proton (Born-Oppenheimer approximation) in the presence of the external magnetic field is given by

$$-\frac{\hbar^2}{2m}\left(\partial_r^2 + \frac{1}{r}\partial_r + \frac{1}{r^2}\partial_\varphi^2 + \partial_z^2 + \frac{2me^2}{\hbar^2\sqrt{r^2+z^2}} - \gamma^2 r^2 + 2i\gamma\partial_\varphi\right)\psi = E\psi, \qquad (II.A.12)$$

where $\gamma = eB/2\hbar c$.

The main problem in the nonrelativistic study of the hydrogen atom in an external magnetic field is to solve the above Schrödinger equation and find the energy spectrum. This equation is not analytically tractable so that one is led to use approximations.

In the approximation of a *very* strong magnetic field, $B \gg B_0 = 2.4 \cdot 10^9$ Gauss, Coulomb interaction of the electron with the nucleus is not important,

in the transverse plane, in comparison to the interaction of the electron with external magnetic field. Therefore, in accord to the exact solution (11.A) for a single electron, one can look for an approximate ground state solution of Eq. (11.A.3) in the form of factorized transverse and longitudinal parts,

$$\psi = e^{-\gamma r^2/2}\chi(z), \qquad (II.A.13)$$

where $\chi(z)$ is the longitudinal wave function to be found. This is so called *adiabatic approximation*. In general, the adiabatic approximation corresponds to the case when the transverse motion of electron is totally determined by the intense magnetic field, which makes the electron "dance" at its cyclotron frequency. Specifically, the radius of the orbit is then *much smaller* than Bohr radius, $R_0 \ll a_0$. The remaining problem is thus to find longitudinal energy spectrum, in the z direction.

Inserting tehe wave function (11.A.3) into the Schrödinger equation (11.A.3), multiplying it by ψ^*, and integrating over variables r and φ in cylindrical coordinate system, one gets the following equation characterizing the z dependence of the wave function:

$$\left(-\frac{\hbar^2}{2m}\frac{d^2}{dz^2} + \frac{\hbar^2\gamma}{m} + C(z)\right)\chi(z) = E\chi(z), \qquad (II.A.14)$$

where

$$C(z) = -\sqrt{\gamma}\, e^2 \int_0^\infty \frac{e^{-\rho}}{\sqrt{\rho+\gamma z^2}}\, d\rho = -e^2\sqrt{\pi\gamma}\, e^{\gamma z^2}[1 - \mathrm{erf}(\sqrt{\gamma}|\mathrm{z}|)], \quad (II.A.15)$$

where $\mathrm{erf}(x)$ is the error function.

The arising effective potential $C(z)$ is of a nontrivial form, which does not allow to solve Eq. (11.A.3) analytically, so one can approximate it by simple potentials, to make an estimation on the ground state energy and wave function of the H atom.

At high intensity of the magnetic field, $\gamma \gg 1$ so that under the condition $\gamma\langle z^2\rangle \gg 1$ one can ignore ρ in the square root in the integrand in Eq. (11.A.3). Then, one can perform the simplified integral and obtain the result

$$C(z) \simeq V(z) = -\frac{e^2}{|z|}, \quad \text{at } \gamma\langle z^2\rangle \gg 1, \qquad (II.A.16)$$

which appears to be a pure Coulomb interaction of electron with the nucleus, in the z direction. Due to the exact result (11.A.3), $C(z)$ tends to zero as $z \to \infty$. However, a remarkable implication of the exact result is that $C(z)$ is *finite* at $z = 0$, namely, $C(0) = -\sqrt{\pi\gamma}\, e^2$, so that the effective potential $C(z)$ can *not* be well approximated by the Coulomb potential.

The exact potential $C(z)$ can be well approximated by the *modified* Coulomb potential,

$$C(z) \simeq V(z) = -\frac{e^2}{|z| + z_0}, \qquad (II.A.17)$$

where z_0 is a parameter, $z_0 \neq 0$, which depends on the field intensity B due to

$$z_0 = -\frac{e^2}{C(0)} = \frac{1}{\sqrt{\pi\gamma}} = \sqrt{\frac{2\hbar c}{\pi e B}}. \qquad (II.A.18)$$

The analytic advantage of this approximation is that $V(z)$ is *finite* at $z = 0$, being of Coulomb-type form. Therefore, Eq. (11.A.3) reduces to *one-dimensional* Schrödinger equation for the Coulomb-like potential,

$$\left(\frac{\hbar^2}{2m}\frac{d^2}{dz^2} + \frac{e^2}{|z| + z_0} + \frac{\hbar^2\gamma}{m} + E\right)\chi(z) = 0. \qquad (II.A.19)$$

In the atomic units ($e = \hbar = m = 1$), using the notation

$$E' = \frac{\hbar^2\gamma}{m} + E, \quad n^2 = \frac{1}{-2E'}, \qquad (II.A.20)$$

introducing the new variable $x = 2z/n$, and dropping $x_0 = 2z_0/n$, to simplify representation, the above equation can be rewritten as

$$\left[\frac{d}{dx^2} + \left(-\frac{1}{4} + \frac{n}{x}\right)\right]\chi(x) = 0, \qquad (II.A.21)$$

where $x > 0$ is assumed. Introducing new function $v(x)$ defined as $\chi(x) = xe^{-x/2}v(x)$, one gets the final form of the equation,

$$xv'' + (2 - x)v' - (1 - n)v = 0. \qquad (II.A.22)$$

Noting that it is a particular case of Cummer's equation,

$$xv'' + (b - x)v' - av = 0, \qquad (II.A.23)$$

the general solution is given by

$$v(x) = C_1\, {}_1F_1(a, b, x) + C_2 U(a, b, x), \qquad (II.A.24)$$

where

$${}_1F_1(a, b, x) = \frac{\Gamma(b)}{\Gamma(b - a)\Gamma(a)} \int_0^1 e^{xt} t^{a-1}(1 - t)^{b-a-1}\, dt \qquad (II.A.25)$$

and

$$U(a, b, x) = \frac{1}{\Gamma(a)} \int_0^\infty e^{-xt} t^{a-1}(1 + t)^{b-a-1}\, dt \qquad (II.A.26)$$

are the confluent hypergeometric functions, and $C_{1,2}$ are constants; $a = 1 - n$ and $b = 2$. Hence, for $\chi(x)$ one has

$$\chi(x) = (|x|+x_0)e^{-(|x|+x_0)/2}\left[C_1^{\pm}{}_1F_1(1-n,2,|x|+x_0) + C_2^{\pm}U(1-n,2,|x|+x_0)\right], \tag{II.A.27}$$

where the parameter x_0 has been restored, and the "$\pm$" sign in $C_{1,2}^{\pm}$ corresponds to the positive and negative values of x, respectively (the modulus sign is used for brevity).

Let us consider first the $x_0 = 0$ case. The first hypergeometric function ${}_1F_1(1-n,2,x)$ is finite at $x = 0$ for any n. At big x, it diverges exponentially, unless n is an integer number, $n = 1, 2, \ldots$, at which case it diverges polynomially. The second hypergeometric function $U(1-n,2,x)$ behaves differently, somewhat as a mirror image of the first one. In the limit $x \to 0$, it is finite for integer $n = 1, 2, 3, \ldots$, and diverges as $1/x$ for noninteger $n > 1$ and for $0 \leq n < 1$. In the limit $x \to \infty$, it diverges polynomially for integer n, tends to zero for noninteger $n > 1$ and for $n = 0$, and diverges for noninteger $0 < n < 1$.

In general, because of the prefactor $xe^{-x/2}$ in the solution (11.A.3) which cancels some of the divergencies arising from the hypergeometric functions, we should take into account *both* of the two linearly independent solutions, to get the most general form of normalizable wave functions.

As a consequence, for $x_0 \neq 0$ the eigenvalues may *differ* from those corresponding to $n = 1, 2, \ldots$ (which is a counterpart of the principal quantum number in the ordinary hydrogen atom problem) so that n is allowed to take some *non-integer* values from 0 to ∞, provided that the wave function is normalizable.

For even states, in accord to the symmetry of wave function under the inversion $z \to -z$, one has

$$C_1^+ = C_1^-, \quad C_2^+ = C_2^-, \quad \chi'(0) = 0. \tag{II.A.28}$$

Also, since $n = 1$ gives $E' = -1/(2n^2) = -1/2$ a.u., one should seek normalizable wave function for n in the interval $0 < n < 1$, in order to achieve lower energy value. If successful, $n = 1$ indeed does not characterize the ground state. Instead, it may correspond to some excited state.

Analysis shows that *normalizable* wave functions, as a combination of *two* linearly independent solutions, for the modified Coulomb potential *does exist* for various *non-integer* n. Focusing on the ground state solution, Aringazin considers values of n ranging from 0 to 1. Remind that $E' = -1/2n^2$ so that for $n < 1$ the energy lower than $E' = -0.5$ a.u.

For $n < 1$, the first hypergeometric function is not suppressed by the prefactor $xe^{-x/2}$ in the solution (11.A.3) at large x so we are led to discard it as an unphysical solution by putting $C_1 = 0$. A normalizable ground state wave function for $n < 1$ is thus may be given by the second term in the solution

(11.A.3). Indeed, the condition $\chi'(x)_{|x=0} = 0$ implies

$$\begin{aligned}\tfrac{1}{2}e^{-(x+x_0)/2}C_2[(2-x-x_0)U(1-n,2,x+x_0)-\\ -2(1-n)(x+x_0)U(2-n,3,x+x_0))]_{|x=0} = 0.\end{aligned} \qquad (II.A.29)$$

The l.h.s of this equation depends on n and x_0, so one can select some field intensity B, calculate associated $x_0 = x_0(B)$ and find n, from which one obtains the ground state energy E'. On the other hand, for the ground state this condition can be viewed, *vice versa*, as an equation to find x_0 at some selected n.

For example, taking the noninteger value $n = 1/\sqrt{15.58} \simeq 0.253 < 1$ Aringazin found $x_0 = 0.140841$. This value is in confirmation with the result $x_0 = 0.141$ obtained by Heyl and Hernquist [14]. On the other hand, x_0 is related in accord to Eq. (11.A.3) to the intensity of the magnetic field, $x_0 = 2z_0/n$, from which one obtains $B \simeq 4.7 \cdot 10^{12}$ Gauss. Hence, at this field intensity the ground state energy of the hydrogen atom is determined by $n = 1/\sqrt{15.58}$.

The total ground state wave function is given by

$$\psi(r,\varphi,x) \simeq \sqrt{\frac{1}{2\pi R_0^2}}e^{-\frac{r^2}{4R_0^2}}(|x|+x_0)e^{(|x|+x_0)/2}U(1-n,2,|x|+x_0), \quad (II.A.30)$$

where n is determined due the above procedure, and the associated three-dimensional probability density is schematically depicted in Fig. 11.A.4.

One can see that the problem remarkably difference than the ordinary three-dimensional problem of the hydrogen atom, for which the principal quantum number n must be integer to get normalizable wave functions, and the value $n = 1$ corresponds to the lowest energy.

The modified Coulomb potential approach provides qualitatively correct behavior, and suggests a *single* Landau-type orbit shown in Fig. 11.A.4 for the *ground* state charge distribution of the hydrogen atom. This is in full agreement with Santilli's study [1, 11] of the hydrogen atom in a strong magnetic field.

Accurate analytic calculation of the ground and excited hydrogen wave functions made by Heyl and Hernquist [14] in the adiabatic approximation leads to the longitudinal parts of the wave functions shown in Fig. 11.A.5, which reproduces the original Fig. 3 of their work; $\zeta = 2\pi\alpha z/\lambda_e$; $B = 4.7 \cdot 10^{12}$ Gauss. They used the modified Coulomb potential of the type (11.A.3), and the additional set of linearly independent solutions of the one-dimensional modified Coulomb problem in the form

$$(|x|+x_m)e^{-(|x|+x_m)/2}{}_1F_1(1-n,2,|x|+x_m)\int^{|x|+x_m}\frac{e^t}{(t\,{}_1F_1(1-n,2,t))^2}\,dt, \qquad (II.A.31)$$

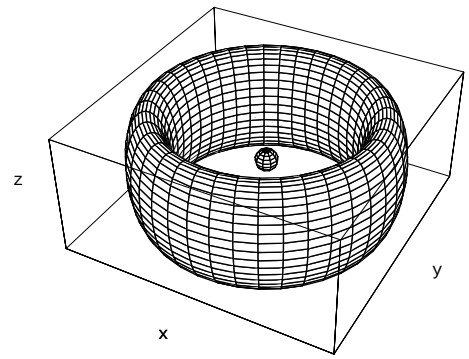

Figure 11.A.4. A schematic view on the H atom in the ground state under a very strong external magnetic field $\vec{B} = (0, 0, B)$, $B \gg B_0 = 2.4 \cdot 10^9$ Gauss, due to the *modified* Coulomb approximation studied in the text. The electron moves on the Landau orbit of small radius $R_0 \ll 0.53 \cdot 10^{-8}$ cm resulting in the toroidal structure used for the new chemical species of magnecules. The vertical size of the atom is comparable to R_0. The spin of the electron is antiparallel to the magnetic field.

where $m = 0$ corresponds to the ground state. For the ground state with $n = 1/\sqrt{15.58}$, they found $x_0 = 0.141$, which corresponds to $B = 4.7 \cdot 10^{12}$ Gauss. This result is in agreement with the study made above.

One can see from Fig. 11.A.5 that the peak of the ground state wave function $|000\rangle$ is at the point $z = 0$, while the largest peaks of the excited wave functions are away from the point $z = 0$ (as it was expected to be). Consequently, the associated longitudinal probability distributions (square modules of the wave functions multiplied by the volume factor of the chosen coordinate system) are symmetric with respect to $z \to -z$, and their maxima are placed in the center $z = 0$ for the ground state, and away from the center for the excited states. The computed ground state $|000\rangle$ binding energy of the hydrogen atom for different field intensities are [14]:

Magnetic field B (Gauss)	Binding energy, $\|000\rangle$ state (Rydberg)
4.7×10^{12}	15.58
9.4×10^{12}	18.80
23.5×10^{12}	23.81
4.7×10^{13}	28.22
9.4×10^{13}	33.21
23.5×10^{13}	40.75
4.7×10^{14}	47.20

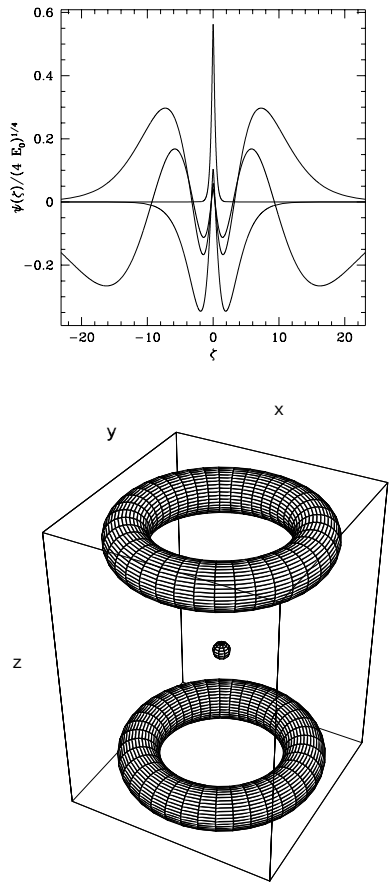

Figure 11.A.5. The axial wavefunctions of hydrogen in an intense magnetic field (analytic calculation) for $B = 4.7 \cdot 10^{12}$ Gauss. The first four even states with axial excitations, $|000\rangle$ (ground state), $|002\rangle$, $|004\rangle$, and $|006\rangle$ (left panel), and odd states $|001\rangle$ and $|003\rangle$ (right panel) are depicted; $n = 1/\sqrt{15.58}$, $\zeta = 2z/n$ corresponds to x in the used notation; z in a.u., 1 a.u. $= 0.53 \cdot 10^{-8}$ cm (reproduction of Figure 3 by Heyl and Hernquist [14]).

Heyl and Hernquist calculated the first-order perturbative corrections to the above energies and obtained the values, which are in a good agreement with the results by Ruder *et al.* [9] and Lai [12].

The associated probability density of the above *excited* states is evidently of a cylindrical (axial) symmetry and can be described as *two* Landau orbits of radius R_0 in different (r, φ) planes, one at the level $z = -L_z$, and the other at the level $z = +L_z$, with the nucleus at $z = 0$, as schematically depicted in Fig. 11.A.6. Presence of two Landau orbits occurs in accord to the excited

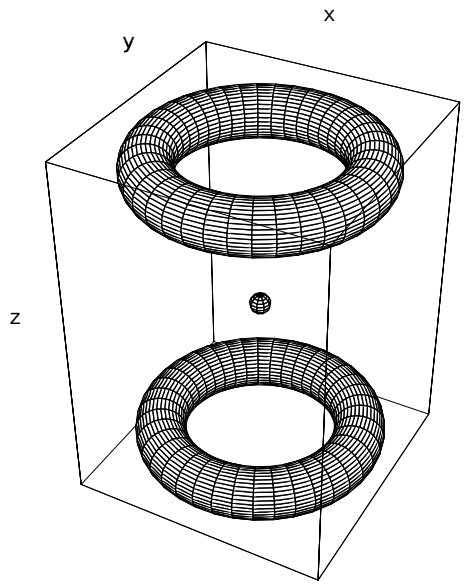

Figure 11.A.6. A schematic view on the H atom in an excited state under a very strong external magnetic field $\vec{B} = (0, 0, B)$, $B \gg B_0 = 2.4 \cdot 10^9$ Gauss. One electron moves simultaneously on two toroidal orbits of radius R_0 which are shown schematically as torii in the different (x, y) planes, one torus at the level $z = -L_z$ and the other at the level $z = +L_z$, with the nucleus shown in the center at $z = 0$. Each torus represents the (x, y) probability distribution as shown in Fig. 11.A.3 but with small Landau radius, $R_0 \ll a_0$. The spin of electron is aligned antiparallel to the magnetic field.

wave functions, which is symmetrical with respect to the inversion, $z \to -z$, and the largest peaks of which are away from the center $x = 0$. The electron moves simultaneously on these two Landau orbits.

A review of approximate, variational, and numerical solutions can be found in the paper by Lai [12]. The accuracy of numerical solutions is about 3%, for the external magnetic field in the range from 10^{11} to 10^{15} Gauss. Particularly, due to the variational results [12], the z-size of the hydrogen atom in the ground state is well approximated by the formula $L_z \simeq [\ln(B/B_0)]^{-1}$ a.u.; the transverse (Landau) size is $L_\perp \simeq (B/B_0)^{-1/2}$ a.u.; and the ground state energy $E \simeq -0.16[\ln(B/B_0)]^2$ a.u., with the accuracy of few percents, for $b \equiv B/B_0$ in the range from 10^2 to 10^6. One can see for $B = 100B_0$, that the variational study predicts the ground state energy $E = -3.4$ a.u. $= -92.5$ eV, the transverse size $L_\perp$ of about 0.1 a.u. $= 0.53 \cdot 10^{-9}$ cm, and the z-size L_z of about 0.22 a.u. This confirms the result of the modified Coulomb analytic approach.

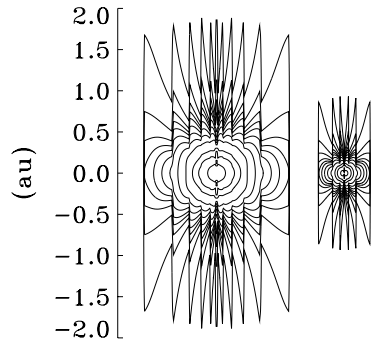

Figure 11.A.7. Contour plots of the (r, z) plane electronic density of iron atom according to the density matrix theory at two different magnetic field strengths, 10^{11} Gauss (left) and 10^{12} Gauss (right). The outermost contour encloses 99% of the negative charge, the next 90%, then 80% etc., and the two innermost 5% and 1% respectively (reproduction of Fig. 5 by Johnsen and Yngvason [13]).

Since a zero-field ground state case is characterized by perfect spherically symmetric electron charge distribution in the H atom, intermediate intensities of the magnetic field are naturally expected to imply a distorted spherical distribution. However, a deeper analysis is required for the intermediate magnetic field intensities because the adiabatic approximation is not longer valid in this case.

As to the multi-electron atoms, an interesting problem is to study action of very strong external magnetic field on He atom (see. e.g., Refs. [12, 14]) and on the multi-electrons heavy atoms, with outer electrons characterized by a *nonspherical* charge distribution, such as the p-electrons in Carbon atom, orbitals of which penetrate the orbitals of inner electrons. In fact, a very intense magnetic field would force such outer electrons to follow *small round* toroidal orbits. In addition to the effect of a direct action of the magnetic field on the inner electrons, a series of essential rearrangements of the whole electron structure of the atom seems to occur with the variation of the field strength. The magnetic field competes with the Coulomb energy, which is different for different states of electrons, and with the electron-electron interactions, including spin pairings. However, it is evident that at sufficiently strong fields, all the electron spins are aligned antiparallel to the magnetic field — fully spin polarized configuration — while at lower field intensities various partial spin polarized configurations are possible.

In accord to the numerical calculations based on the density matrix theory by Johnsen and Yngvason [13], which is in good agreement with the Hartree-Fock treatment of a very strong magnetic field, the inner domain in iron atom (26 electrons) is characterized by a slightly distorted spherically symmetric distribution, even at the intensities as high as $B = 100B_0 \ldots 1000B_0$. The outer domain appears to be of specific, highly elongated distribution along the direction of the magnetic field as shown in Fig. 11.A.7. The possible interpretation that the inner electrons remain to have a spherical distribution while outer electrons undergo the squeeze seems to be not correct unless the spin state of the iron atom is verified to be partially polarized. So, we can conclude that all the electrons are in the highly magnetically polarized state (Landau state mixed a little by Coulomb interaction), and the electronic structure is a kind of *Landau multi-electron cylindrical shell*, with the spins of all the electrons being aligned antiparallel to the magnetic field (fully spin polarized configuration).

Another remark regarding Fig. 11.A.7 is that the contours indicating a nearly spherical distribution will always appear since the Coulomb center (nucleus) is not totally eliminated from the consideration (non-adiabatic approximation), and it forces a spherical distribution to some degree, which evidently depends on the distance from the center (closer to the center, more sphericity). We note that outer contours in Fig. 11.A.7 is in qualitative agreement with Fig. 11.A.6 in the sense that the predicted charge distribution reveals symmetry under the inversion $z \to -z$, with the characteristic z-elongated Landau-type orbits.

An interesting problem is to study H_2 molecule under the action of a strong external static uniform magnetic field using Schrödinger's equation. However, prior to that study, it would be useful to investigate the simpler two-center H_2^+ ion, since it can give valuable information on the features of the full hydrogen molecule under the action of a strong magnetic field. We refer the interested reader to Refs. [12, 14, 15] for studies on H_2^+ ion and H_2 molecule in strong magnetic field. Figure 11.A.8 displays the ground and first excited state wave functions of H_2^+ [14].

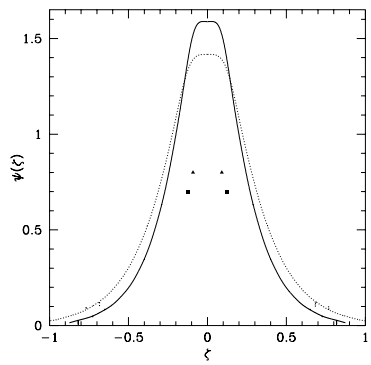

Figure 11.A.8. A schematic view of the ground and first-excited state of H_2^+ ion. The solid line traces $|000\rangle$, and the dashed line follows $|0\text{-}1\,0\rangle$. The triangles give the positions of the protons for the ground state and the squares for the excited state. The magnetic field $B = 4.7 \cdot 10^{12}$ Gauss is pointed along the internuclear axis; $\zeta = 2\pi\alpha z/\lambda_e$ denotes z in a.u.; 1 a.u. $= 0.53 \cdot 10^{-8}$ cm (reproduction of Figure 5 by Heyl and Hernquist [14]).

APPENDIX 11.A

Table 11.A.1. Basic units and their conversions.

1 kWh	860 Kcal = 3413 BTU	1 cf	28.3 liters
1 Kcal	3.97 BTU	1 cf[a]	1.263 mol
1 eV	3.83×10^{-23} Kcal	N_A	6.022×10^{23} mol^{-1}
1 cal	4.18 J	$N_A k/2$	1 cal/(mol·K)
1 mole[a]	22.4 liters = 0.792 cf	R	8.314 J/(mol·K) = 1.986 cal/(mol·K)

[a] An ideal gas, at normal conditions.

Table 11.A.2. Specific heat capacities. $p = 1$ atm, $T = 25^o$ C.

H_2(gas)	29.83 J/(mol·K)	7 cal/(mol·K)	
H_2O (liquid)	4.18 J/(gram·K)	1 cal/(gram·K)	18 cal/(mol·K)
Graphite (solid)	0.71 J/(gram·K)	0.17 cal/(gram·K)	2 cal/(mol·K)
O_2 (gas)	29.36 J/(gram·K)	7 cal/(gram·K)	
H (gas)	14.3 J/(gram·K)	3.42 cal/(gram·K)	
O (gas)	0.92 J/(gram·K)	0.22 cal/(gram·K)	
Fe (solid)	0.45 J/(gram·K)	0.11 cal/(gram·K)	6 cal/(mol·K).

Table 11.A.3. Average binding energies, at T=25° C.

	Kcal/mol		Kcal/mol		Kcal/mol
H–H	104.2^a	C=O	192.0^d	O=O	119.1^b
C–C	82.6	O–H	110.6	C=C	145.8
C–O	85.5	C≡C	199.6	C=O	255.8^c

^{a} in H_2; ^{b} in O_2; ^{c} in carbon monoxide; ^{d} in carbon dioxide.

Table 11.A.4. Evaporation heats and first ionization potentials.

	Kcal/mol	Atoms	eV
Water	10.4	H	13.6
Graphite	171.7	C	11.26
		O	13.6

References

[1] Santilli, R.M.: Hadronic J. **21**, 789 (1998).

[2] R. M. Santilli, *Foundations of Hadronic Chemistry with Applications to New Clean Energies and Fuels,* Kluwer Academic Publishers (2001) (Russian translation available in pdf file at http://www.i-b-r.org)

[3] Kucherenko, M.G. and Aringazin, A.K.: Hadronic J. **21**, 895 (1998).

[4] Settle, F.A.: Editor, *Handbook of Instrumental Techniques for Analytic Chemistry*, Prentice Hall, Upper Saddle River, New Jersey (1997).

[5] R. M. santilli, U.S. patents numbers 6,926,872; 6,673,322; 6,663,752; 6,540,966; and 6,183,604 [5a]. Magnegas website http://www.magnegas.com [5b].

[6] Sachse, T.I. and Kleinekathöfer, U.: "Generalized Heitler–London Theory for H_3: A Comparison of the Surface Integral Method with Perturbation Theory", e-print arXiv: physics/0011058 (November 2000).

[7] Kadomtsev, B.B. and Kudryavtsev, V.S.: Pis'ma ZhETF **13**, 15, 61 (1971); Sov. Phys. JETP Lett. **13**, 9, 42 (1971) (English Translation); ZhETF **62**, 144 (1972); Sov. Phys. JETP **35**, 76 (1972) (English Translation). Ruderman, M.: Phys. Rev. Lett. **27**, 1306 (1971); in: IAU Symposium 53, *Physics of Dense Matter*, C.J. Hansen (ed.), Dordrecht, Reidel (1974). Lai, D., Salpeter, E. and Shapiro, S.L.: Phys. Rev. **A45**, 4832 (1992). Lai, D. and Salpeter, E.: Phys. Rev. **A52**, 2611 (1995); Phys. Rev. **A53**, 152 (1996); Astrophys. J. **491**, 270 (1997).

[8] A. K. Aringazin, Yayli and E. Soyturk, Hadronic Journal **24**, 395 (2001).

[9] Sokolov A.A., Ternov I.M., and Zhukovskii, V.Ch.: *Quantum mechanics*, Nauka, Moscow, 1979 (in Russian). Landau, L.D. and Lifshitz E.M.: *Quantum Mechanics:*

Non-Relativistic Theory, 3rd ed., Pergamon, Oxford, 1989. Ruder, H., Wunner, G., Herold, H. Geyer, F.: *Atoms in Strong Magnetic Fields*, Springer, Berlin-Heidelberg-New York, 1994. Kadomtsev, B.B.: Soviet Phys. JETP **31** 945 (1970). Kadomtsev, B.B. and Kudryavtsev, V.S.: JETP **13** 42 (1971); JETP Lett. **13** 9 (1971).

[10] Faddeev, L. and Niemi, A.J.: Magnetic geometry and the confinement of electrically conducting plasmas, physics/0003083, April 2000. R. Battye, R., Sutcliffe, P.: Phys. Rev. Lett. **81**, 4798 (1998); and Proc. R. Soc. Lond. **A455**, 4305 (1999). Hietarinta, J, Salo, P.: Phys. Lett. **B451**, 60 (1999); and The ground state in the Faddeev-Skyrme model, University of Turku preprint, 1999; for video animations, see `http://users.utu.fi/hietarin/knots/index.html`

[11] Santilli, R.M.: *The Physics of New Clean Energies and Fuels According to Hadronic Mechanics*, Journal of New Energy **4**, Special Edition, No. 1 (1999), 318 pages. Santilli, R.M. and Shillady, D.D.: Intern. J. Hydrogen Energy **24**,
943 (1999); Intern. J. Hadrogen Energy **25**, 173 (2000).

[12] Lai, D.: Matter in strong magnetic fields, chem-ph/0009333, September 2000.

[13] Johnsen, K. and Yngvason, J.: Density Matrix Functional Calculations for Matter in Strong Magnetic Fields: I. Atomic Properties, chem-ph/9603005, March 1996.

[14] Heyl, J.S. and Hernquist, L.: Hydrogen and Helium Atoms and Molecules in an Intense Magnetic Field, chem-ph/9806040, June 1998. Jones, M.D., Ortiz, G., and Ceperley, D.M.: Spectrum of Neutral Helium in Strong Magnetic Fields, chem-ph/9811041, November 1998.

[15] Lopez, J.C., Hess, P., and Turbiner, A.: H_2^+ ion in strong magnetic field: a variational study, Preprint ICN-UNAM 97-06, chem-ph/9707050. Turbiner, A., Lopez, J.C., and Solis, U.: H_3^{++} molecular ions can exist in strong magnetic fields, Preprint ICN-UNAM 98-05, chem-ph/9809298. Lopez, J.C. and Turbiner, A.: One-electron linear systems in a strong magnetic field, Preprint ICN-UNAM 99-03, chem-ph/9911535.

[16] R. M. Santilli, Alarming oxygen depletion caused by oxygen produced from regenerating methods, Contributed paper, International Hydrogen Energy Forum 2000, Munich, Germany, September 11-15, 2000, `http://www.magnegas.com/technology/part4.htm`

[17] Liphardt and Associates: Certification of MagneGas Exhaust `http://www.magnegas.com/technology/part5.htm`

[18] R. M. Santilli, Intern. J. Hydrogen Energy **28**, 177 (2003)

[19] R. M. Santilli, "A new gaseous and combustible form of water", Intern. J. Hydrogen Energy, in press (2006).

[20] D. Eisenberg and W. Kauzmann, *The Structure and Properties of Water,* Oxford University Press, Oxford (1969) [1a]. J. A. Plambeck, *Electroanalytical Chemistry, Principles and Applications,* 2-nd edition, Wiley & Sons, New York (1982) [1b].

[21] Yull Brown, U. S. patent number 4,014,777 issued issued on March 29, 1977, and U. S. patent number 4,081,656 issued on March 28, 1978.